Sofie Kopperstad Gjerde

Hydrodynamic design of an autonomous ROV vessel

Master's thesis in Marine Technology

Supervisor: Sverre Steen

June 2020

Master's thesis

NTNU
Norwegian University of Science and Technology
Faculty of Engineering
Department of Marine Technology

NTNU

Norwegian University of
Science and Technology

NTNU Trondheim
Norwegian University of Science and Technology
Department of Marine Technology

MASTER THESIS IN MARINE TECHNOLOGY

SPRING 2020

FOR

Sofie K. Gjerde

Hydrodynamic design of an autonomous ROV vessel

ROV operations for installation and maintenance of subsea offshore installastions are currently performed using ROVs launched and controlled from large, manned offshore vessels. These vessels are costly to build and to operate, and with the rapidly increasing capability of autonomous ship technology, remote and autonomous operation of the mother ship of large ROVs seems increasingly possible. Making the mother ship unmanned means that it can be made much smaller and therefore cheaper to build and to operate than current ROV vessels. However, there are many unsolved challenges – some are related to motions and accelerations, and their impact on the operability of the ROV launch and recovery operations. This again depends on the size and hydrodynamic design of the ship. The master thesis shall evaluate the operability of small ROV motherships, with focus on the ROV launch and recovery operations, and subsequently optimize the dimensions and hydrodynamic design to maximize the operability.
The master project is part of a funded research project, headed by Kongsberg Maritime (formerly Rolls-Royce Marine), with SINTEF Ocean and NTNU as partners. The requirements set for ROV launch and recovery operations will be provided by other parts of the project team.

The objectives of this project are:
- To identify the most critical limitations for the ROV operation, including the limiting motions
- To develop a SWATH hull design, compute it's motion characteristics and operability for ROV operations, and compare that to the performance of the comparable existing monohull design.
- Participate in the planning of a seakeeping model test with the SWATH
- Observe the model test and analyse and report the results of the model test
- Discuss the results of the comparison and give recommendations for development of an optimum design.

In the thesis the candidate shall present her personal contribution to the resolution of problem within the scope of the thesis work.

Theories and conclusions shall be based on mathematical derivations and/or logic reasoning identifying the various steps in the deduction.

The thesis work shall be based on the current state of knowledge in the field of study. The current state of knowledge shall be established through a thorough literature study, the results of this study shall be written into the thesis. The candidate should utilize the existing possibilities for obtaining relevant literature.

The thesis shall be organized in a rational manner to give a clear exposition of results, assessments, and conclusions. The text should be brief and to the point, with a clear language. Telegraphic language should be avoided.

The thesis shall contain the following elements: A text defining the scope, preface, list of contents, summary, main body of thesis, conclusions with recommendations for further work, list of symbols and acronyms, reference and (optional) appendices. All figures, tables and equations shall be numerated.

The supervisor may require that the candidate, in an early stage of the work, present a written plan for the completion of the work. The plan shall include a budget for the use of laboratory or other resources that will be charged to the department. Overruns shall be reported to the supervisor.

The original contribution of the candidate and material taken from other sources shall be clearly defined. Work from other sources shall be properly referenced using an acknowledged referencing system.

The thesis shall be submitted electronically (pdf) in Inspera:
- Signed by the candidate
- The text defining the scope (this text) (signed by the supervisor) included

Supervisor   : Professor Sverre Steen
Advisors: : Mohd Atif Siddiqui
Start   : 13.01.2020
Deadline   : 10.06.2020

Trondheim, 13.01.2020

Sverre Steen
Supervisor

Preface

This master thesis has been written in the spring semester to end the studies in Marine Technology at the Norwegian University of Science and Technology (NTNU). The thesis is written in cooperation with Kongsberg Maritime, for the project "ROV Revolution Project". Through the project I have learned allot about planning experiments and how to post process data, which has been very educational.

There are several that should be acknowledged for their contribution. First of all, I would start to thank my supervisor, Sverre Steen, for giving me the opportunity to be a part of this project and giving me good advice's throughout the thesis. Thank you for pushing through to make the experiment happen due to the difficult times during COVID-19.

I would also like to express my sincerest appreciation to my co-supervisor, Mohd Atif Siddiqui, for the numerous conversations and discussion we have had throughout the project. Thank you for always being available and answering my many questions. Also, thank you for making the mesh files for the SWATH and ROV that was needed in for the simulations done in WAMIT. I have learned a lot when discussing the projects topics such as design of the SWATH and planning of seakeeping model test during out weekly supervision. The experiment would not been possible to perform without you, for that I am very grateful.

Reza Firoozkoohi at Sintef has been very helpful by providing data and geometry files for numerical simulations of the existing monohull. Thank you for being helpful with guidance for numerical simulations done in WAMIT.

Finally, thanks to my parents, Nina and Richard, for the unconditional love and endless support.

Abstract

The first full-scale autonomous cargo container vessel is currently under construction, known as "Yara Birkeland". As technology is rapidly increasing, it is likely that the autonomous technology could expand to other vessel segments when the autonomous technology has been more proven. By developing an autonomous ROV support vessel more safe operations and large overall costs in the industry will be saved. The funded research project "ROV Revolution Project" by Kongsberg Maritime wants to investigate the hydrodynamic design of an ROV support vessel. A SWATH has been designed and compared against a monohull developed by Kongsberg Maritime. The thesis investigates the design motion characteristics and operability for ROV operations for two different designs.

Seakeeping experiments on the SWATH model were carried out in two phases in the extended part of the towing tank at Sintef Ocean, Trondheim. In the first phase of the experiments, both regular and irregular wave test was carried out on the hull with stabilizer fins of two different sizes. In phase two, regular and irregular wave tests were done for bare hull and hull with stabilizer fins and an ROV mounted to the vessel. Both phases of the experiments were done in three different wave headings; 0°, 90° og 45°. The experiments gave a good understanding of the seakeeping abilities of the SWATH and also the operability of the ROV.

Due to limited time, experiments were only possible to carry out on the SWATH. Comparison between the monohull and the SWATH was, therefore, done in WAMIT. Response Amplitude Operators (RAO's), significant motion amplitude in a given sea state, and relative vertical motion amplitude between the vessel and the ROV were investigated. A comparison of the results gave an indication of the performance of the existing monohull design and the SWATH design.

The experiments of the SWATH were successfully carried out. Results from both regular and irregular wave tests proved that to achieve sufficient stability in heave and pitch motion, stabilizer fins have to be implemented in the SWATH design, even though it will increase the design and building costs. The mounted ROV on the hull made it clear that the support vessel motion does not change due to the large mass difference. The measured heave force on the ROV also gave an important understanding of that the heave force is largest for smaller waves. This means that the relative motions will be significant for small wave periods. The results from the simulations done in WAMIT showed that the SWATH has less significant motion amplitude than the monohull. For the vertical relative motion amplitude, the results indicate

that the monohull gave zero vertical velocity after wave period of five seconds. Each design has its advantages and disadvantages that need to be compared against each other to give a final decision on what fits the best for the operational requirements.

Samandrag

Tittel: Hydrodynamisk design av eit autonomt ROV fartøy

Den fyrste autonome fullskala lastekontainerfartøyet er for tida under bygging, kjend under namnet «Yara Birkeland». Ettersom teknologien stadig blir bedre, er det sannsynleg at den autonome teknologien kan utvidast til andre fartøyssegment når den autonome teknologien har blitt meir utvikla. Ved å utvikle eit autonomt ROV forsyningsfartøy, vil operasjonar for offshore bransjen bli tryggare og store kostnadar vil bli spart. Forskingsprosjektet «ROV revolusjon prosjekt» av Kongsberg Maritime har som formål å forske på det hydrodynamiske designet av eit autonomt ROV forsyningsfartøy. Ein SWATH har blitt designa og samanlikna mot eit eksisterande mono skrog designa av Kongsberg Maritime. Oppgåva ser på designa sine bevegelseseigenskapar.

Eksperiment har blitt utført på SWATH designet og blei gjennomført i to ulike fasar i den forlenga delen av slepetanken ved Sintef Ocean i Trondheim. I den fyrste delen av eksperimentet, blei både regulere og irregulære bølge testar utført på skroget med stabilisator finnar med to ulike størrelsar. I fase to, blei også regulere og irregulære bølger testa på skroget uten stabilisator finnar og for skroget med stabilisator finnar og ein tilkopla ROV. Begge fasene blei testa i tre ulike bølgeretningar; 0°, 90° og 45°. Eksperimenta gav ein god forståelse av sjøeigenskapane til SWATHen og for operabiliteten av ROVen.

På grunn av tid, var det kun mogleg å utføre eksperiment på SWATH designet. For å samanlikne mono skroget og SWATH designet, blei numeriske analyser gjennomført i WAMIT. Respons amplitude operatørar (RAO), signifikant bevegelse amplitude og relativ vertikal bevegelse amplitude mellom kvart enkelt skrog og ROVen vart undersøkt. Samanlikning av resultata gav ein indikasjon på ytelsen til det eksisterande mono skroget og SWATH skroget.

Eksperimenta utført på SWATHen blei vellukka utført. Resultata frå både regulær og irregulære bølge testar viser at for å oppnå tilstrekkelig stabilitet i hiv og stamp bevegelse, må stabilisator finnar bli integrert i designet, uansett om at det vil auke design og byggings kostnadane. Resultata frå hiv kreftene som blei målt på ROVen viste at skroget sine bevegelsar blir ikkje endra på grunn av dei store forskjellane i vekt. Den målte hiv krafta på ROVen gav ein god indikasjon om at hiv krafta er størst for bølger med liten periode. Det betyr at dei relative bevegelsane mellom skroget of ROVen er størst for bølger med liten periode. Resultata frå analysene gjort i WAMIT viste at SWATHen har mindre signifikant bevegelse amplitude samanlikna med mono skroget. Resultata av dei vertikale hastigheit amplitudene viste at mono

VI

skroget gav null vertikale hastigheit amplitude for bølge periode større enn fem sekund. Kvart design har sine fordelar og ulemper som må bli samanlikna mot dei operasjonelle krava for å gi ei sluttvurdering om kva som passar best til dei operasjonelle krava.

Contents

List of Figures

XIII

List of Tables

Nomenclature

The next list describes abbreviations, symbols and constants that will be used within the body of this document

Abbreviations

COG Center of gravity

DOF Degree of freedom

FFT Fast Fourier Transform

$IMCA$ International Maritime Contractors Association

$JONSWAP$ Joint North Sea Wave Project

$LARS$ Launch and recovery system

PSD Power Spectrum Density

RAO Response Amplitude Operator

ROV Remotely operated vessel

RSV ROV support vessel

$SWATH$ Small waterplane area twin hull

TMS Tether management system

$WAMIT$ Wave Analysis MIT

$WROV$ Work-class remotely operated vehicle

Physics Constants

μ Dynamic coefficient $1 * 10^{-3} \ Ns/m^2$

ν	Kinematic coefficient	??
ρ	Volumetric mass density	$1025 \ kg/m^3$
g	Gravitational constant	$9.81 \ m/s^2$

Other Symbols

$\ddot{\eta}$	Acceleration
$\dot{\eta}$	Velocity
ϵ_j	Phase angle
η	Displacement
λ	Waveheight
ζ_a	Wave amplitude
A_{jj}	Added mass
B_{jj}	Damping
C_D	Drag coefficient
c_e	Phase velocity
C_{jj}	Restoring coefficient
H_s	Significant wave height
M	Mass
R_e	Reynolds number
S	Surface area
T	Draft
T	Period
t	Time
T_P	Peak period
V	Volume

w Wave frequency

w_p Peak frequency

w_e Encounter frequency

Chapter 1

Introduction

1.1 Background

The maritime industry is moving towards more autonomous solutions to create safer and less costly operations. One of the segments that are seeing the potential of going autonomous is the segment for ROV operations. Today, ROV operations for repair, maintenance, and installation of subsea offshore structures require support from large IMR and subsea vessels. The people working onboard are needed to ensure that the ROV operation is conducted safely and correctly. Due to the accommodation and ROV tools, the support vessels often have a length of 100 meters and above. Depending on the size of the ship, the day rates end up at 100000-30000 dollars per day (Schjølberg & Utne 2015). Making the support vessel unmanned by going towards autonomy solutions, great cost and time savings is expected, and it may lead to more safe operations. Since an autonomous ship is unmanned, this means that the main dimensions of the support vessel can be reduced, which again reduces the overall cost.

Making the support vessel smaller gives the ship designers many questions that need to be explored and solved. The autonomous support vessel will still work in the same area as the traditional support vessels. In these operation areas, it can be harsh weather conditions. Reducing the length of the support vessel will lead to challenges due to motions and accelerations and the operability of the ROV in launch and recovery operations. How will a small ship respond to the given sea state, and is there an increased risk of impact between the support vessel and the ROV during the launch and recovery of the ROV? These are some questions that will be looked upon in this thesis.

Developing a small autonomous vessel that can launch and recover the ROV safely and controlled will be a game-changer towards autonomy in the offshore industry. Kongsberg Maritime has designed a conceptual monohull design as an autonomous vessel. The monohull has its natural period in the given sea state, and can, therefore, enhance large motions, which is un-

wanted during launch and recovery. A Small Waterplane Twin Hull (SWATH) will be designed and compared directly against the vessel designed by Kongsberg Maritime.

1.2 Motivation

The first full-scale autonomous vessels are currently under construction, and the autonomous technology could likely expand to other vessel segments when the ships and technology have proven to be reliable. Several new challenges arise when designing an autonomous ROV vessel. Autonomous ships will be a part of the future, but the industry don't know yet how this will be developed. The oil and gas industry have an enormous environmental impact. Solving this problem could contribute to lowering the emissions and reduce both the building and operating cost of the ROV vessel fleet.

There is also a personal aspect behind the motivation of solving these problems. I have a strong passion for ship design and believe that the future for some vessel segments is autonomous. I want to be able to contribute to this technological development and progress.

1.3 Objectives

The objective of this thesis is to evaluate the hydrodynamic performance of a small autonomous ROV support vessel. The emphasis will be the most critical aspect, which is the ROV launch and recovery operation, where the relative motion between ROV and the support vessel is the most vital. The primary tool for this evaluation will be that model experiments shall be supplemented by numerical analyses. Also, analysis of the experimental results will be part of the work, as well as planning the experiments.

The main objectives of the project can be summarized as:

1. To identify the most critical limitations for the ROV operation, including the limiting motions

2. To develop a SWATH hull design, compute it's motion characteristics and operability for ROV operations, and compare that to the performance of the comparable existing monohull design.

3. Participate in the planning of a seakeeping model test with the SWATH.

4. Observe the model test and analyze and report the results of the model test.

5. Discuss the results of the comparison and give recommendations for the development of an optimum design.

Chapter 2

Literature Review

This literature review aims to understand the functionality of an unmanned support vessel (USV) and the operational criteria for the launch and recovery of an ROV. In section 2.1, the reason for going autonomous will be studied, and section 2.2 looks at what equipment is needed for a USV. Most important, section 2.3 is trying to establish operational limitations for the launch and recovery of the ROV from a support vessel.

2.1   Why go autonomous?

The interest around unmanned vessels is growing, and the knowledge is rapidly increasing. Multiple companies are developing sustainable solutions for autonomous vessels. An unmanned surface vessel (USV) is defined as a vessel with no crew offshore, and the ship is controlled on-shore from a control center. There are many reasons for the shipowner for wanting unmanned vessels. Ahvenjärvi (2017) states that the two central aspects for going full autonomous are more safety in the maritime industry and reduction of costs.

The article states that safety is the most important factor when looking at the solution of an unmanned vessel. The goal of an unmanned ship is to make safety better than on a manned ship. People working offshore are exposed to rough work conditions and long working hours. The combination of harsh working conditions and long working hours may lead to fatigue of the worker. Porathe et al. (2018) states that our decision making gets worse during the night since the humans are designed to work by day time and sleep in the night time. That is in relation to human errors that may cause unwanted and dangerous situations for the people working onboard a ship. Club (2007) describes that 80 % of accidents in the maritime industry are related to human errors. The number of accidents in the maritime industry caused by humans is high, so it is desirable to reduce this number. A solution can be to move people onshore and develop autonomous and unmanned vessels. Then they are not exposed to dangerous working conditions and the risk of a maritime accident will be reduced.

The reduction of cost is also a driving factor for going autonomous. The main dimensions of an unmanned ship will be reduced compared to a manned ship. These ships require much space for accommodation and service for different equipment as an ROV. An unmanned ship does not need space for accommodation so that the main dimensions can be reduced. By reducing the length building costs and operational costs will be saved. Smaller vessels will not use so much fuel as a large ship, which is also beneficial for the environment. Therefore, one can say that the life cost cycle for an autonomous vessel will be lower than a crewed vessel.

When going autonomous, the designers have to predict many scenarios that can arise during a voyage for the vessel. Ahvenjärvi (2017) raised the question: "*Are the designers of autonomous vessels able to anticipate all different operational situations to make the vessel always behave in a safe way?*". This question states that it is still the humans that design the whole system, and need to understand and predict different scenarios that can happen when the ship is at sea.

2.2   Unmanned Support Vessel (USV)

When designing a ship, it is essential to understand what the vessel shall do and where to operate. A vessel is often fitted with various support systems that will help the vessel to complete its primary mission in a safe and controlled way. As stated by Bai & Bai (2012), an ROV support vessel (RSV) is a dynamically positioned vessel, where the operations are performed. Its primary mission is to provide support for marine operations such as drilling decommissioning or abandonment. The RSV primary assignment is to support the ROV through all phases of the operation.

When an ROV system shall be installed on a ship or a platform, there is a wide variation in the complexity and requirements of ROV systems regarding the ROV class. The needed support equipment is related to the specific ROV the ship will have. The International Maritime Contractors Organisation (IMCA) has listed the different size classifications of ROVs (Sandford 1987). Figure 2.1 describes the five different ROV classes, where the complexity increases from lower to a higher class. The different classes vary in size and weight, and they can be deployed by various systems depending on their size. The ROV can be deployed in general by two methods: over-the-side deployment or moonpool deployment. Over the side, deployment is a cost-effective method and is frequently used in ROV operations. Moonpool deployment is a more expensive and complicated method where the operation window can be increased. An increased weather window means that the ROV operation can be performed in more extreme sea conditions, which is not possible in other ROV deployment methods. It is also a more stable method for launching and recovery of the equipment. The ROVs can be deployed by a tether management system (TMS), or the vehicle can be free swimming. When the ROV is freely swimming, a surface winch umbilical is directly connected to the vehicle.
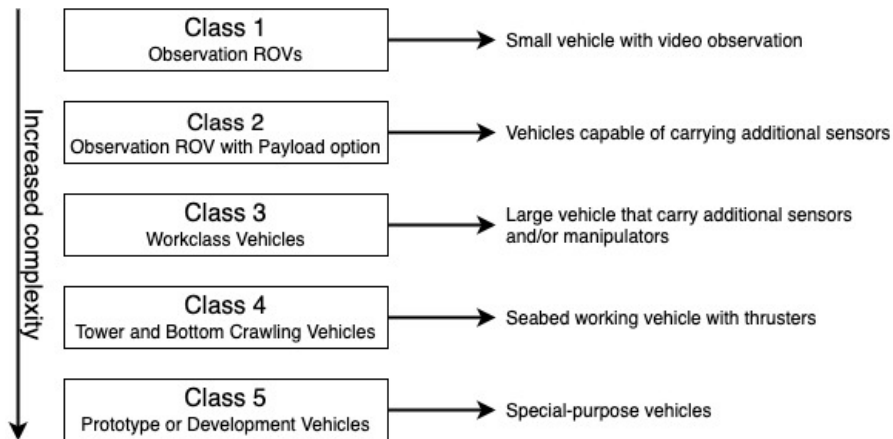
Figure 2.1: ROV classification from class 1 to class 5

The information about the ROV and its support systems comes from the ROV Manual book (Christ & Wernli 2014). Several support systems need to be implemented when performing the ROV's launching and recovery from a support vessel. Various systems need to be implemented so that the ROV will efficiently be launched without danger. The necessary support systems for the ROV operation is the launch and recovery system (LARS) and tether management systems (TMS) and the tether itself, as shown in Figure 2.2. Figure 2.2 is the arrangement for over-the-side deployment.
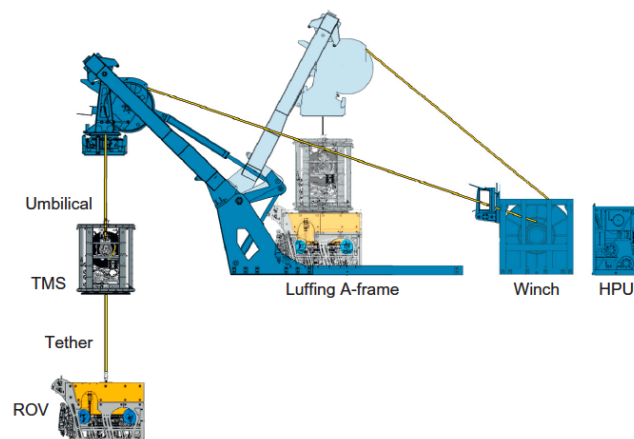
Figure 2.2: Illustration of ROV, LARS and TMS used for over-the-side deployment. (Christ & Wernli 2014)
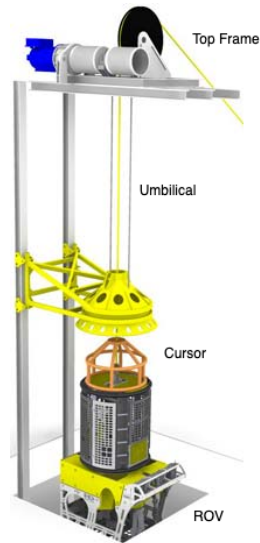
Figure 2.3: Illustration of the moonpool deployment system. (*Kongsberg moonpool deployment system* (n.d.))

In general, the TMS is the tether-handling machinery which shall support the tether cable. The tether cable is soft and is the link between the ROV and the TMS that provides power and sensors to the ROV. It describes the link between the entire subsea mechanism from the umbilical to the start of the tether. A winch system often handles the umbilical. The winch system can also be heave compensated. The mission of the LARS is to move the vehicle from the deck through the splash zone. This operation has to be performed in a safe and controlled movement, not to harm any equipment.

Figure 2.3 shows the deployment system for operation through a moonpool. When operating in the splash zone through a moonpool, the ROV is guided by wires or rails with the conjunction of a cursor. The cursor restricts horizontal movement while transitioning through the splash zone. In this way, it will stabilize and centralize the ROV and TMS. If it is large waves and powerful wind, it can cause a risk of damage to the ROV or any other component. The shape of the cursor is an upside-down bowl that fits the top of the TMS. The cursor travels on a constructed path down the side of the vessel on guided wires or rigid rails. The cursor will follow the ROV and TMS until it reached an endpoint, where the wires or rails are terminated subsea. At the endpoint, the cursor and the wires are often terminated at the deepest possible level on the ship's structure. At this endpoint, the ROV and TMS will disconnect from the cursor and be free to descend to the worksite.

2.3   Operational limitations

When assessing the characteristic of a vessel, the characteristic of the vessel must fit the operational limitations. For a USV, the owner of the vessel want it to be efficient so that it is easy to transport and operate and is affordable. It is also essential that the vessel has good operational capabilities in a rough sea. In the recommended practice DNV-RP-H103 (DNV 2011) the main phases of a subsea lift are as follow:

- Liftoff from deck and maneuvering object clear of the transport vessel

- Lowering through the splash zone

- Further lowering down to sea bed

- Positioning and landing

All these phases need to be considered in a lifting procedure, but some phases are more critical than others, especially for the launch and recovery of the ROV. When performing launch av recovery of an ROV from a support vessel, there are some operational requirements and limiting motions that need to be considered. Lifting through the splash zone is referred to as the most critical phase during the operation (Oritsland & Lehn 1989). It is desirable to avoid interference between the ROV and the hull through the launching and recovery of the ROV. When the ROV is guided through the splash zone, the heave motion is of interest. The heave motion decides the tether snatching, which is often referred to as snap loads. These snap loads can be caused by slamming from waves on the ROV or its launching frame. Also, the magnitude of the resulting large dynamic loading on the ROV and tether can lead to snapping loads (P et al. 1996). The relative motion between the support vessel and the ROV becomes one of the critical aspects.

The problem with launching a marine construction from support vessels is that the ocean is in a constant movement. The optimal would be if the vessel and the ROV were not exposed to any wave forces. This implicit state that it is the weather conditions that are limiting the operation of the ROV from the support vessel. Wernli & Chapman (1986) listed up two limiting criteria for the launch and recovery of the ROV through a moonpool.

- To launch and recover safely without damaging the hull or the ROV systems and maintaining no personal harm

- The ability to the support vessel to keep its position over the ROV due to weather-induced forces

For an autonomous vessel, the comfort on board is not an issue since it will be crewless. The operator of the vessel wants to have as little downtime as possible. Launching and recovery through a moonpool compared to conventional over-the-side launch has been proved to increase the weather window for operation. The over-the-side launch will cause a force induced by the motion of the support vessel, which can cause high vertical accelerations. This force is trans-

lated from the support vessel's roll and pitch. Operating through moonpool, which is placed in the center of the support vessel, roll and pitch motion will be reduced. Since the snap loads are a crucial limiting factor in the launch and recovery process, the use of moonpool can also minimize the vertical water motion so that snap loads on the ROV is reduced (Wernli & Chapman 1986).

Jamieson & Wilson (2015) explained that lifting constraints that shall be considered of any heavy object from a vessel at sea, are nearly related to the motion of the vessel and sea state. Different class societies have developed guidelines for design and build of launch and recovery of equipment like this. He mentioned that one of the most limiting factors is to avoid slack wire, which is when the lift line goes slack due to the vessels or wave motion. The slack wire is no problem in a low sea state, but when the sea state gets high, the chance for slack wire is increasing. He underlined that when the significant wave height exceeds 5.5 meters, slack-wire is likely to appear.

DNV states that a large ROV should not be launched over-the-side when the significant wave height exceeds 2.5 to 3.0 meters. If wished to operate in a higher sea state, launch and recovery should be taken place in moonpool operation, on leeward, and if heavy weather side system is used. It is hard to specify the operational limitations of a moonpool, but it is clear that it gives an increased weather window. What needs to be studied is the vertical accelerations for the ship (DNV GL 2016).

In addition to the sea state that needs to be taken into account for the operation, other factors need to be considered. The factors that will be considered in addition to the sea state is as listed:

- Vessel Heading

- Wind speed

- Wave direction and interaction

- Surface current

- Visibility

- General weather forecast

These factors need to be considered by a supervisor that should decide if the ROV can be conducted or not. It is therefore desirable to investigate the vertical acceleration, snap loads, and the relative velocity between the vessel and ROV. When knowing how the vessel will behave, the LARS system has to be designed to minimize the chance of slackline Jamieson & Wilson (2015).

Chapter 3

Designs

3.1 Tentative design goals

ROV operations for installation and maintenance of subsea offshore installation are currently performed using ROVs launched and controlled from large, crewed offshore vessels. These vessels are costly to build and operate. With the rapidly increasing capability of autonomous ship technology, remote and autonomous operation of the mother ship of large ROVs seems increasingly possible. Making the mother ship crew less means that it can be made much smaller and, therefore, cheaper to build and to operate.

When designing a vessel, tentative design goals need to be established. Since this vessel will be an autonomous ROV support vessel, the ship should have excellent seakeeping abilities, so that the launch and recovery of the ROV will be completed without any harm. The executive goal of the design of the alternate design to the monohull proposed by Kongsberg is to increase the sea keeping abilities and ensure a sufficient operation.

The designer also has ambitions of keeping the lightweight ship around 100 *tonnes*. The underlying goal of keeping the weight of the autonomous vessel around a specific weight is because the autonomous vessel can be lifted on board on, for example, a subsea construction vessel. Many subsea construction vessels have installed a 150 tonnes crane on board and can be used to lift the autonomous ship onboard the subsea construction vessel.

In addition to excellent seakeeping abilities, it also needs to be robust. There is a wish that the vessel can provide 24/7 operation. During the 24/7 service, there may be weather conditions exciting the operation limitation for the ROV operation. The ship will then be on stand by and wait for calmer weather. The vessel needs to be robust to withstand the harsh condition. The survivability of the vessel, therefore, needs to be taken into consideration.

Procedure of launch and recovery of the ROV:

- 1 m below the moonpool will be the realise point for the ROV. Taking the basis from the monohull.

- Timeframe for launch and recovery: 10 min launch and 10 min recovery. The hatches will be closed in the meetime between launch and recovery. This implies that it can be a 24/7 operation for the ROV.

3.2   Comparison between designs

In the design phase, hull types are studied to determine what hull is most suited for the operational requirements. For the support vessel's operability, it is desirable to choose a ship that gives the least motions and accelerations in the launch and recovery stage. A small waterplane area twin-hull (SWATH) vessel will be studied and compared with the original monohull design proposed by Kongsberg Maritime. Figure 3.1 is a 2D illustration showing the submerged transverse area of the SWATH and the monohull, to get a better understanding of the most significant features of each design.

The designer of the autonomous ROV vessel has the ambition to keep the lightweight ship around 100 tonnes. This requirement is established to lift the autonomous vessel onboard, for example, a subsea construction vessel. Also, a 150 tonnes crane can be used, since many subsea vessels have that implemented. To achieve excellent seakeeping abilities is more important than having the ability to lift the autonomous vessel on board a support vessel. Therefore, the requirement of lifting the vessel will be a sub-requirement, and the seakeeping abilities will be more critical.
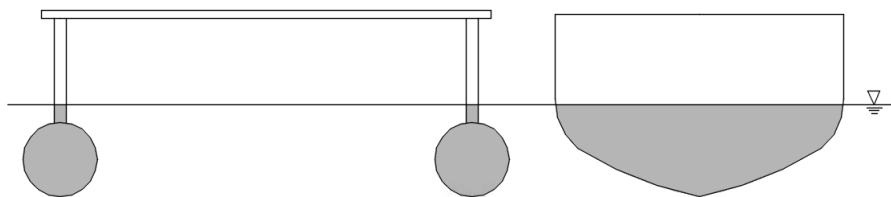
Figure 3.1: Illustration of a transverse section of SWATH (left) and monohull (right)

When making a direct comparison of the monohull and the SWATH, it is challenging because the vessel's geometry is so different. One of the great benefits of the SWATH compared to a monohull is the enclosed deck area due to the large beam that can be used for storing equipment and operations. The beam is typically twice as large as the beam to a monohull. Even though the SWATH has large deck area compared to the monohull, the reduced waterplane still gives problems related to the choice of machinery system. A small SWATH is restricted not to fit large and complex machinery systems into the design, and the machinery may have to be
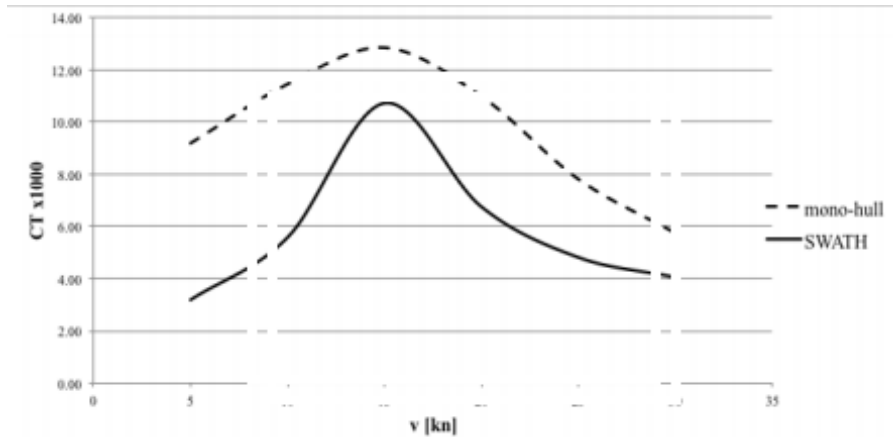
Figure 3.2: Comparison between total resistance coefficient for a SWATH and monohull done by Medaković et al. (2013)

placed on deck if there is limited space in the lower hull. Nagai (1987) states that the most common machinery configuration is Diesel engines with fixed or controllable pitch propellers, due to limited space. The monohull design does have a more comprehensive range of choosing machinery and propulsion systems since it is not so sensitive to weight and does not have have a limitation of space due to the fitting of propulsion.

Resistance is an important parameter when evaluating different designs. Medaković et al. (2013) made a resistance comparison between a SWATH and a monohull with a length of 25 meters, which is comparable to the length of the SWATH and monohull that will be compared in this study. Figure 3.2 shows the total resistance comparison between a SWATH and a monohull, where the monohull has a higher total resistance coefficient than the SWATH. Less resistance will reduce fuel consumption, which is preferable. Cost is also an important criterion that needs to be evaluated in the early design phase when selecting a design. G (1960) confirmed that the SWATH does have a higher building cost due to the nontraditional design parameters compared to the monohull. Still, the designer needs to take into account the greater seakeeping abilities when looking at the total cost.

3.2.1 Monohull

Kongsberg has developed a tentative design of an autonomous support vessel that should support an ROV. The preliminary hull design is formed as a monohull. A monohull is, in general, a hull that only has one hull, compared to the SWATH that has two submerged hulls connected, as illustrated in Figure 3.1. The ROV will be launched through a moonpool. For monohulls, rolling tends gives large motions. Therefore, a roll damping tank has been implemented in the design of the monohull to reduce the roll motion of the hull. The monohull will be fitted with hatches that can be closed and opened during launch and recovery. When the ROV is launched and working, the bottom hatches will be closed, and water will still be inside the moonpool. The main dimensions of the ship is given in Table 3.1.

Table 3.2 was used as an basis for the development of the monohull geometry used for analyses is this thesis. The geometry file in made out from the launch and recovery minus the water in the moonpool, which resulted in the parameters presented in Table 3.3 Table 3.4.

Table 3.1: Main dimensions to the tentative design of the support vessel

Dimensions	Value	Unit
L_{hull}	24.00	m
B	7.00	m
$T_{Lifting}$	3.1	m
$T_{Transit}$	3.4	m
$T_{L/R}$	3.9	m

Table 3.2: Weight estimation of monohull

Category	Lifting [t]	Transit [t]	Launch and Recovery [t]
Hull	49.00	49.00	49.00
Cargo equipment	29.00	29.00	29.00
Ship equipment	3.00	3.00	3.00
Crew equipment	1.00	1.00	1.00
Machinery main comp.	8.00	8.00	8.00
Systems for machinery	2.00	2.00	2.00
Ship common systems	13.00	13.00	13.00
Payload	1.70	1.70	1.70
Consumables	0.00	26.40	26.40
Fixed ballast	1.70	1.70	1.70
Ballast water	0.00	0.00	27.80
Water in moonpool	0.00	0.00	30.00
Total	108.00	134.00	192.00

Table 3.3: Monohull displacement and COG values used in WAMIT

Draft	Displacement [t]	LCG [m]	TCG [m]	VCG [m]
3.80	153.00	0.00	0.00	0.16

Table 3.4: Moment of inertia and radius of gyration for the monohull used in WAMIT

R_x [m]	R_y [m]	R_z	I_x [tm^2]	I_y [tm^2]	I_z [tm^2]
2.50	5.34	5.27	952.82	4363.19	4247.83

Prior to this project, SINTEF did an experiment on the monohull, to understand its motions. In the experiment a free decay test were also performed to characterise the linear and quadratic

damping coefficients. The damping coefficient will be used for the simulations done in WAMIT, and has the values:

$$
C_{jj} = \begin{bmatrix}
1525 & 0 & 0 & 0 & 0 & 0 \\
0 & 14489 & 0 & 0 & 0 & 0 \\
0 & 0 & 200000 & 0 & 0 & 0 \\
0 & 0 & 0 & 1120000 & 0 & 0 \\
0 & 0 & 0 & 0 & 18000000 & 0 \\
0 & 0 & 0 & 0 & 0 & 186600
\end{bmatrix}
\tag{3.1}
$$

3.2.2 SWATH

A SWATH has been developed on similar guidelines as the monohull. The name SWATH describes the vessel features that it has a small waterplane area and two demi-hulls. The reason for comparing a SWATH with the proposed monohull is that the SWATH has higher natural periods in heave and pitch than a monohull, as stated by Faltinsen (2006). The idea of designing a SWATH as the ROV mothership is to move the vessels natural period out of the wave range.

One of the characteristic design parameters of the SWATH is that is has reduced waterplane. The reduced waterplane will give less motions and be preferable due to the design requirement of low relative motions and velocities. The relative velocities are important during the launching and recovery of the operation and are described more in detail in section 4.2. The SWATH will also have a large deck area due to the large beam, which is preferable due to the large ROV system.

The two demi-hulls that is the characteristic of the SWATH is often made up of two semi-submerged hulls and a strut which break the water surface. To connect the demi-hulls, a box cross-structure is used. Figure 3.3a and Figure 3.3b shows a simple arrangement of the SWATH hull and its design parameters.

Table 3.5: Main dimensions of SWATH

Dimensions	Value	Unit
Dimension between hulls, B	10.00	m
Length of individual hull, L	30.00	m
Strut length, S_1	20.00	m
T	2.90	m
Depth of struts	8.00	m
Height from deck to base of hull, D	4.20	m
Hull radius, R	0.90	m
Thickness of strut, t1	0.18	m
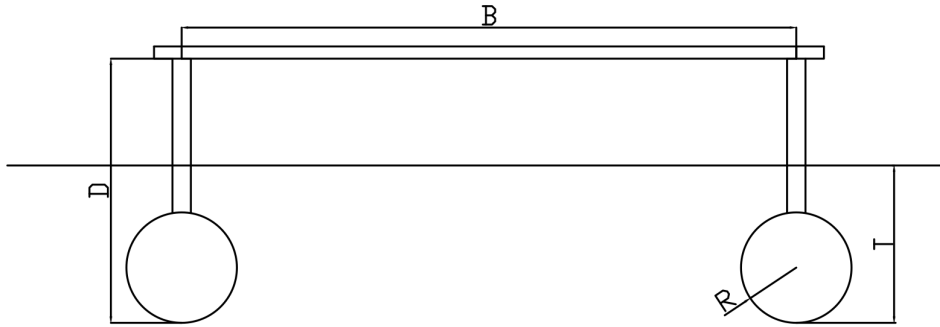
(a) Arrangement of SWATH without stabiliser fins, transverse view
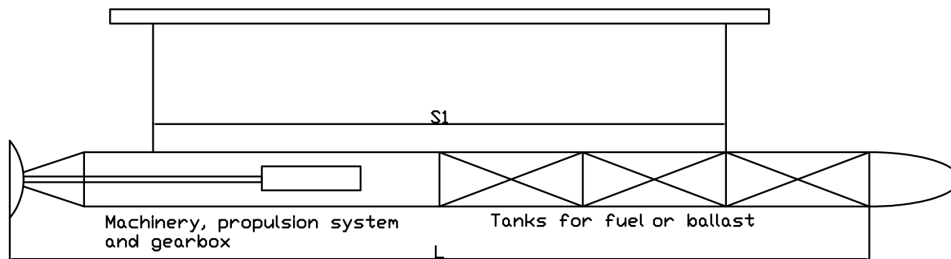
(b) Arrangement of SWATH without stabiliser fins, longitudinal view

Figure 3.3: Arrangement for SWATH in transverse and longitudinal view

Table 3.6: Weight estimation of SWATH

Category	L/R [t]	KG [m]	W*KG
Hull	40.00	2.63	105.20
Cargo equipment	29.00	4.00	116.00
Ship equipment	3.00	4.00	12.00
Crew equipment	1.00	4.00	4.00
Machinery main comp.	8.00	0.90	7.20
Systems for machinery	15.00	0.90	13.50
Ship common systems	15.00	0.90	13.50
Payload	1.70	3.00	5.10
Consumables	26.40	0.90	23.76
Fixed ballast	26.40	0.90	1.53
Ballast water	27.80	0.90	25.02
Total	153.60	2.04	313.31

The COG with respect from vessels origo in full scale model is presented in Table 3.7. The vertical direction is relative to the keel (the lowest point on the model). These values will be used for further calculations.

Table 3.7: SWATH COG from vessels origo

Draft [m]	Displacement [t]	LCG [m]	TCG [m]	VCG [m]
2.90	168.00	−2.23	0.00	−1.858

The required moment of inertia about the COG is presented in Table 3.8 and will be used in further calculation.

Table 3.8: SWATH required moment of inertia

Type	I_{xx} [tm^2]	I_{yy} [tm^2]	I_{zz} [tm^2]
Hull	1600	1200	0.00
Fins 1 fore	1.35	15.33	0.00
Fins 1 aft	1.35	12.73	0.00

The exceptional seakeeping abilities do also have their drawbacks. Slamming loads can cause severe problems for the cross-structure when operating in heavy sea. When designing a SWATH, several things need to be considered. One of the drawback with the SWATH is that it is susceptible to an increase in weight compared to the monohull. As seen in Figure 3.1 for the illustration of the SWATH (to the right), the SWATH has a large air gap between the waterline and the cross deck. Increasing the weight one will automatically increase the draught, which can be critical for the SWATH, for example, for the required air gap. It can lead to wave impact on the bottom of the cross-structure, which is not preferable. Lee & Martin (1976) have pointed out that due to the small waterplane area, it can cause pitch-mode instability from the Munk moment, when the ship is cruising. The Munk-moment is proportional to the square of the speed and will then provide a destabilizing pitch moment. To achieve stability, stabilizer fins can be mounted on the inner side of both hulls. These stabilizer fins can have either a passive or active control system. The fins are often formed as foils that will generate lift at operating speeds and improve the stability. The foils will also cause a viscous effect and vortex shedding. This will provide damping in the vertical motions, as heave, roll and pitch motion.The stabilizer fin size must be designed to ensure stability, to obtain damping for heave and pitch, and to maintain reasonable natural periods. Lee & Martin (1976) suggests that the forward fin should be located at approximately 0.15 L at the inside of each of the two hulls and aft fin at 0.84 L position at the inside of the two hulls. To understand the effect of fin sizes on vessels seakeeping behavior two fin sizes are tested with the dimension presented in Table 3.9.

Table 3.9: Dimensions and details of stabiliser fins

Aspect Ratio	Span	Root Chord length	Tip Chord length	Surface area
1.25	1.463	1.281	0.640	–
2.00	1.463	1.286	0.640	–

Vertically the foils will act as a flat plate. The foils will be formed as flat plates both at zero and non-zero speed due to simplifications in the experiment. Since the stabilizer fins are providing added damping in the vertical direction, this has to be accounted for. For similarity, the thickness overall is set to 6 *mm*. The stabilizer fins will cause viscous damping due to vortex shedding when the vessel moves in the water. The numerical analyses done in WAMIT external viscous damping due to the fins have to be added, since WAMIT does not take into account viscous effects. The added damping from the fins will be found in the experiments. Figure 3.4 shows how the SWATH with single strut is modelled and will be used for the numerical simulations.
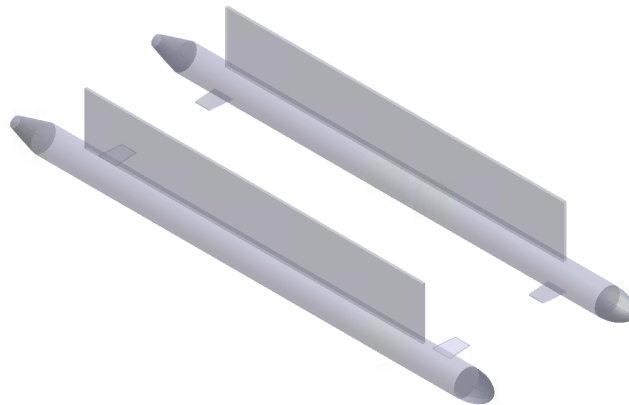
Figure 3.4: SWATH with single strut model

The SWATH can also have problem with slamming on the underside of the deck between the two hulls and piston-mode resonance. This two phenomena are discussed in section 4.3.

3.3 SAAB Seaeye

Over a couple of years, ROVs have been used for demanding underwater operations. The SAAB Seseye Leopard is proposed as an example of a work-class ROV (WROV) that can be used in such an operation that is described above. Therefore, the SAAB Seaeye will be used as a basis for the ROV in numerical and experimental analysis. Figure 3.5 shows the design of the WROV. In Table 3.10 the different parameters for the ROV is listed. The ROV is delivered with 7 or 11 vectored $SM9\ 500v$ brushless DC thrusters providing 6-axis control (*SAAB Seaeye leopard* n.d.).
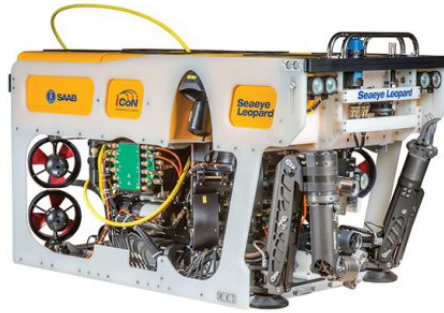
Figure 3.5: SAAB Seaeye leopard work ROV, (*SAAB Seaeye leopard* n.d.)

Table 3.10: ROV: Seaeye Leopard specifications

Parameters	Value	Unit
Depth Rating	$2000 - 3000$	m
Length	2.150	m
Height	1.20	m
Width	1.20	m
Launch weight	< 1200	kg
Forward velocity	> 1.80	m/s
Thrust forward	493	kgf
Thrust lateral	377	kgf
Thrust vertical	225	kgf
Payload	200	kgf

The ROV can recover quickly in surge and sway using thrusters. Heave, roll, and pitch are the most critical motions relative to the vessel. When considering that the ROV is an independent body just after launch and recovery, the USV and the ROV is moving independently to each other. Even though they are moving independently, they can have hydrodynamic interaction with each other that can cause an unwanted situation. When the ROV is fully submerged, it does not have a natural period, but its motions can be affected by the motions to the USV. Therefore, it is of interest to find out if the ROV can manage to "swim" away fast enough to avoid interactions with the USV right after launch and recovery.

For the numerical calculations and the experiment, the ROV is modeled as a cubic box, with the dimensions presented in Table 3.10. This gives a total weight of 2000 kg and the mass moment of inertia has been estimated to be:

Table 3.11: Mass moment of inertia estimation for ROV

I_{xx}	I_{yy}	I_{zz}	Unit
480	975	975	kgm^2

The estimates COG for the ROV related to the SWATH is $(0, 0, -2.30)$ and for the ROV related to the monohull the COG is found to be $(0, 0, -5.30)$ From Table 3.10 the ROV forward velocity is found to be $v_x < 1.80 \ m/s$. The ROV vertical velocity is an important criterion when studying the relative velocity between the vessel and ROV to see if the ROV has enough time to "swim" away to avoid collision between the two systems. The vertical velocity can be found by using relative expense when knowing the forward velocity, thrust forward, and the vertical thrust.

$$\frac{U_x}{U_y} = \frac{T_x}{T_y} \tag{3.2}$$

$$\frac{18}{U_y} = \frac{493}{225} \tag{3.3}$$

$$U_y = 0.82 \tag{3.4}$$

From the calculation above the vertical velocity is found to be $U_y = 0.82 \ m/s$, and an execcutive vertical velocity can be set to $U_y = 1.0 \ m/s$. In section 4.2, one can read more about relative motions and velocity, where a operational requirement is established.

When the ROV is submerged, wave forces are minimal, but drag forces cannot be neglected. Viscous effect dominates and needs to be accounted for in the numerical calculations. Since WAMIT is based on potential theory, the viscous effect is ignored. Therefore, it is desirable to establish the damping due to viscous effects to get correct relative motions and velocities between the hull and the ROV. Holven (2018) investigated the control system for *ROV Minera II* and had then to investigate hydrodynamic parameters for the ROV. The drag coefficient for that ROV was found to be $C_D = 0.85$, and will be used in this work.

When knowing the drag coefficient, one can use Morrison's equation to calculate the drag coefficient. Morrison's equation calculates wave loads on circular cylindrical structural members of fixed offshore structures when viscous forces are important. Chakrabarti (2005) suggested that Morrison equation can also be used on a structure that is free to move, such as an ROV. A modified form of the Morison's equation is written that describes the in-line force resulting from oscillatory motions imposed on submerged ROV:

$$F_d(t) = \frac{1}{2}\rho C_D A_c u(t)|u(t)| + (C_M \rho \forall + m)\, \dot{u}(t) \tag{3.5}$$

where $f(t)$ is the in-line force acting on the ROV, u(t) is the ROVs velocity, $\dot{u}(t)$ is the ROVs

acceleration, C_D, and C_M is the drag and inertia coefficient, A is the characteristic area of the ROV and $\forall$ is the volume of the fluid displaced by the vehicle.

The characteristic area of the ROV is defined as $\forall^{2/3}$. The characteristic area for the SAAB Seaeye Leopard ROV is calculated to be 2.05. From the equation of motion below, a simplified expression for the damping can be found.

$$A\ddot{u}(t) + B\dot{u}(t) + Cu(t) = F_d(t) \tag{3.6}$$

By using the equivalent coefficient B, the damping force can be written in an alternate way

$$B = \frac{F_d(t)}{\dot{u}} = 732.30N \tag{3.7}$$

Chapter 4

Numerical analysis

In this chapter the theory for the numerical analysis is described.

To be able to satisfy operational requirements and safety criteria, seakeeping has to be studied. That means that the vessel needs to operate safely and reliably under its given requirements. The forecast of seakeeping parameters like ship response, slamming, wave loads, or relative velocities, is some of the essential parameters that need to be accounted for the ship design. The theory is based on the book Sea loads on ships and offshore structures (Faltinsen 1998) and DNV-RP-H103 (DNV 2011).

For the numerical analysis, the program WaveAnalysisMIT (WAMIT) has been used. As stated in INC. (n.d.), WAMIT is a tool that solves the radiation and diffraction problem and gives out the body's motion. The program assumes linear potential flow theory in the frequency domain. WAMIT assumes that the body stays at its mean position, which is right in the fact that the launch and recovery of the ROV from the USV will happen when the ship is dynamically positioned. One of the advantages of using WAMIT is that only the wetted body boundary needs to be established. This is because the WAMIT uses the Green's function satisfies the free-surface condition and radiation due to far-field waves. The geometries used for simulation are mesh files, named *.gdf*.

The disadvantage with simulations in WAMIT is that viscous effects are not considered, and the flow fields are potential without circulation. The solution to this problem is to add damping coefficients manually, which will depend on the frequency. From the decay test in the experiment, the damping coefficient was found and was implemented in the model for the SWATH, to get more realistic calculation. From the small-scale experiment done by Reza Firoozkoohi of the monohull, the damping coefficients were also estimated.

4.1 Seakeeping

The seakeeping ability is of significant interest during the preliminary design stage to understand how the ship will behave. When somebody states that a ship has functional seakeeping abilities, it is said to be seaworthy and can operate efficiently in high sea states. For crewed vessels, the comfort of the vessel has to be sufficient to be a good workplace. The ROV support vessel will, as stated, be crewless, the comfort onboard is not a requirement. On the other side, the seakeeping abilities for launch and recovery must be considered to find the limiting motions for the operation.

There are different principle terms to describe a seakeeping performance when having the measure of seakeeping ability to a ship. St. Denis proposed four factors to identify seakeeping performance in 1976 Lewi (1989).

1. **Mission**.
   Missions are assigned to the ship, including appropriate condition of loading.

2. **Environment**.
   Where should the ship operate? This includes sea state, wind speed or geographic region. A wave spectrum and oceanographic databases can be used to describe the environment.

3. **Ship responses**.
   The ship responses that is characteristic to the ship. Is a function of the vessels characteristics regarding to hull form and weight distribution. This gives the response amplitude operator (RAO) and evaluates the six DOFs. The response is also affected by the given sea state ship is suppose to operate in.

4. **Seakeeping performance criteria**.
   Key element in developing a methodology for assessing a ship's seaway operational performance.

4.1.1 Response in regular waves

In waves, a ship has six degrees of freedom, which are the primary dynamic responses to the wave loads that is acting on the ship. The coordinate system for a ship has three principal axes with two degrees of freedom for each axis. As shown in Figure 4.1 the motion of the vessel is
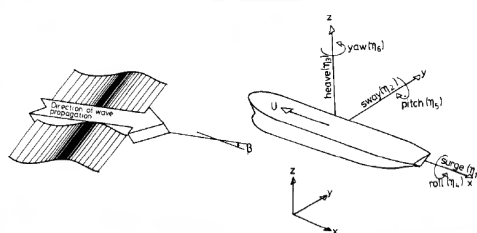
Figure 4.1: Coordinate system for ship (Faltinsen (1998))

characterized by three translations and three rotations. The translations and rotations can be expressed by:

$$\eta_j(t) = \eta_{ja}cos(\omega_e t + \epsilon_{j\zeta}) \tag{4.1}$$

for $j = 1..6$: surge, sway, heave, roll, pitch and jaw, respectively.
where:

ω_e = Wave frequency $[rad/s]$
ϵ_j = Phase angle in j^{th} mode $[rad]$
t = Time $[s]$

As known, the dimensions of the ship affects seakeeping and dynamic responses. A small ship will generally have higher motions than a larger vessel. A smaller ship will have larger motions because of its relative length to the wave. When a small ship gets encountered by big waves, the ship will move allot around compared to its size, and a larger ship will move less in the same wave. This is because a larger ship is longer relative to the wave. For smaller ships, rolling in combination with either wind, water on deck, or motion of the cargo can cause the ship to capsize. Another important reason is for the capsizing of smaller ships is breaking waves. Heave, roll, and pitch are the most critical motions, for the launch and recovery operation of the ROV.

The Response Amplitude Operator (RAO) refers to the movements of a floating ship in its six degrees of freedom due to an incoming hydrodynamic wave, as shown in Figure 4.1. The name *Response amplitude operator* is set up in two parts. Response amplitude refers to the degree of movement induced in a vessel by an incoming wave. The movement created by the incoming wave is absolute. The operator refers to the factor that must be multiplied by a specific value, such as wave height, to define the absolute movement. The operator is a transfer function of the body motions amplitude. The parameter is used to determine the expected behavior of a ship when operating at sea. The effect of different sea states on the ship can be analyzed and given valuable information about the ship's behavior in the early design stage. The RAOs can be found by implementing a frequency domain analysis or through experimental analyses. Frequency-domain analysis can be used when a large volume structure gets analyzed in regular incident waves. Assuming linear potential theory, the hydrodynamic problem can be divided into radiation and diffraction problems.

In this report, WAMIT has been used to establish the RAOs numerically. WAMIT is a diffraction and radiation panel program developed for linear analyses of the interaction with surface waves.

The diffraction problem is when the structure is fixed and is interacting with incident regular waves — resulting in hydrodynamic loads that are called wave excitation loads. This, again, is divided into Froude-Kriloff and diffraction forces and moments. The diffraction force can be written as

$$F_k^{(d)} = f_k(\omega)e^{-iwt}; k = 1, 6 \tag{4.2}$$

The restoring force appears when the vessel is forced to oscillate with the wave excitation frequency in any rigid-body motion mode. In this problem, there is no incident wave. These hydrodynamic loads can be found as added mass, damping, and restoring terms. The radiation force can be written as

$$F_k^{(r)} = -A_{kj}\frac{d^2\xi_j}{dt^2} - B_{kj}\frac{d\xi_j}{dt} - C_{kj}\xi_j \tag{4.3}$$

4.1.2 Natural resonance period

Important parameters that determine the amplitude of motion of a ship are the natural or often named resonance period, damping level, and wave excitation level. Relatively large motions occur when the structure is excited with oscillation periods equal to the resonance period. It is therefore important to locate the resonance periods for the ship to know its operation range. The equation of rigid body motion has to be implemented to describe the resonance frequencies. The equation of rigid body motion is established by using the equation of linear and angular moment, and the steady-state sinusoidal motion can be written as:

$$\sum_{k=1}^{6}\left[(M_{jk} + A_{jk})\ddot{\eta}_k + B_{jk}\dot{\eta}_k + C_{jk}\eta_k\right] = F_j e^{i\omega_k t} \tag{4.4}$$

for $j = 1..6$: surge, sway, heave, roll, pitch and jaw, respectively.

Where M_{jk}, A_{jk}, B_{jk} and C_{jk} are the components of the generalized mass, added mass, damping, and restoring matrices of the ship. M_{jk} are the components of the generalised mass matrix for the structure. Equation 4.5 shows the mass matrix. The mass matrix is also important in WAMIT to represent the mass of the structure.

$$M_{jk} = \begin{bmatrix} M & 0 & 0 & 0 & Mz_G & 0 \\ 0 & M & 0 & -Mz_G & 0 & 0 \\ 0 & 0 & M & 0 & 0 & 0 \\ 0 & -Mz_G & 0 & I_4 & 0 & -I_{46} \\ Mz_G & 0 & 0 & 0 & I_5 & 0 \\ 0 & 0 & 0 & -I_{46} & 0 & I_6 \end{bmatrix} \tag{4.5}$$

4.1.3 Response in irregular waves

The theory in this section is taken from the Marine Dynamics compendium (Myrhaug et al. 2014). When designing a ship, it is desirable to calculate the response in a particular sea state that represents the real world. The spectrum depends on different factors such as wind, geographic site, and other factors. One can say that ocean waves are often random or irregular. The difference between a regular wave and an irregular wave is that a regular wave has a single frequency and amplitude. In contrast, irregular waves are a result of adding together results from regular waves of different amplitudes, wavelengths, and directions.

Short term statistics

Short term statistics can be explained as the probability distribution of wave heights in a sea state or wave record. When having the RAO, the short-term response statistic can be established. This is done by using a standardized wave spectrum. This is an important part of the design strategy to avoid significant response; one can make the peak of the transfer function of the linear system away from the peak of the wave spectrum. The RAO can be describes as:

$$H_j(\omega) = \frac{\bar{\eta}(\omega)}{\bar{\zeta}(\omega)} \tag{4.6}$$

where $\bar{\eta}e(iwt)$ is the wave amplitude and $\bar{\zeta}e(iwt)$ is the motion response. By considering it as a linear system the response spectrum for a given sea spectrum can be found by:

$$S_{\eta j}(\omega) = |H_j(\omega)|^2 S_{\zeta j}(\omega) \tag{4.7}$$

where $|\eta(\omega)|$ is the amplitude of the RAO or it can be explained as a transfer function of the linear system and $_{\zeta j}(\omega)$ is the wave spectrum. One can say that a standardized wave spectrum is a mathematical representation over a sea state. The spectrum can be used to explain how energy is distributed for different frequencies. When just having the RAO, it can be hard to relate and to understand the given results. That is why the user can have an advantage of giving the results for a particular sea state that can occur in units like displacement in m, velocity in m/s and accelerations in m/s^2.

When the response function is known, it is of interest to find the significant wave height, denoted as H_s or H_{m0}. When assuming a stationary, normally distributed and ergodic process, the significant wave height can be written as

$$H_s = H_{m0} = 4\sqrt{m_0} \tag{4.8}$$

m_0 is a moment of the spectrum and is often used to express the significant wave height or characteristic wave periods, as in Equation 4.8. The moments can be defined as

$$m_n = \int_0^\infty \omega^n S_{\eta j}(\omega) d\omega; \text{n} = 0, 1, 2, \dots \tag{4.9}$$

To calculate the significant motion amplitude, m_0 is used. m_0 is the sea surface variance and the equation for the moments can be calculated as

$$m_0 = \int_0^\infty S_{\eta j}(\omega) d\omega \tag{4.10}$$

By having the relation for the significant waveheight the same relation can be used to find the amplitude of significant response motion and the amplitude of significant relative motion. This is done by integration over the response spectrum.

The JONSWAP spectrum (Joint North Sea Wave Project)

Different spectrums are established that gives frequency distribution of energy. Well-known spectrums are Pierson Moskovitz and the JONSWAP spectrum. The JONSWAP spectrum is a multinational project which took place in the south-east part of the North Sea. In general, the JONSWAP spectrum is a Pierson-Moskowitz spectrum that is multiplied by a peak enhance, the coefficient of γ. γ is proportional to the ratio between the maximum energy in the JONSWAP spectrum and the maximum energy in the PM spectrum. The JONSWAP spectrum is defined as:

$$S(\omega) = \frac{\alpha g^2}{\omega^5} \exp\left\{-1.25\left(\frac{\omega_p}{\omega}\right)^4\right\} \cdot \gamma^{\exp\left\{-0.5\left(\frac{\omega-\omega_p}{\sigma\omega_p}\right)^2\right\}} \tag{4.11}$$

where w_p is the peak frequency factor that can be found by $w_p = \frac{2\phi}{T_p}$ and α is a parameter which determines the spectrum shape in high frequency range. This parameter can be calculated by:

$$\alpha = 5.061\left(\frac{\omega_p}{2\pi}\right)^4 H_s^2[1 - 0.287\log\gamma] \tag{4.12}$$

$$\sigma = \begin{cases} 0.07 & \text{for} \quad w \leq w_p \\ 0.09 & \text{for} \quad w > w_p \end{cases} \tag{4.13}$$

The environmental parameters that will be used as input for the numerical and experimental analysis is presented in Table 4.1. Mainly there are two different significant wave height, denoted H_S, with varying peak period, that is denoted T_p.

Table 4.1: Environmental parameters

H_S	T_p	γ	H_S	T_p	γ
1.5	4.5	4.6	-	-	-
1.5	5.5	1.8	2.5	5.5	5.0
1.5	6.5	1.0	2.5	6.5	2.8
1.5	7.5	1.0	2.5	7.5	1.3
1.5	8.5	1.0	2.5	8.5	1.0
1.5	9.5	1.0	2.5	9.5	1.0
1.5	10.5	1.0	2.5	10.5	1.0
1.5	11.5	1.0	2.5	11.5	1.0
1.5	12.5	1.0	2.5	12.5	1.0
1.5	13.5	1.0	2.5	13.5	1.0

Waves can influence the stability of a ship and, in some cases, lead to extreme situations like ship or sinkage damage. Waves will always exist, so it is important to predict the different situations that may appear when the ship will be at sea operating. The designs will be tested in three different wave heading; *head sea*, *quartering sea* and *beam sea*. Biran & López-Pulido (2013) explains that beam seas are when the crests of the wave are parallel to the ship. Beams sea is often referred to as the most dangerous condition because it can cause a large angle of heel. A large angle of heel can create loads that get loose and expose stability. In beams sea the

possibility for creating excessive roll is known. Also, there is a risk of getting breaking waves over the side of the boat, which can be very dangerous. In head seas, the waves are traveling against the ship. Quartering seas is a combination of beam and following seas and is known as one of the most critical conditions to operate a ship in. Table 4.2 shows the three different wave headings in degrees.

Table 4.2: Wave headings used in experiment of numerical calculations

Heading	[°]	Critical motions
Head	0	Heave and pitch
Quartering	45	Heave, roll and pitch
Beam	90	Heave and roll

4.2   Relative motion and relative velocity

One limiting criterion for the operation is the relative motion between the ROV and the USV. This is important to assess the chance of impact between the two objects before and after launch and recovery. The relative motions are considered as the motion between one object regarding one other moving object. When the relative motion is equal to zero, it means that there is no danger for the hull and ROV to interact. The goal is then to have the amplitude between the hull and ROV as small ass possible. In Equation 4.1, the linear motion in its six DOF is shown. The equation can be used when the relative motion between the hull and the ROV is of interest.

The displacement to an object is defined as:

$$\eta_j = \eta_{jA} * sin(wt + \varepsilon_{jA}) \tag{4.14}$$

From Equation 4.14 the relative motion between the hull and ROV can be defined as:

$$\eta_{3r} = \sqrt{\left(|\eta_{3rov}|\sin\left(\varepsilon_{rov}\right) - |\eta_{3hull}|\sin\left(\varepsilon_{\text{hull}}\right)\right)^2 + \left(|\eta_{3rov}|\cos\left(\varepsilon_{\text{rov}}\right) - |\eta_{3\text{hull}}|\cos\left(\varepsilon_{\text{hull}}\right)\right)^2} \tag{4.15}$$

When the displacement is known the relative velocities amplitude can be found. The relative velocity amplitude is a significant parameter in combination with the relative motion. By differentiate Equation 4.14 the velocity be defined as:

$$\dot{\eta} = w * \eta_{jA} * cos(wt + \varepsilon_{jA}) \tag{4.16}$$

The relative velocity amplitude can be expressed as:

$$\dot{\eta}_{3r} = \omega\sqrt{\left(|\eta_{3hull}|\sin\left(\varepsilon_{\text{hull}}\right) - |\eta_{3rov}|\sin\left(\varepsilon_{\text{rov}}\right)\right)^2 + \left(|\eta_{3rov}|\cos\left(\varepsilon_{\text{rov}}\right) - |\eta_{3hull}|\cos\left(\varepsilon_{\text{hull}}\right)\right)^2} \tag{4.17}$$

In section 3.3 the ROV vertical velocity was found to be $< 1.0m/s$. To avoid collision between

the ROV and vessel the following operational criteria is established:

$$\text{Vessels relative vertical velocity} < \text{ROV relative vertical velocity} \qquad (4.18)$$

This means that the relative vertical velocity needs to be less than around $1 \; m/s$ to avoid any unwanted situation.

4.3 Piston-mode resonance

The SWATH and the monohull with the moonpool have one phenomenon that can occur and must be studied in the design process. The phenomenon is referred to as piston-mode resonance. Faltinsen & Timokha (2009) describes sloshing in external flow. Sloshing can, for example, occur in confined liquid spaces with a free surface in the external flow of a ship. Resonance oscillations between hulls of a SWATH or in a moonpool is an example of where these oscillations can arise. Far-field waves can be generated since the confined space is a part of the ship's external water domain. This will cause wave radiation damping of the resonance oscillation. The piston mode resonance frequency can be calculated by using Equation 4.19. Figure 4.2 describes the different parameters used in Equation 4.19.
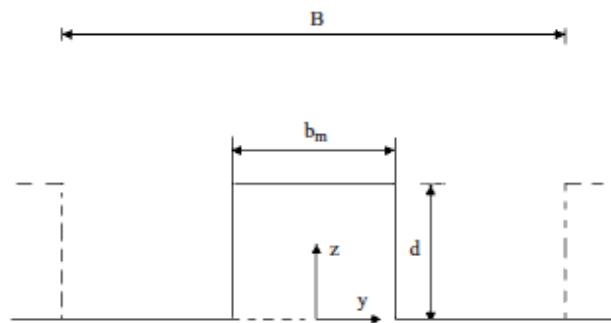
Figure 4.2: Definitions used to describe piston-mode resonance between two hulls (Faltinsen & Timokha (2009))

$$\omega_n = \sqrt{\frac{g}{d}} \sqrt{\frac{1}{1 + \frac{b_m}{\pi t}\left(1.5 + \ln \frac{B}{2b_m}\right)}} \qquad (4.19)$$

where d is the draught, b_m is the distance between the two hulls and B is the beam of the ship. As stated above there may occur piston mode resonance for the SWATH. Figure 4.3 illustrates what parameters that will be used to calculate the piston mode resonance, since the transverse section of the SWATH is slightly different from the monohull.
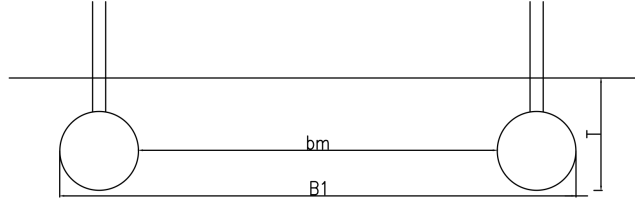
Figure 4.3: Definitions used to describe piston-mode resonance for the SWATH

The piston mode resonance for the SWATH can be calculated as

$$w_{n_S} = \sqrt{\frac{9.81}{2.90}} \sqrt{\frac{1}{1 + \frac{8.20}{\pi \cdot 2.9}\left(1.5 + \ln\frac{11.80}{2 \cdot 8.20}\right)}} = 1.28 \tag{4.20}$$

$$T_{n_S} = \frac{2\pi}{1.28} = 4.90s \tag{4.21}$$

The piston mode resonance for the monohull with moonpool can be calculated as

$$w_{n_M} = \sqrt{\frac{9.81}{3.90}} \sqrt{\frac{1}{1 + \frac{3.00}{\pi \cdot 3.9}\left(1.5 + \ln\frac{7.00}{2 \cdot 3.00}\right)}} = 1.34 \tag{4.22}$$

$$T_{n_M} = \frac{2\pi}{1.34} = 4.70s \tag{4.23}$$

The calculations above shows that piston mode resonance can occur for the SWATH for piston mode period $T = 4.90$ s and it can occur for the monohull with moonpool with the piston mode period $T = 4.70$ s. The piston mode resonance for the monohull is slightly lower than the SWATH.

Chapter 5

Experiments

Experiments have been performed on the SWATH model, presented in subsection 3.2.2, to assess seakeeping abilities as compared to the monohull. Due to time constraints, experiments are performed only on the SWATH and Kongsberg Maritime will conduct experiments on the monohull in Spring 2020. Experiments also serve to complement the numerical analysis performed using WAMIT. This chapter will describe the procedure of planning, executing, and post-processing of the seakeeping experiments of the SWATH with and without a ROV.

Seakeeping experiments in zero forward speed were conducted on the SWATH model in regular and irregular waves for three different wave headings (0 °, 45°, and 90 °). The experiments were performed in the extended part of the towing tank at SINTEF Ocean, Trondheim. The extended part of the towing tank is 85 m long, 10.5 m wide and has a depth of 10 m.

The experiments are divided into two phases:

Phase 1 The model was tested with two fin sizes in various waves and headings (April 2020)

Phase 2 The model was tested in bare hull condition without any fins and with the ROV fixed to the hull (May 2020)

section 5.1 descirbes the details of the SWATH model. Further in section 5.2 the setup of the experiments is describes, section 5.3 presents the different parameters and section 5.4 describes the different tests performed, respectively. Finally, data analysis and possible error sources are addressed in section 5.5 and section 5.6.

5.1   Ship Model

The model to full scale ratio is 1 : 18, and the particulars of the model are provided in Table 5.1. The model was designed such that the stabilizer fins could be taken on and off, and the ROV could be easily be mounted to the top of the model. The end portion of the bosses was made

such that they can be unscrewed to load ballast. In the middle of the aluminum tubes center tubes are inserted so that they can be filled with ballast.

To understand the effect of damping and stabilizing fins, two fin sizes were tested. Stabilizer fins were placed in the aft and fore part of the model in the experiment. The model were also tested a box-shaped, neutrally buoyant, ROV fixed to the model. The dimensions of the ROV in model scale is presented in Table 5.3 and is illustrated in Figure 5.1. Two fin sizes with different sizes were tested in the experiment in phase one, to understand th effect of fin sizes on vessel's seakeeping behavior. The dimension of the fins in the model scale is presented in Table 5.2. Each test condition were tested for three wave headings; head (0°), beam (90°) and quartering sea (45°).

Table 5.1: Main properties of the ship model with scale 1 : 18

Model Particulars	Value	Unit
Scale	1 : 18	-
Breadth	0.60	m
Length	1.68	m
Depth	0.31	m
Draft aft, TA	0.16	m
Draft fore, TF	0.16	m
Displacement, total	30.06	kg

Table 5.2: Dimensions and details of stabiliser fins in model scale

Type	Aspect Ratio	Span	Root Chord length	Tip Chord length	Unit
Fin 1	1.25	0.0813	0.0712	0.0575	m
Fin 2	2.00	0.0813	0.0712	0.0356	m

(a) Aspect ratio 1.25
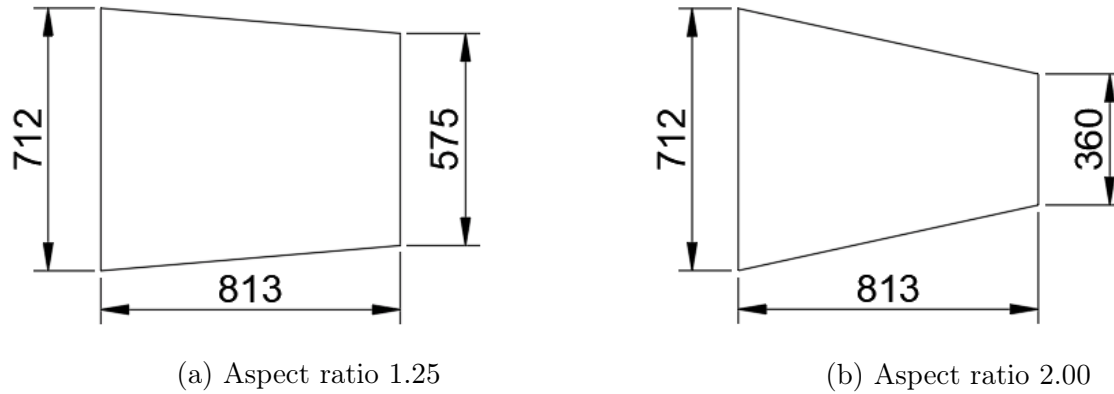
(b) Aspect ratio 2.00

Figure 5.1: Illustration of the stabiliser fin used in the experiment with aspect ratio 1.25 and aspect ratio 2.00. The dimensions is shown in mm in the illustrations.

Table 5.3: ROV dimensions in model scale

Parameters	Value	Unit
Length	0.119	m
Height	0.067	m
Width	0.067	m

Figure 5.2: Model in the extended part of the main towing tank at Sintef Ocean in Trondheim, Norway. Here equipped without stabiliser fins and the ROV. The model is equipped with marker spheres to measure six DOF using Oqus and three accelerometers. The model is moored with four horizontal mooring lines.

5.2   Experimental Setup

The model is equipped with three body-fixed wave probes and three accelerometers, as shown in Figure 5.3. Table 5.4 gives a detailed description of the type and location of the accelerometers. There were also three wave probes outside the model in the towing tank, as illustrated in Figure 5.4. To measure the ship's motion in its six DOF, Oqus position system was used.

Table 5.4: Description of location and type of accelerometers used in the experiment fixed on the body

Name	Type	Location
Acc 1	Three-Axis	Starboard Midship
Acc 2	Vertical	Port Aft
Acc 3	Vertical	Port Fwd

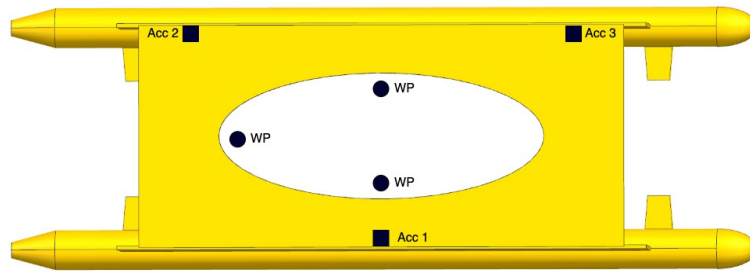Figure 5.3: Placement of wave probes and accelerometers on the SWATH in the seakeeping experiment

Soft mooring lines were used to help the model to maintain heading (0°, 45° and 90°) and to prevent large surge, sway, and yaw motions. The springs were connected to the model and attached to the tank's sidewalls by using wires. The spring stiffness was designed to have large natural periods associated with the spring system. For the three wave headings, the location of the moorings on the tank side was fixed, and the length of the wires was modified according to the wave heading, as shown in Figure 5.5. The length of the mooring lines in head sea is estimated to be 7 meters, and in beam sea, the length changes to 6.7 meters. The model was moored with four horizontal mooring lines, each with the stiffness of 33, 32, 31, and 33 N/m. The pre-tension of the mooring lines is $2-3$ N.

5.2.1   ROV connected to ship model

In phase two of the experiments, the aim was to measure the forces on the ROV and how it would impact the motions of the SWATH in regular and irregular waves in three different headings. The ROV was mounted to the model, which means that the ROV moves with the vessel. It will give an essential understanding of how the forces are influencing the ROV in different wave periods. The ROV was made as a box-shaped block of plastic/fiber. The ROV
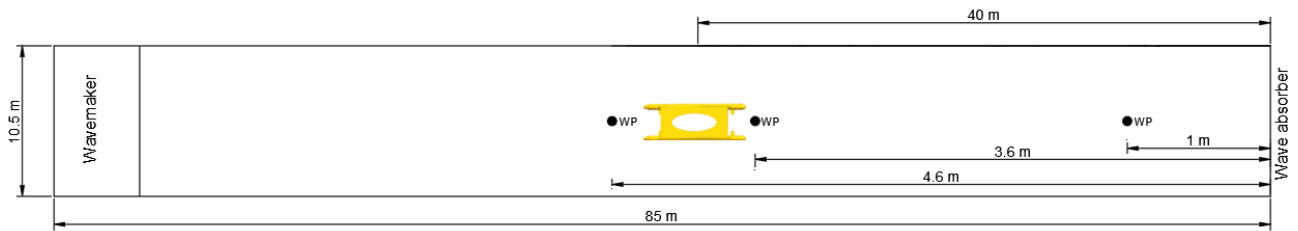
Figure 5.4: Illustration of bird's eye view of the end part of the towing tank with the location of the wave probes outside the model. In the towing tank there is a wave maker at the end and on the opposite end there is a wave absorber.
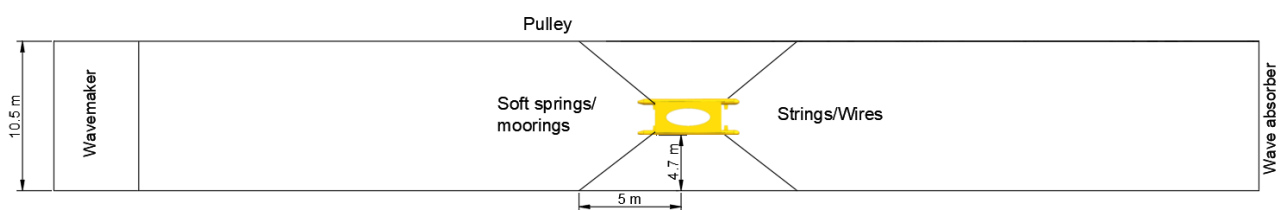
Figure 5.5: Illustration of the model moored in head sea

was fixed to the hull by vertical supports, which was connected to force transducers. Figure 5.6 shows the geometry of the ROV and how the ROV was mounted to three vertical tubes. On top of the tubes, force transducers are attached that measures the heave force on the ROV. Figure 5.7 shows the ROV mounted to the SWATH model in phase 2 of the experiments.

Figure 5.6: ROV that were fixed to the model in phase two of the experiment

Figure 5.7 shows the ROV when it is fixed to the model in the experiment. Also, stabiliser fins are shown in this figure.
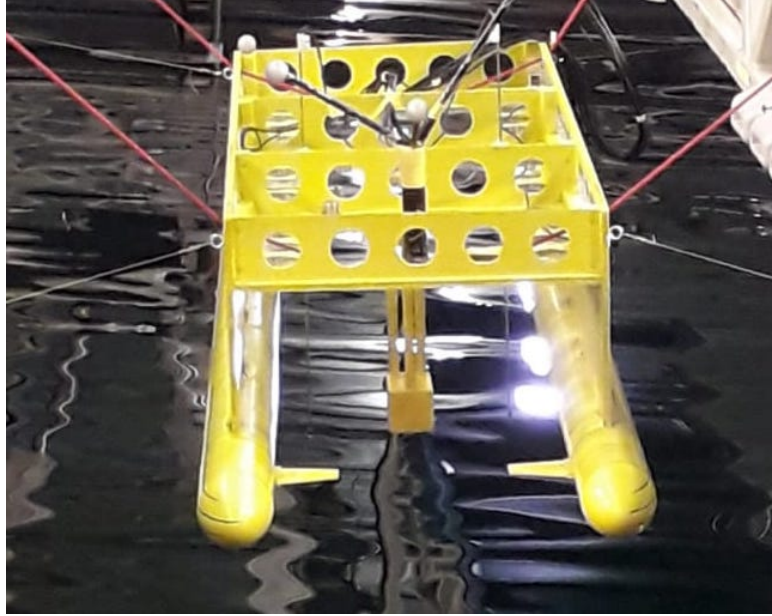
Figure 5.7: Setup of ROV mounted to the ship hull with stabiliser fins in phase 2 of the experiments

5.3   Experimental Parameters

The experimental parameters used in the experiments are presented. Table 5.5 presents the regular wave parameters used in the experiment and Table 5.6 presents the irregular wave parameters used in the experiments. In the experiment, there are different conditions tested to evaluate the operability for the SWATH model. Table 5.7 and Table 5.8 presents the test matrices for regular and irregular waves.

Table 5.5: Regular wave parameters used in the experiment

T [s]	H [m]	λ [m]	k	Wave steepness
0.900	0.020	1.264	4.97	0.05
1.000	0.025	1.559	4.02	0.05
1.300	0.042	2.636	2.38	0.05
1.500	0.056	3.509	1.78	0.05
1.800	0.100	5.054	1.24	0.062
2.000	0.100	6.239	1.00	0.05
2.200	0.100	7.549	0.83	0.0416
2.500	0.200	9.734	0.64	0.0645
2.700	0.200	11.370	0.55	0.0553
2.900	0.200	13.117	0.47	0.048
3.200	0.200	15.971	0.39	0.039

In Table 5.5 T is the wave period, H is the wave height λ is the wavelength and k is the wavenumber.

Table 5.6: Irregular wave test parameters used in the experiment

T_P [s]	H_{m0} [m]	γ
1.00	0.10	3.30
1.30	0.14	3.30
2.50	0.20	3.30

Table 5.7: Test matrix for experiment in regular waves

Test condition	Nr of wave periods	Wave heading [deg]	Repetitions
Bare hull	7	0	1
Bare hull	9	90	1
Bare hull	7	45	-
Fin 1	11	0	1
Fin 1	9	90	1
Fin 2	8	0	-
Fin 2	7	90	-
Fin 2	6	45	-
ROV and fin 2	9	0	-
ROV and fin 2	7	90	-
ROV and fin 2	6	45	-

Table 5.8: Test matrix for experiment in irregular waves

Test condition	Nr of wave periods	Wave heading [deg]	Repetitions
Bare hull	1	0	-
Bare hull	1	90	-
Bare hull	1	45	-
Fin 1	3	0	-
Fin 1	1	90	-
Fin 2	1	0	-
Fin 2	-	90	-
Fin 2	1	45	-
ROV and fin 2	1	0	-
ROV and fin 2	1	90	-
ROV and fin 2	1	45	-

5.4 Tests

5.4.1 Wave Calibration

Wave calibration tests were performed before the seakeeping tests of the model. Calibration is done to ensure that the required wave amplitude is achieved during wave generation from the wavemaker.
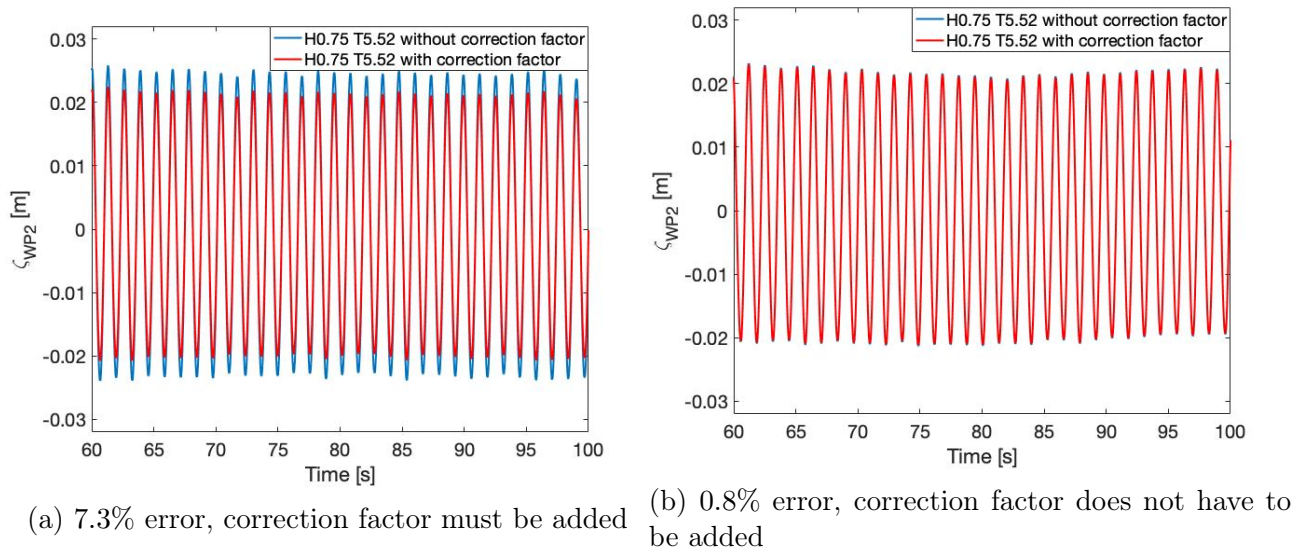

(a) 7.3% error, correction factor must be added

(b) 0.8% error, correction factor does not have to be added

Figure 5.8: Regular wave calibration with H=0.756 and T=5.52, full scale values.

Figure 5.8 shows the calibration of the same regular wave with H=0.756m and T=5.52 seconds, which are full scale values. A correction factor is implemented if the deviation of the mean experimental wave height compared to the required value is higher than 5%. The correction factor is found by dividing the input wave height by the observed wave height. The output wave height has a deviation of 7.3% for Figure 5.8a, and a correction factor of 7.3% is added to get the required wave amplitude. After application of correction factor, the wave amplitude measured can be seen in Figure 5.8b where the deviation is under 5%, and therefore correction is not applied any further.

5.4.2 Pendulum Test

To find the center of grqavity (COG) and moment of inertias (I_{xx} and I_{yy}) of the model, a pendulum test as has been performed (Huse 1994). Especially in a sea keeping test, it is important that the mass distribution is correct. Therefore, the pendulum test was conducted to determine the COG and the radius of gyration in pitch and roll. During the process, the total mass of the model was also measured.

SINTEF Ocean recommended procedure for the pendulum test says that in theory, the test

needs to be conducted at two heights, as described by Ravinthrakumar (2020). The COG and moment of inertia I, which are unknown and need to be found, are determined given τ at two different heights. Below a simplified analysis is described how the unknown parameter can be found.

The pendulum test is performed on the cradle at two different heights (lower knife and upper knife). This was done so that the moment of inertia in pitch and roll and COG of the platform was established. The orientation of the model on the cradle must be changed for pitch and roll moments of inertia. Table 5.9 shows the results from the pendulum test performed at Sintef Ocean. The full report made by Sintef Ocean of the pendulum test is attached in Appendix A.
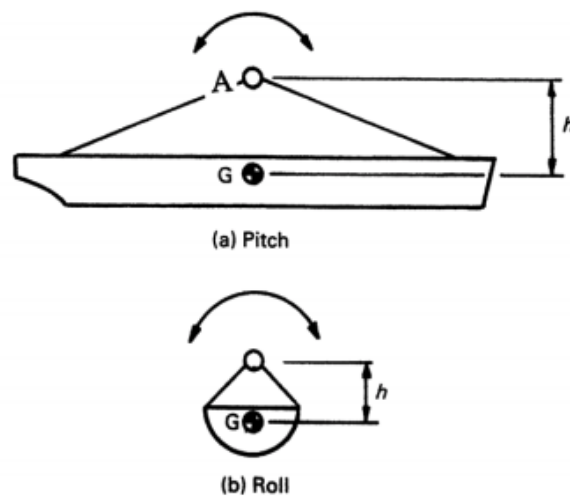

(a) Pitch

(b) Roll

Figure 5.9: Sketch that shows the principle of the pendulum test by Steen (2015)

The period of a physical pendulum is expressed as:

$$T_0 = 2\pi\sqrt{\frac{I}{Mgh}} \tag{5.1}$$

where M is the mass of the model, h is the distance form point A to the COG and acceleration due to gravity is g. The period of a physical pendulum comes from:

$$4\pi^2 I - MgT_0^2 h = 0 \tag{5.2}$$

Firstly, the period of oscillation of the pendulum, T_0 is measured. Secondly, two weights with mass m, are placed at each end of the pendulum. They are placed with a distance a from the rotation center A. After the two weights are added, the pendulum period T_1 can be found. Same as for Equation 5.2 the equation can be written as

$$4\pi^2(I + \Delta I) - (M + 2m)gT_1^2(h + \Delta h) = 0 \tag{5.3}$$

where $\Delta I = 2ma^2$ and $\Delta h = \frac{2mh}{(M+2m)}$. With the expressions of I and Δh on can insert it in

Equation 5.3 and can write

$$4\pi^2\left(I + 2ma^2\right) - MmgT_1^2h = -8\pi^2ma^2 \tag{5.4}$$

With the two unknown I and h, they can be written as

$$h = \frac{8\pi^2ma^2}{Mg\left(T_1^2 - T_0^2\right)} \tag{5.5}$$

$$I = \frac{2ma^2T_o^2}{T_1^2 - T_0^2} \tag{5.6}$$

When calculating the h and I the moment of inertia of the model, I_m, which referring to the COG, can be written as

$$\mathrm{I_m} = I - Mh^2 \tag{5.7}$$

Table 5.9: Results from pendulum test for pitch and roll

	Pitch	Roll	Unit
Moment of inertia about COG	2.110	6.858	kgm^2
KG	0.102	0.100	m
Radii of gyration	0.265	0.478	m

5.4.3 Free decay tests

Free decay test for the fully ballasted model was conducted for heave, roll, and pitch motion in calm water. The results from the decay test gave important information about the natural frequency and damping of the system. Since the free decay test of a ship model can be challenging to get accurate, the free decay test was performed two to three times for each DOF. Decay test was conducted for three different conditions as shown in Table 5.10.

Table 5.10: Description of the three test conditions that were conducted in the free decay test

Condition	Description
Condition 1	Bare hull
Condition 2	Model fitted with fin type 1
Condition 3	Model fitted fin type 2 and ROV

Figure 5.10 shows the decay in roll for the SWATH model with two successfully decay tests within the same record period. The decay test in roll for bare hull was hard to conduct in the experiment as seen in Figure 5.11.

(a) Three decay tests performed for the same condition
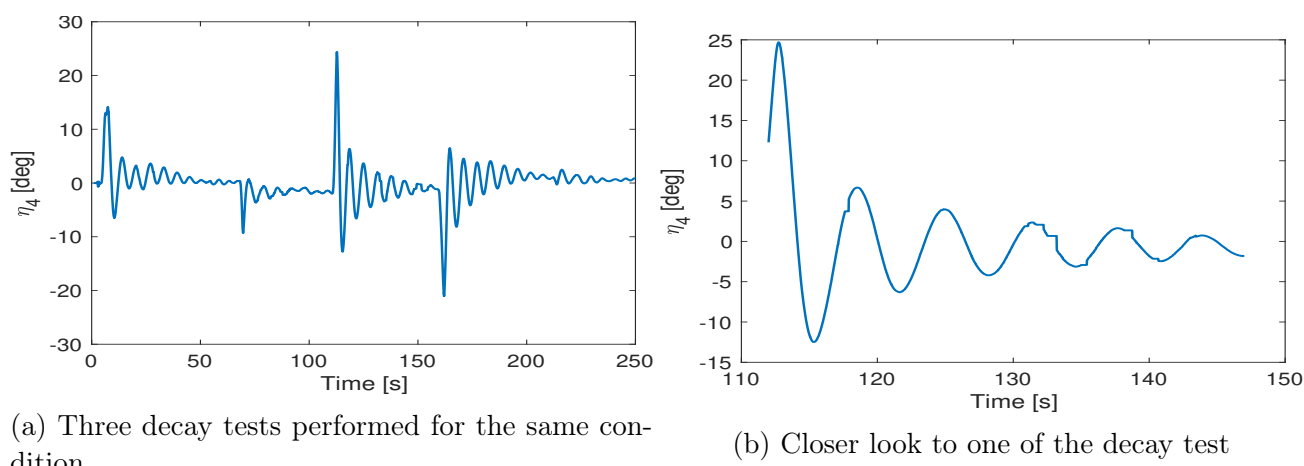

(b) Closer look to one of the decay test

Figure 5.10: Decay test in roll for model with stabiliser fins. Three decay tests were performed per test condition to get an accurate result.
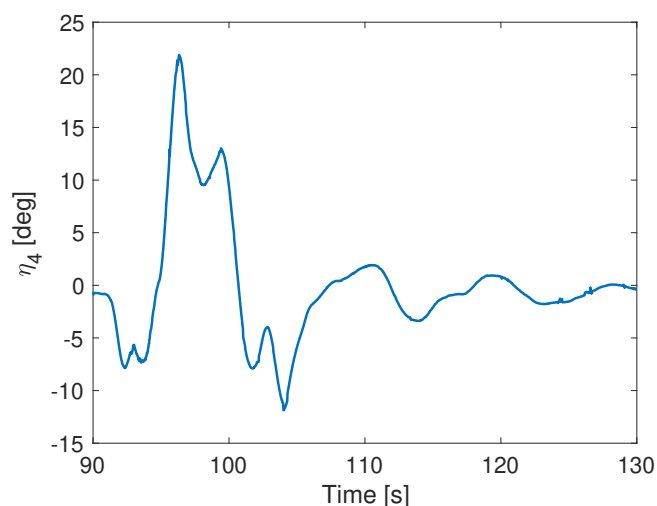

Figure 5.11: Decay test of the bare model in roll motion. We were not able to conduct reasonable decay test in roll motion.

5.4.4 Regular wave test

In the experiment, regular waves with the parameters, as shown in Table 5.5 can be used to obtain the RAOs for the SWATH model. A regular wave is generated using a wavemaker. Waves are generated by specifying wave period and height using which an in-house software provides sinusoidal input calculated from wavemaker theory. One can, therefore, control the amplitude and steepness of the wave. When generating regular waves, one can find the amplitude and phase of the body response with respect of incoming waves, as explained by Steen (2015). Duration varied between 2-4 minutes. Waiting time between experiments was 6-12 minutes.

5.4.5 Irregular wave test

As known, irregular waves are used to represent a realistic sea state. Therefore, conducting irregular waves can give valuable information on how the vessel will behave in a given sea state. It can give valuable information on the survivability of the ship or the load impact of a ship in a given sea state. Table 5.6 shows the parameters for the irregular waves that were tested. As introduced in section 4.1.3, JONSWAP spectrum was used for the irregular wave test in the experiment:

$$S(\omega) = \frac{\alpha g^2}{\omega^5} \exp\left\{-1.25\left(\frac{\omega_p}{\omega}\right)^4\right\} \cdot \gamma^{\exp\left\{-0.5\left(\frac{\omega-\omega_p}{\sigma\omega_p}\right)^2\right\}} \tag{5.8}$$

ITTC (2014a) recommends that the model have to encounter waves more than 20 minutes of full-scale measurements to get satisfying results. The time series for the irregular waves were 45 minutes, with 20 minutes waiting time between each run.

5.5 Data analysis

Raw data obtained from the measurements on board the model, wave probes outside the model and Oqus system has to be filtered to remove noise from the instruments. Following this Fast Fourier transform (FFT) was used to transform the time series into the frequency domain. FFT is an efficient computational technique for evaluating the discrete Fourier transform. It gives the amplitude and phase of the response at the measured wave frequency, and the primary period (T) of the signal is determined. The sampling frequency of the FFT is set to 200 Hz. Figure 5.12 is an example of how the FFT is performed. Here, shown for regular wave with $H_s = 0.02$ m in head sea.

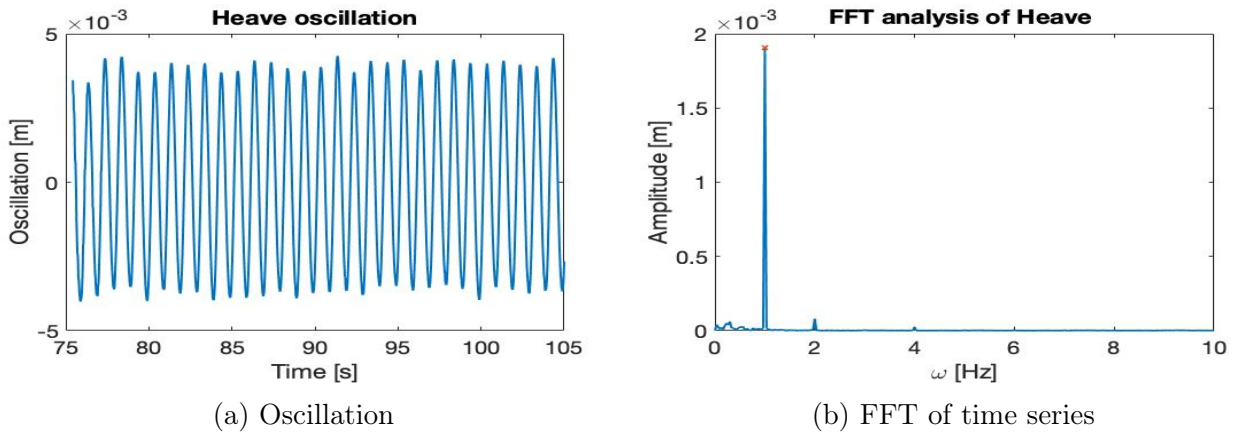(a) Oscillation   (b) FFT of time series

Figure 5.12: Example of how the FFT is performed

5.5.1 Regular wave data

For the post-processing of the regular wave data, the common ratio that shall be found in the RAO of motions and loads. The RAO or transfer function is the ratio between the response

amplitude and input wave amplitude and can be defined as:

$$RAO = \frac{Y_A}{X_A} \tag{5.9}$$

where Y_A is the amplitude from the signal output and is easily obtained from the maximal and minimal of the output signal. For the rotational motions the output is in degrees so the amplitude from the signal output also needs to be divided on the wave number and the wave amplitude from the from the harmonic wave signal. $x(t)$ is defined as the harmonic wave signal and is defined as:

$$x(t) = X_A sin(w_1 t) \tag{5.10}$$

where X_A is the wave amplitude, and w_1 is the wave frequency.

5.5.2   Irregular wave data

The RAO can also be obtained from the calculations of the spectrum from the irregular waves. When processing the measurements from the irregular test, it is advantageous to transform the measured time history $x(t)$, to the frequency domain. Transforming the history signal to the frequency domain can be done by first finding the power spectrum, S_{xx}. S_{xx} is defined as the Fourier transform of the autocorrelation function R_{xx}. The power spectrum can be expressed as:

$$S_{xx}(\omega) = \int_{-\infty}^{\infty} R_{xx}(\tau)e^{(-i\omega\tau)}d\tau \tag{5.11}$$

The next step is to find the cross spectrum between two signals $x(t)$ and $y(t)$ where $x(t)$ is the reference signal and y(t) is the measured response. The cross spectrum can be found by:

$$S_{xy}(\omega) = \int_{-\infty}^{\infty} R_{xy}(\tau)e^{(-t\omega\tau)}d\tau \tag{5.12}$$

when knowing the power spectrum and the cross spectrum the linear transfer function can be established as:

$$H(\omega) = \frac{S_{xy}(\omega)}{S_{xx}(\omega)} \tag{5.13}$$

The relation between the input wave spectrum measured at the wave probe, measure the response of the model, and the RAO is shown in Figure 5.14. The power spectrum densities (PSD) is established by using the current source density function in MatLab, where the sampling frequency is set by 1/0.005. An example of the raw measured response signal is shown in Figure 5.13. The input spectrum, which is measured at the wave probe, the output spectrum, which is the response of the model, and the response function is shown in Figure 5.14c.
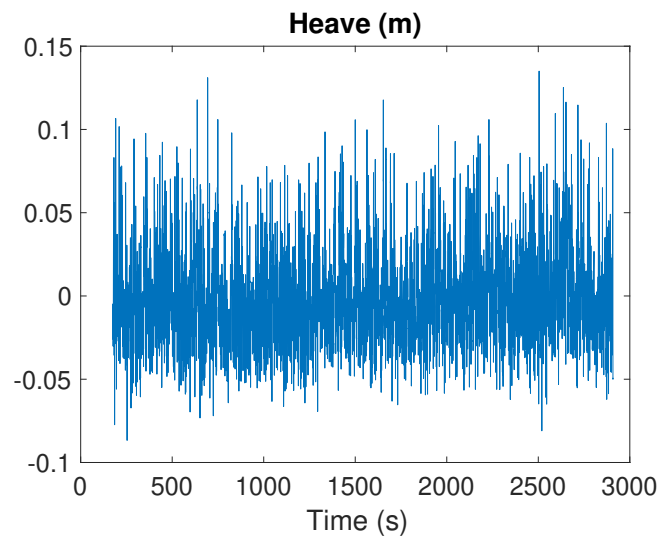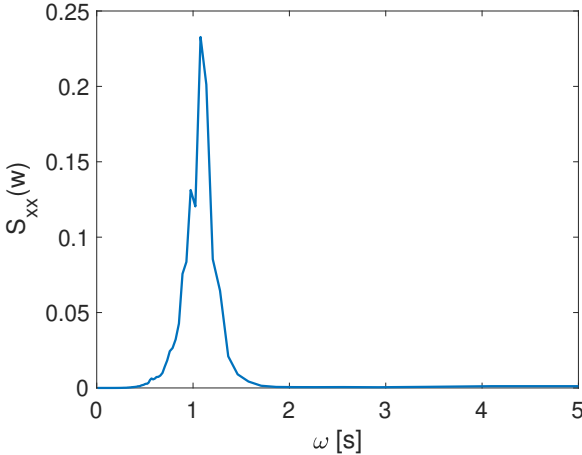
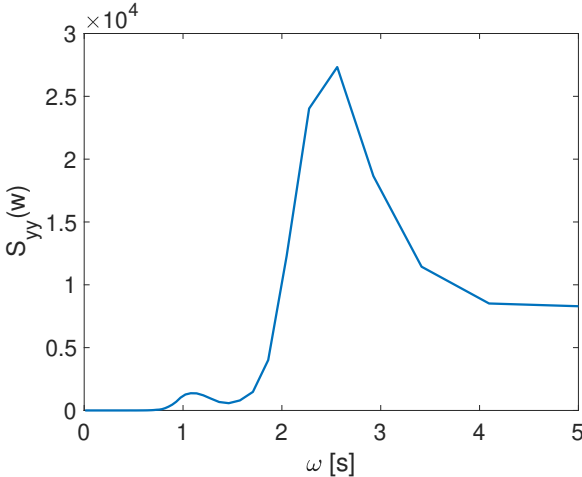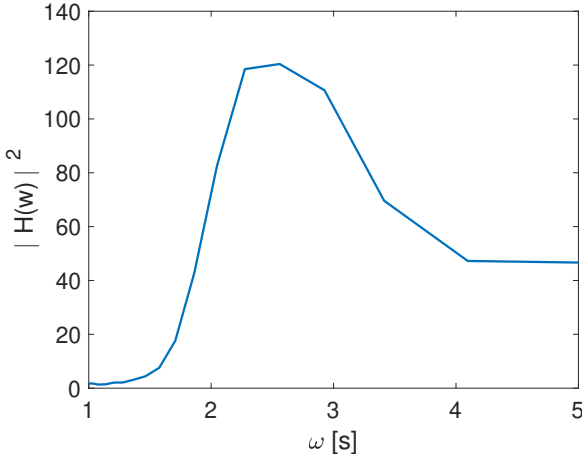Figure 5.13: Measured heave response for bare hull in beam sea for irregular waves

(a) Input spectrum

(b) Output spectrum

(c) Response function, RAO

Figure 5.14: Calculation of the response function, which gives the natural period of the system. It shows the relation between the input spectrum measured at the wave probe, the output spectrum measured from the motions of the model and the response function which is the RAO.

The irregular wave is tested for $T_p = 1.0$, $T_p = 1.3$ and $T_p = 2.5$ values as shown in Figure 5.15.
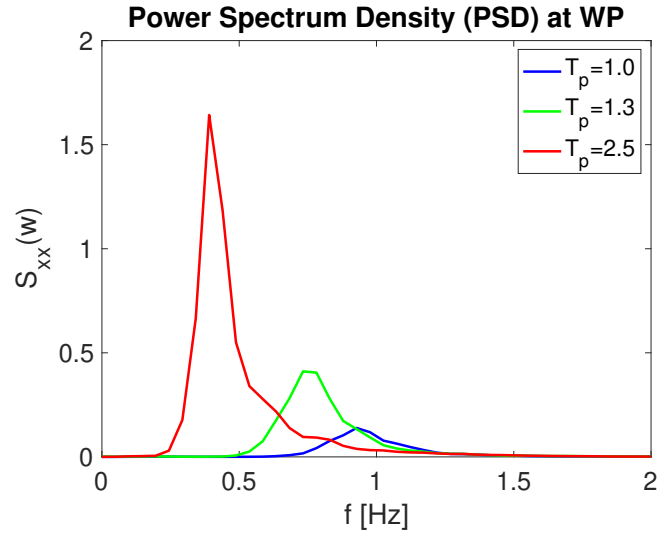
Figure 5.15: Power spectrum density measured at the wave probe for different periods, $T_p = 1.0$, $T_p = 1.3$ and $T_p = 2.5$.

5.5.3 Heave force on ROV

As explained and illustrated in subsection 5.2.1, the ROV has force transducers that measured the vertical heave force on the ROV. The transducers' values are given in the model scale, so the force shall not be scaled when processing the data. To find the total heave force on the ROV, the force on all the three transducers are summed up. The total force is obtained by summing up the force signals from the three transucers. Figure 5.16 shows the individual force signal from the three transducers. The total force is found by $F_{Total} = F_1 + F_2 + F_3$. The phase and amplitude to each force transducers can have different amplitudes and phases.
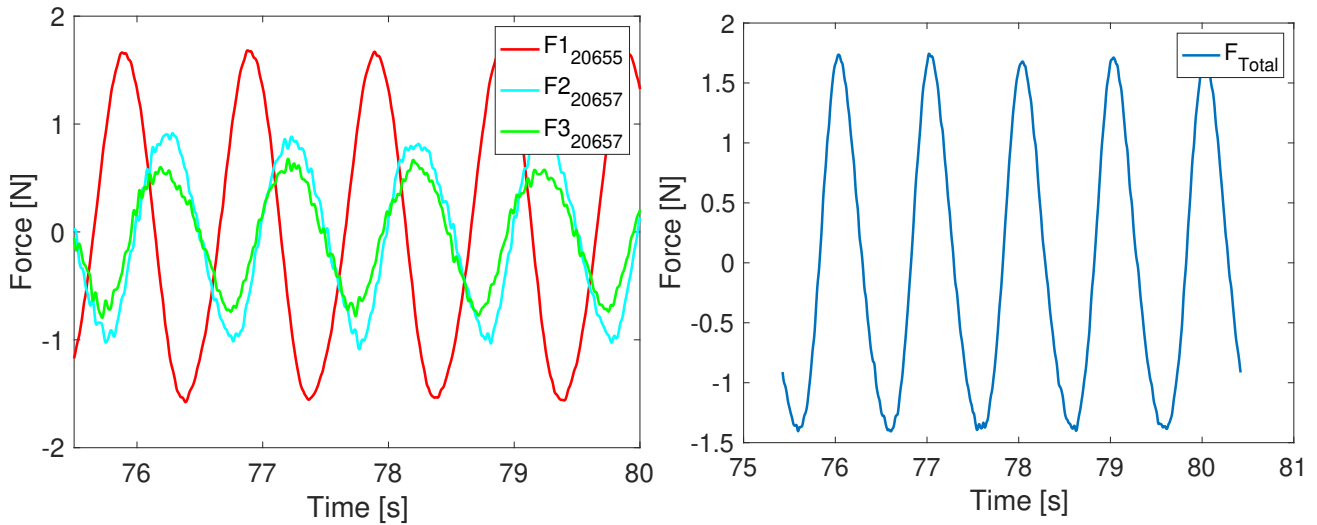
(a) Signal showing the three force transducers and how they are varying in amplitude and phase

(b) Total heave force by summing all the three forces

Figure 5.16: Plot of individual force transducers that were attached to the ROV and the total heave force

5.6 Sources of error

When doing an experiment it is desirable that the experiment represents the model in real conditions. There can be errors arising from various phenomena during experiments. These have to be minimized. Therefore, it is essential to have a good test plan and be aware of the possible error sources affecting the experiments. First, it is essential to identify all error sources to limit the uncertainty of the experiment. The primary sources in the model test are listed below.
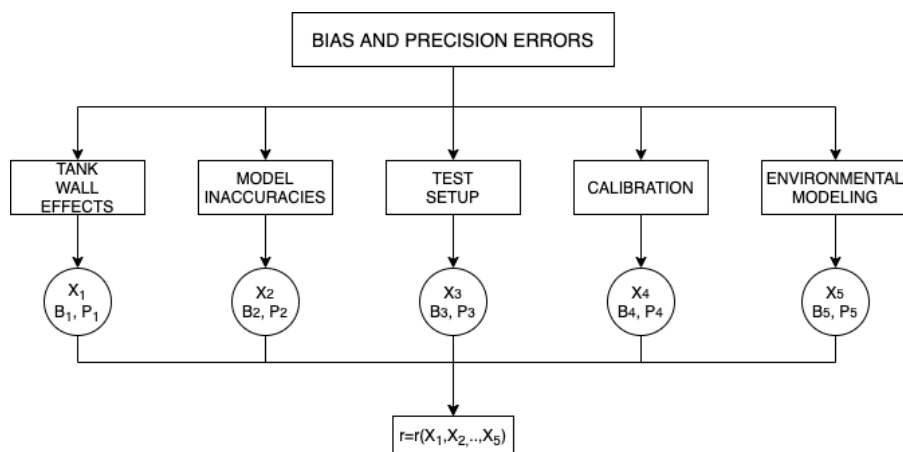

Figure 5.17: Errors due to interaction in seakeeping model tests

Tank wall effects

Figure 5.17 identifies the primary bias and prediction errors in the seakeeping experiment of the SWATH. A towing tank has a limited width and length. Due to the limited width, tank wall effects, or sidewall effects, a vital bias error can impact the results when running zero speed tests in a towing tank. It is not only the width of the tank that determines the side wall effects. Yuan et al. (2018) explains that the geometry of the model, depth of the tank, and forward speed of the model also impact the tank wall effects. In the experiments, there will be zero forward speed. In the twenty-first towing tank conference, Messalle (1987), stated that when testing ships at slow or zero speed, the results will be affected by large experimental scatters due to thank wall effects. This will create wave reflections from the moving model because of radiated and diffracted waves by the model. To minimize the wave reflection problem for zero and low speed can be done by keeping the small model relative to the size of the basin or width of the tank. In some basins, there are also installed effective wave damping devices. Table 5.11 provided details about the error quantification for the instruments used in the test.

Reflections from beaches

Another source of error can be wave reflection from the beach. The wave reflection in this experiment has not been calculated.

Model inaccuracies

Model inaccuracies are a more distinct and understandable error that is related to the model. First of all, if the shape of the model is inaccurate, it will give a wrong result of the full-scale hull. It is, therefore, important that the production of the model is correct. In an experiment, the model often needs to be ballasted to achieve the required draught. Error due to inaccurate draught can be minimized by ballasting to correct weight, not to the specified draught. It is also crucial that the model surface is not too rough.

Meniscus effect

Faltinsen & Timokha (2009) explained the error source named meniscus effect could appear for the measured wave elevation due to the steel wires that the wave probes are made of. The meniscus effect can cause an error if the measured wave elevation is less than the diameter of the steel wire.

Calibration

The test setup can influence the results. First of all, the right equipment has to be used to ensure that the measurements wished to measure, gets measured. Moffat (1988) describes that errors in measurement systems can arise, for example, in the strain gain, ripple in power supplies, or drift due to temperature changes in the instrument. Calibration procedures should be implemented to minimize measurement errors during the experiments. Errors due to environmental modeling

is a factor that needs to be accounted for. Wave parameters and spectral shape are the two essential factors. It is, therefore, important to always calibrate the waves used in the experiment. The result of the calibration can then be used instead of specific waves.

Oqus system and accelerometers

The model was equipped with three Oqus markers. For heave, RAO significant variance was shown in the uncertainty analysis. This must come due to fault in the measurement from the Oqus system.

Repetition test

Repetition tests were only carried out for regular waves, as shown in Table 5.5, with one repetition for four different test conditions, due to limited time. Repetitions test should be carried out for both regular and irregular test for five repetitions to get an accurate result.

Table 5.11: Error/uncertainty for the instruments used in the experiment

Instrument	Error/Uncertainty	Unit
Wave Probes	0.001-0.002	m
Accelerometers	0.05-0.1	m/s^2
Oqus system	1	deg °
Oqus system	0.01-0.02	m

5.6.1 Calculation of precision error

The error in an experiment can be described as the difference between the real results and the test results. It is difficult to predict the error, and it is a sum of bias (systematic errors) and precision (random errors) sources. The bias and precision error can be estimated with a confidence level of 95%. Five runs are often the recommended amount of repeated runs to get a proper uncertainty analysis. As presented in Table 5.7, one additional set of repetitions were conducted for four different test conditions. The repetitions were done to check the uncertainty and repeatability of the experiment. Unfortunately, repetition of all periods was not performed due to limited time available in the tank.
ITTC (2014b) gives a guide to the expression of uncertainty in experimental hydrodynamics. For standard uncertainty, the best available estimate of the expected value of a batch "q" that alter randomly for "n" observations. From this, the mean or average is expressed as:

$$\bar{q} = (\frac{1}{n}) \sum_{k=1}^{n} q_k \tag{5.14}$$

n is the number of observations that have been done during the experiment. The number of observations depends on how many repeated tests that get performed during the experiment. When the test is repeated, a standard deviation can be found. ITTC (2014b) suggests that

at least ten repeated test needs to be performed to get a reasonable estimate of the standard deviation. Repeated tests are expensive and time-consuming. Therefore, typically about five repeated runs are performed.

When the mean or average value if found the experimental variance of the observation can be calculated. This estimates the variance, s, of the normal probability distribution of "q":

$$s = \sqrt{[\frac{1}{n-1}] \sum_{k=1}^{n} (q_k - \bar{q})^2} \tag{5.15}$$

In experiments correlation is often mentioned. In a stationary time series, the uncertainty is dependent on the correlation which is white noise. In a situation where there is no white noise, the standard uncertainty can be expressed as:

$$u(\bar{q}) = \frac{s}{\sqrt{n}} \tag{5.16}$$

When having a series of measurements which has given a mean value, standard deviation and that one measurement has given a large deviation, δ, from the mean value. One can then choose a criterion for disregarding the the measurement that the probability of exceeding δ with one of the measurement in the series (Huse 1994). When having n measurements the probability that one of them will exceed the given boundary is

$$p = n(1 - A) \tag{5.17}$$

A traditional choice is to set $p = 0.5$ and one have the criterion for disregarding the measurements by
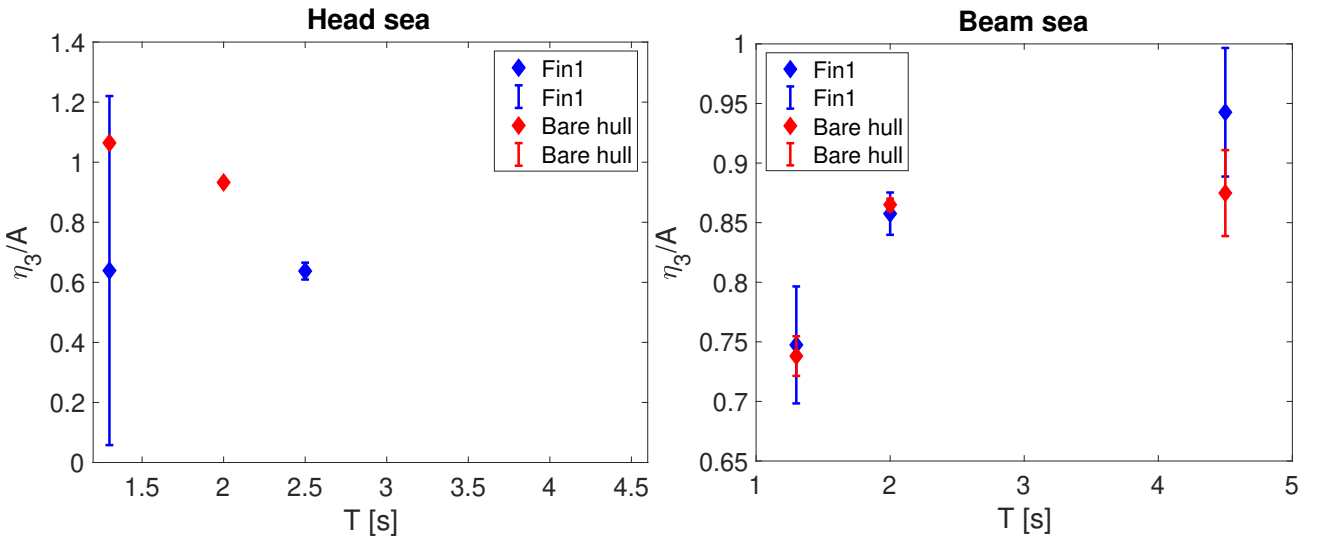
$$A = \frac{n - p}{n} \tag{5.18}$$

Figure 5.18: Standard deviation with mean values as a function of heave RAO for bare model and model with fin type 1 in regular waves

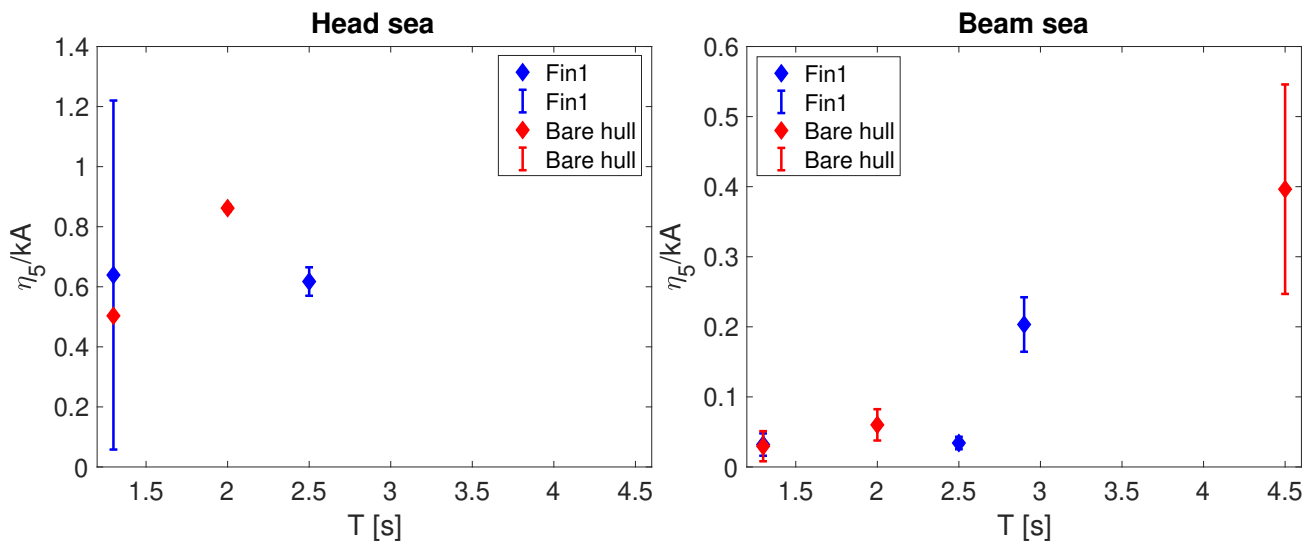Figure 5.19: Standard deviation with mean values as a function of pitch RAO for bare model and model with fin type 1 in regular waves

Figure 5.18 shows a large standard deviation for heave motion, especially for head sea. The error is linked ether to phase 1 or phase 2, where some faults in the measurement of heave motion must have been wrong. A standard deviation of 0.58 is found for $T = 1.3$ s.

Chapter 6

Results

This chapter will present the results from the experiments and the numerical simulations done in WAMIT. First, the results from the experiments on the SWATH is presented. Next, the two different designs' motion characteristics and operability of the ROV will be compared.

6.1 Experimental results

In this section, the results from the experimental work are presented. Different analyses have been performed for regular and irregular wave tests to understand the motions of the SWATH in different conditions. There were no unexpected phenomenons that exceeded during the experiment.

6.1.1 Estimation of the natural period and damping coefficients from decay test

The natural damping period is found by taking FFT of the measured damping. From the FFT, the eigenfrequency of the system is found, and the natural period is then found by the relation $T_n = \frac{1}{f}$. Faltinsen (1998) describes the method of determining the linear and quadratic damping coefficient from a free decay test. The damping coefficient can be found by assuming that the motion can be written as:

$$x + p_1 \dot{x} + p_2 |\dot{x}|\dot{x} + p_3 x = 0 \tag{6.1}$$

where p_1 is the linear damping, p_2 is quadratic damping and p_3 is the restoring stiffness. By assuming that the damping is constant with respect to the amplitude of oscillation, p_1 and p_2 can be determined from the relation

$$\frac{2}{T_{\mathrm{m}}} \log\left(\frac{X_{n-1}}{X_{n+1}}\right) = p_1 + \frac{16}{3}\frac{X_{\mathrm{n}}}{T_{\mathrm{m}}} p_2 \tag{6.2}$$

where T_m is the damping period, X_n is the amplitude of the nth oscillation. Between X_n and X_{n+1} for any n there is one half period $\frac{T_m}{2}$. By plotting the left side of the Equation 6.2 versus $\frac{16}{3}X_n/T_m$ and fitting the points to a straight line by the least square method, the damping coefficients are found.
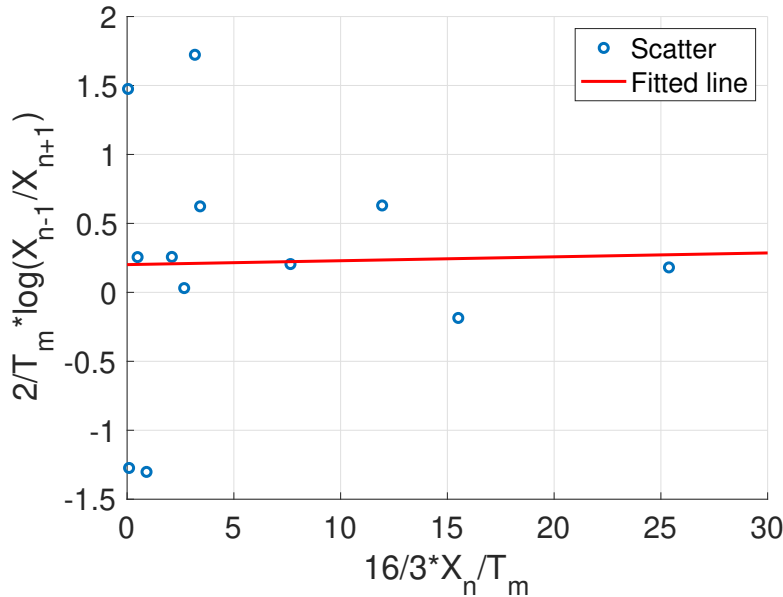

Figure 6.1: Illustration of how the linear and quadratic coefficient are obtained from the free decay test. Here presented for decay test 1 (as described in Table 5.10) in roll motion.

Figure 6.1 shows the linear and quadratic damping. The linear damping, q_1, is where the fitted linear line crosses the y-axis, and the quadratic damping, q_2, is the slope of the fitted linear line. The coefficient strongly depends on the amplitude, and as seen in Figure 5.10a, the amplitude for the same test is not equal and can strongly vary. The decay test needs, therefore, to be conducted safely and without any disturbance from the environment to get a reasonable estimate of the natural period and the linear and quadratic coefficient.

Each test was done two to three times to get an accurate result as possible. As seen in Figure 5.10, it was not easy to get the same result for each test. It was difficult for roll and pitch to obtain consistent results as the motions were quickly damped out. Table 6.1 - Table 6.3, shows the result of the calculated natural period and the damping coefficients. For the damping in heave, Table 6.1 shows that the damping in condition 2 (hull with fin 1) is higher than condition 1 (bare hull), which is reasonable since the stabilizer fins will apply more damping to the system. In condition 3, when the ROV is mounted to the hull, it is reasonable to assume that the damping would be higher than the bare hull and when fins are mounted. The damping calculated for condition three is lower than conditions one and two. Damping in heave can be hard to conduct, which in this case resulted in a quickly damped out system. In Table 6.2 its seen that the damping coefficient for condition 3 has less damping than condition 2, which seems unreasonable. When the ROV is attached, the damping should be higher than

condition 1 and 2, since that ROV will add damping to the system.

Table 6.1: Natural period for heave and linear and quadratic damping coefficient in model scale

Condition	Natural heave period T_{n3} [s]	Linear damping coefficient B_{33}	Quadratic damping coefficient B_{33}	Total damping term B_{33}^*
Condition 1	4.05	0.13	0.58	10.54
Condition 2	4.38	0.27	0.63	17.71
Condition 3	2.90	0.0056	4.90	12.78

For the calculation of the natural period and damping coefficient for roll motion is presented in Table 6.2. The damping increases from condition 1 to condition 3. The natural period is also changing as the damping increases.

Table 6.2: Natural period for roll and linear and quadratic damping coefficient in model scale

Condition	Natural roll period T_{n4} [s]	Linear damping coefficient B_{44}	Quadratic damping coefficient B_{44}	Total damping term B_{44}^* $[\frac{rad}{s}kgm^2]$
Condition 1	4.81	0.2	0.0028	0.70
Condition 2	6.3	0.027	0.717	0.75
Condition 3	4.91	0.26	0.019	0.95

The damping in pitch is presented in Table 6.3, and the damping seems reasonable as the damping is increasing from condition 1 to condition 3.

Table 6.3: Natural period for pitch and linear and quadratic damping coefficient in model scale

Condition	Natural pitch period T_{n5} [s]	Linear damping coefficient B_{55}	Quadratic damping coefficient B_{55}	Total damping term B_{55}^* $[\frac{rad}{s}kgm^2]$
Condition 1	4.18	0.013	0.24	0.77
Condition 2	4.70	0.18	0.049	2.21
Condition 3	4.00	0.17	0.00	1.98

6.1.2 RAO from regular wave test

In this subsection, the RAO calculated from the regular wave test is presented. Regular wave test is mostly used to obtain RAO's of motions, but it then needs to have sufficiently large

enough wave periods to reach the peak over the RAO's. Sinusoidal waves were tested with periods from T=0.9-2.9 s. In some cases, the period domain was not high enough to reach the natural period, so one could not define the natural period for the model in different conditions. Anyhow, interesting results were found when studying the impact of stabilizer fins on the model and when the ROV was mounted to the model.

The RAO found from the experiment for head, quartering and beam sea for the most decisive motions in each heading are presented below. The remaining DOFs not presented in this section can be found in Appendix C. Figure 6.2 presents the RAO results from the regular wave test in head sea for heave and pitch motion. For head sea, its shown that the bare hull has higher amplitudes than the hull with stabilizer fin 1 and stabilizer fin 2. In the early design stage of the SWATH, it was decided to study the effect of stabilizer fins to increase heave and pitch stability. Two fin sizes were tested to see if the size of the fins were important. Figure 6.2 shows that the RAO for fin size 1 and fin size 2 is more or less the same, and it was therefore decided to only test fin 2 in the remaining tests. In head and quartering sea, the stabilizer fins show a significantly reduced motion with stabilizer fins compared to the bare hull. It shows a slight decrease in pitch motion when comparing bare hull to hull with stabilizer fins. For quartering
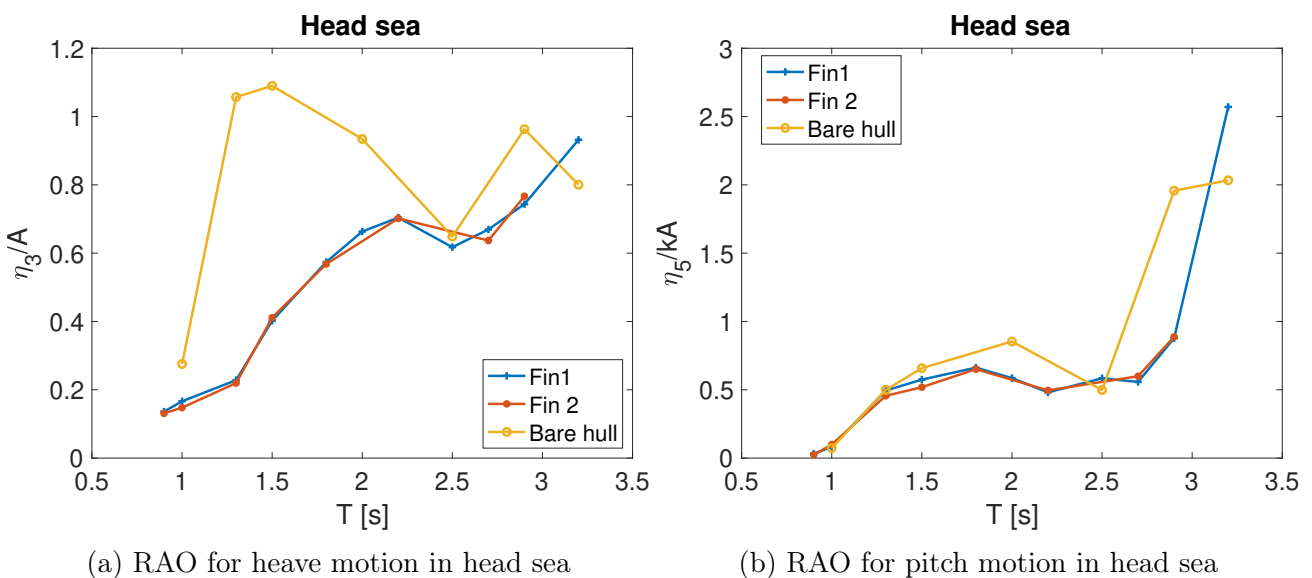

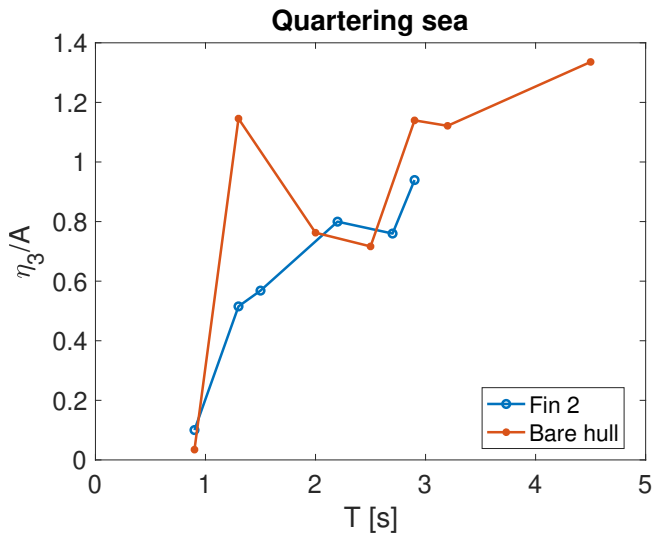(a) RAO for heave motion in head sea   (b) RAO for pitch motion in head sea

Figure 6.2: Heave and pitch RAO in head sea from experiments in regular waves
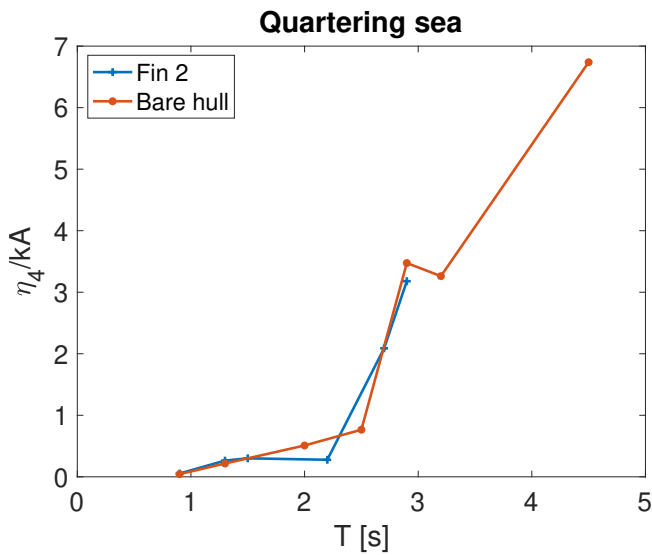
sea the bare hull were only compared against fin 2, since fin 1 were only tested in head and beam sea. Figure 6.3 shows that the fins are decreasing the motion in heave. For pitch and roll motion there are not any significant change in motion.

(a) RAO for heave motion in quartering sea
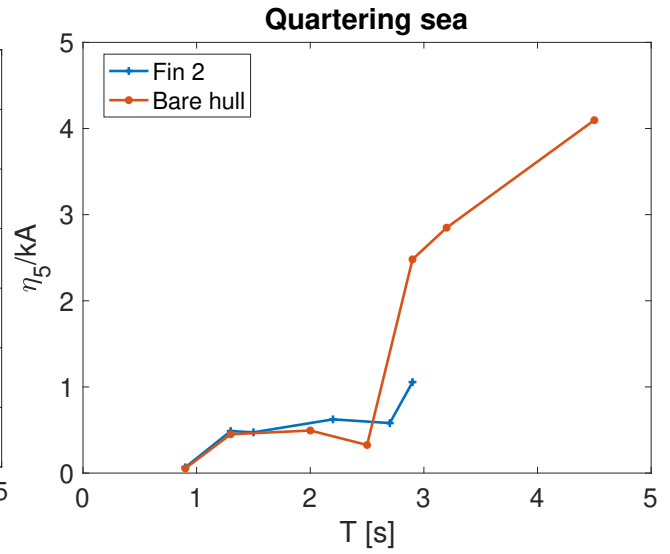
(b) RAO for pitch motion in quartering sea

(c) RAO for roll motion in quartering sea

Figure 6.3: Pitch and roll RAO in quartering sea from experiments in regular waves

Comparison of the bare hull and the hull with stabilizer fins in beam sea, as presented in Figure 6.4, shows that the motions for the three tested conditions did not vary as much as for head and quartering sea. Beam sea will give the most impact in roll motion, but it will also impact the heave motion.
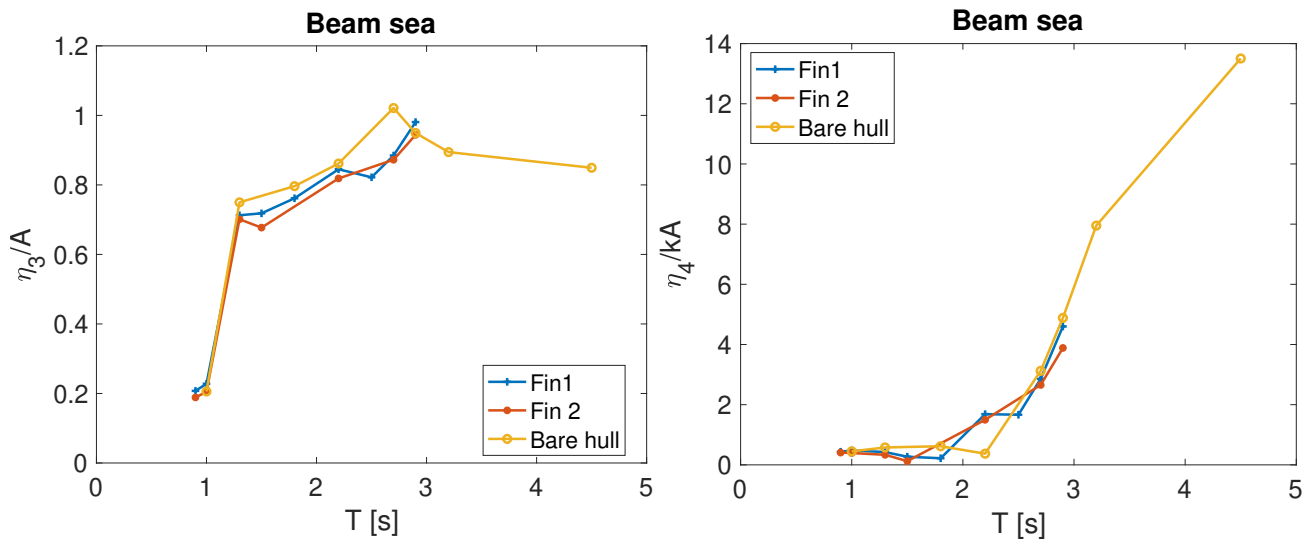
(a) RAO for model in heave motion in beam sea   (b) RAO for model in heave motion in beam sea

Figure 6.4: Head and roll RAO in beam sea from experiments in regular waves

6.1.3 Impact of ROV on the SWATH

One important aspect of the experiment was the interaction between the USV and an ROV. Due to limited time, the feasible solution was to mount the ROV to the hull. Since the ROV was mounted to the hull, it automatically stated that the ROV follows the motions to the model. It is reasonable to assume that the ROV will not impact the motions to the USV since the weight of the ROV is very small compared to the weight of the vessel. The results of the calculated RAO's for the monohull with the connected ROV shows that for all heading, the pitch and roll motion with the hull connected to the ROV is equal to the motions for the hull with fin 2. At the same time, Figure 6.5a and Figure 6.5a shows that the heave motions to the USV changed when connecting the ROV. It is not reasonable to accept the substantial changes in heave motions. As presented in Figure 5.18, a large standard deviation for heave in head sea was found for $T = 1.3$ s. When calculating the uncertainty, all cases were checked, and all data for the measurement system were the same except for heave motion. Therefore, it is conceivable that there were some faults in the measurement of heave in phase two.
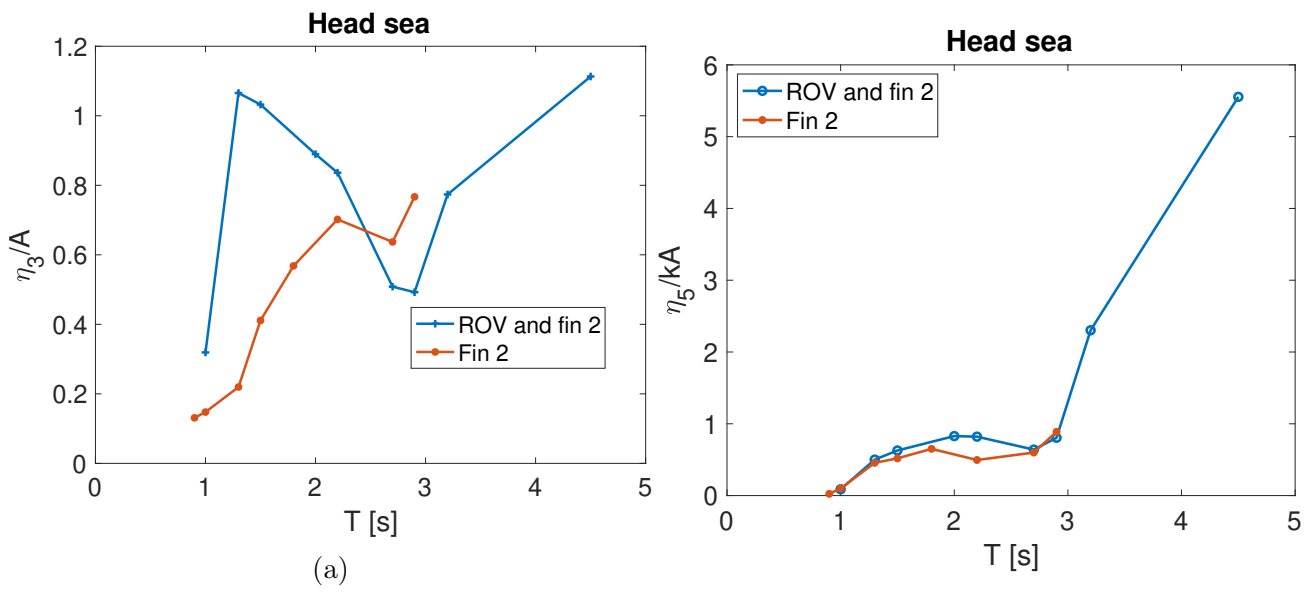
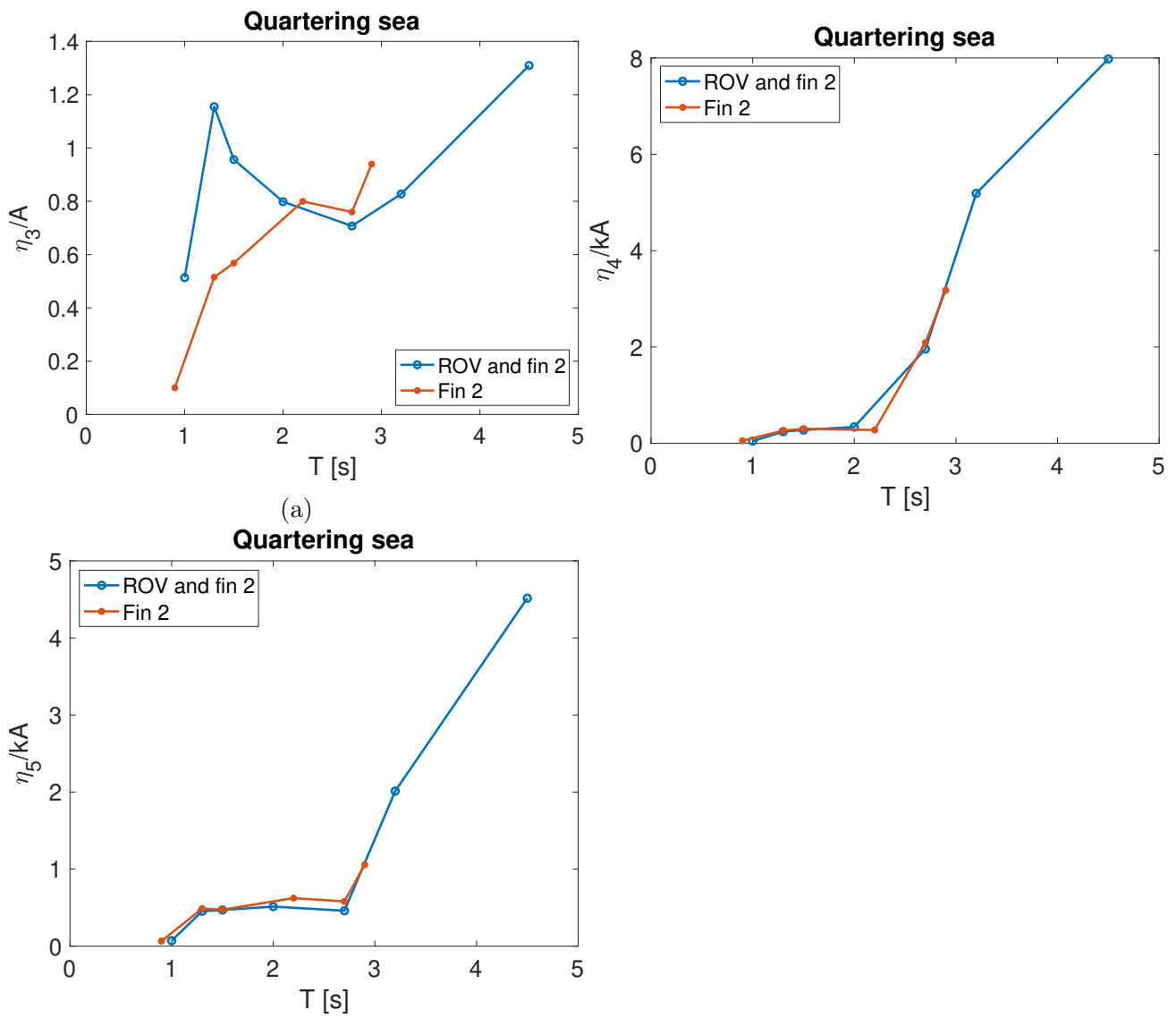Figure 6.5: Impact of ROV on the SWATH for head sea

(a)

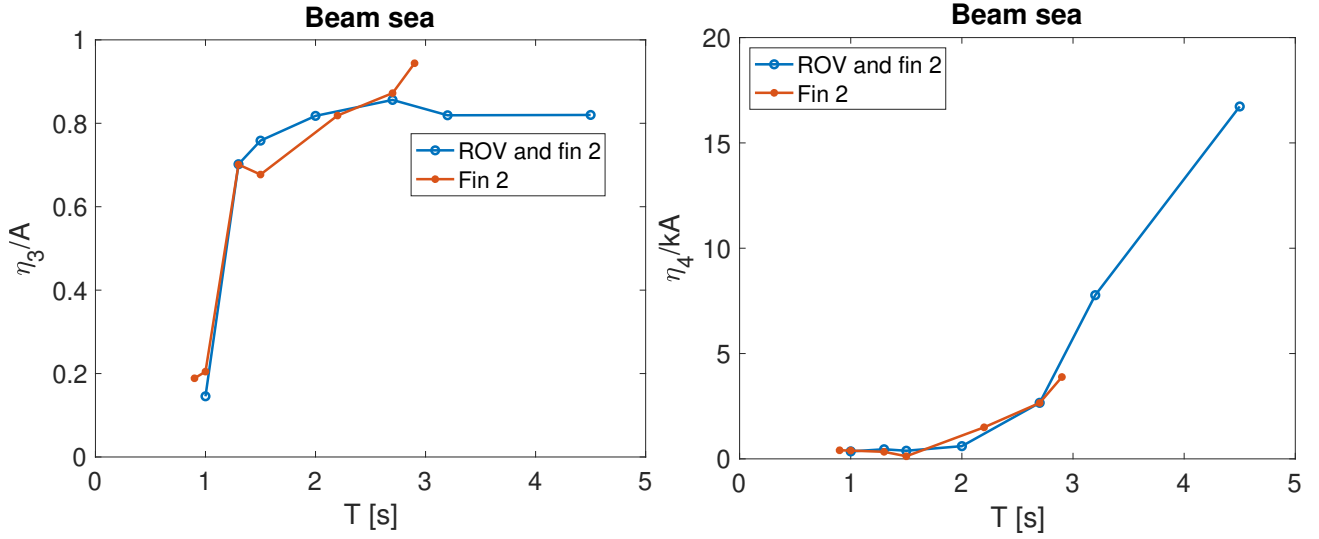Figure 6.6: Impact of ROV on the SWATH for quartering sea

Figure 6.7: Impact of ROV on the SWATH for beam sea in roll

6.1.4 Force on ROV

To measure the heave force on the ROV, three force transducers were attached to the ROV. By summing up the force from each force transducer, the total heave force was found. The undimensional total heave force was found as follows:

$$F_{TOTAL} = \frac{F_{TOTAL}}{\rho g A B^2} \tag{6.3}$$

where A is the wave amplitude and B is the breadth of the ROV, which is 0.119m in model scale, as presented in Table 5.3. Figure 6.10, Figure 6.9 and Figure 6.8 shows that the force reaches a minimum at $T = 2.0$ s and has maximum undimentional force at $T = 1.0$ s. This means that the forces on the ROV is most critical for small wave periods smaller than $T = 2.0$ s, and the heave force on the ROV decreases as the period is increasing. For the small periods, the ROV tries to push against the model, which results in a large force. When the waves are large, the ROV tries to follow the ship. For long periods the force will be small, which implicitly says that the relative motion between the ship and ROV will be low. When the wave period is small, the relative motion between the ship and the ROV will be more significant.
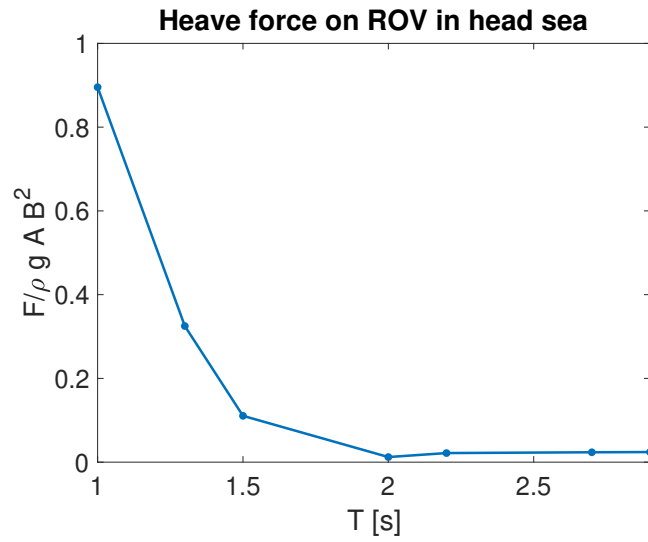
Figure 6.8: Heave force on the ROV in beam sea from experiment in regular waves
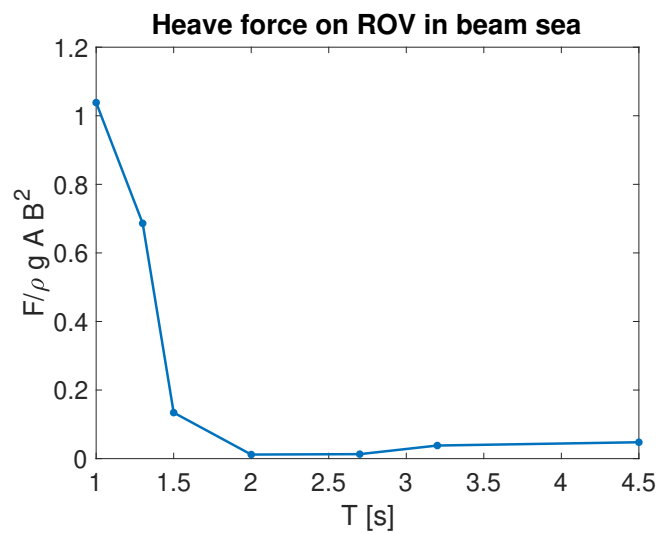

Figure 6.9: Heave force on the ROV in quartering sea from experiment in regular waves
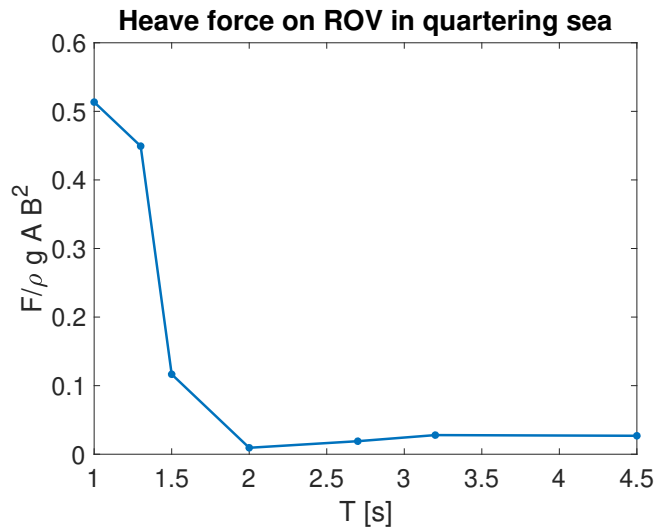
Figure 6.10: Heave force on the ROV in head sea from experiment in regular waves

6.1.5 Comparison of RAO from regular and irregular wave test

Figure 6.11 compares the irregular and regular RAO found for the hull with fin 1 in head sea for heave and pitch motion. The irregular wave test corresponds well with the regular wave test. For hull with fin 1 in head sea, three different wave periods were tested. To get the RAO's from regular wave test, numerous test has to be performed for different frequencies. From the irregular wave test, multiple frequencies can be covered in one run.
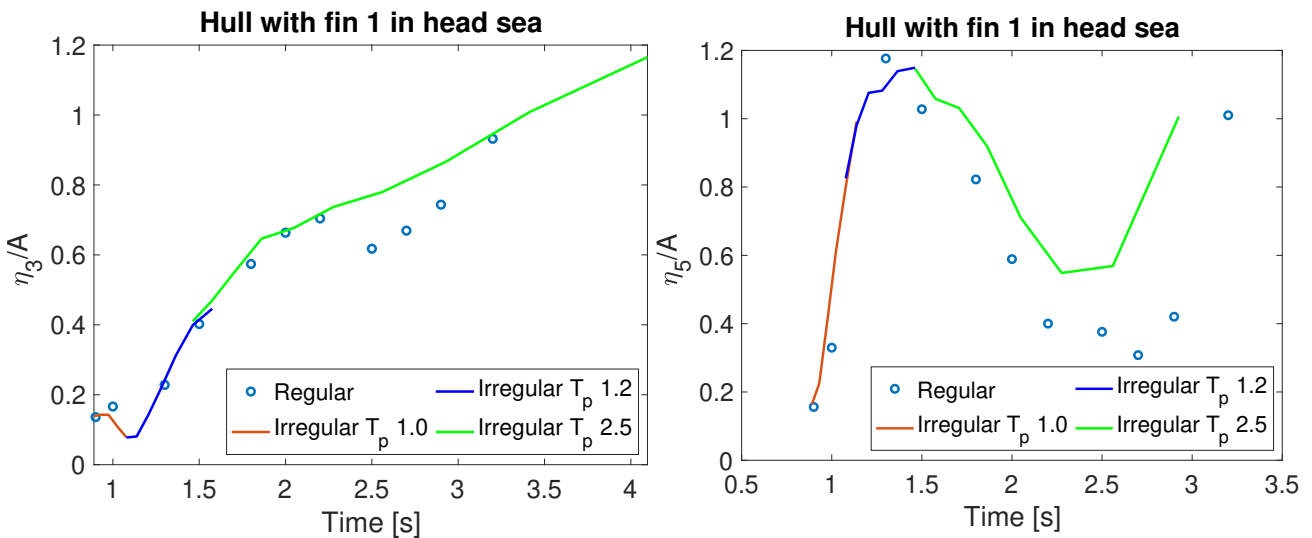
Figure 6.11: Comparison of RAO from regular and irregular wave test. Shown for hull with fin 1 in head sea.

6.1.6 RAO from irregular wave test

The RAO's were obtained from the irregular wave test. The results found in the regular wave test support the results found from the regular wave test, but some cases are divergent from

the regular wave test. Figure 6.12, Figure 6.13 and Figure 6.14 shows clearly that the bare hull has the largest motions and that stabilizer fins need to be implemented in the design, to get lower motions in heave and pitch. In Figure 6.4 there were not any significant changes between the bare hull and the model with fin-type 1 and 2. Figure 6.14 shows changes in the motions comparing the bare hull and the model with stabilizer fins.

The irregular wave test also shows change in RAO's for heave motion when the ROV is mounted to the model, which has been discussed above as an error.

Figure 6.12: Heave and roll RAO from irregular wave test with $T_p = 1.3$ in head sea

Figure 6.13: Heave, roll and pitch RAO from irregular wave test with $T_p = 1.3$ in quartering sea sea

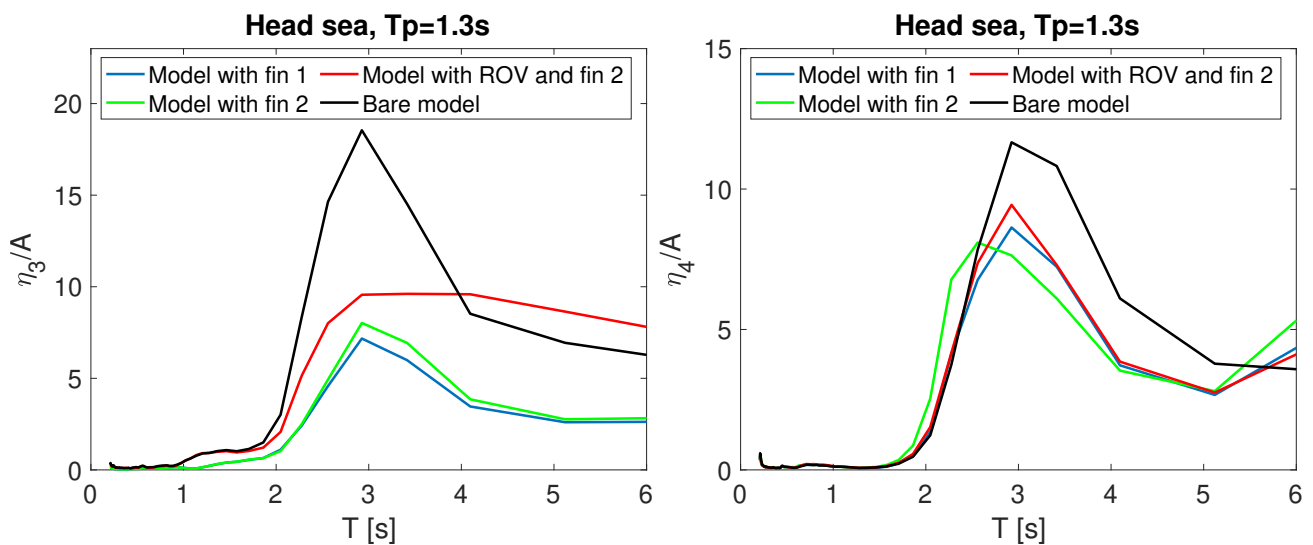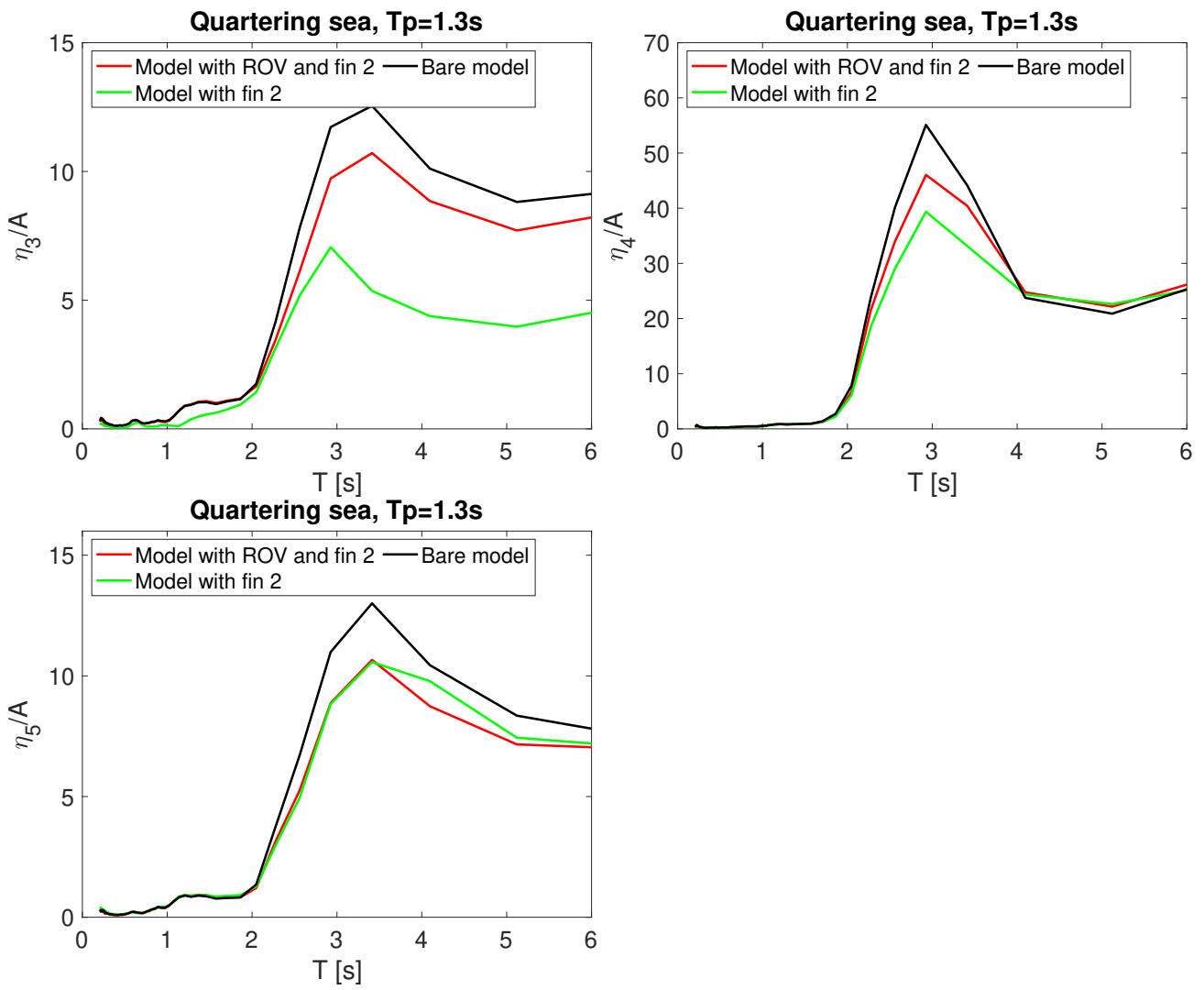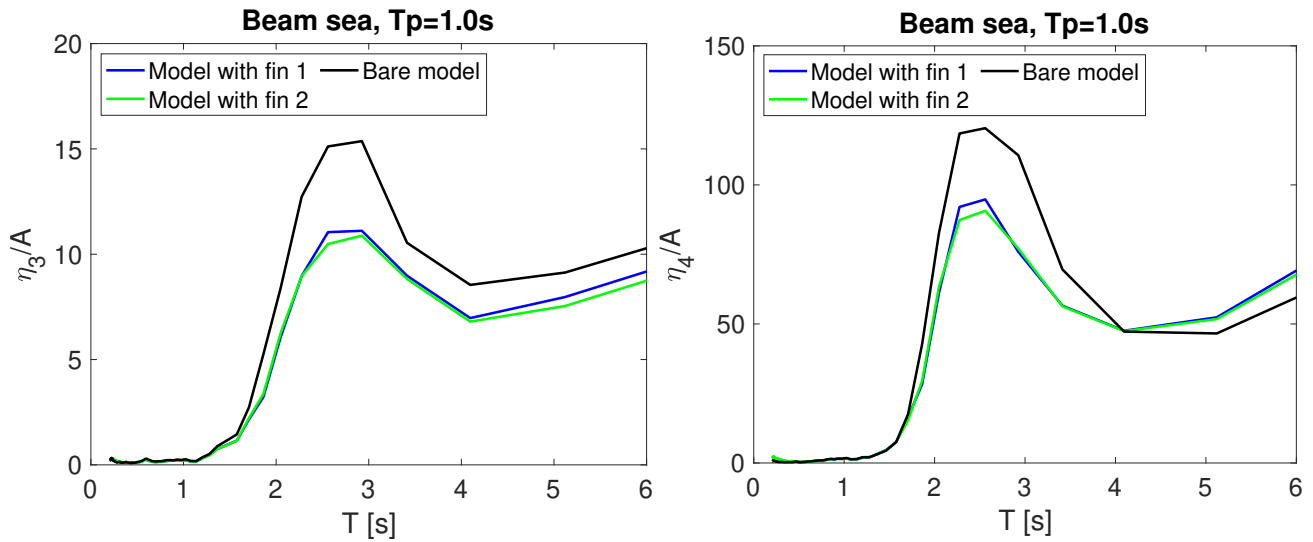Figure 6.14: Heave and roll RAO from irregular wave test with $T_p = 1.0$ in beam sea

6.1.7 Standard deviation and significant response value

The standard deviation and significant response value is found from the irregular wave test. Table 6.4 and Table 6.5 presents the calculated standard deviation of response. Table 6.6 and Table 6.7 presents the calculated significant value of response from the irregular wave test. The standard deviation is an indication of how close the values is to the mean value. The significant response values shows large significant response values for roll motion for hull with fin 2 in beam sea. For bare hull the most significant response value is in roll motion for beam sea. For the hull with stbailiser fins and ROV quartering sea gave large significant response values.

Table 6.4: Standard deviation for hull with fin 1 and fin 2

σ	Head sea Fin 1			Beam sea Fin 1	Head sea Fin 2	Beam sea Fin 2	Quartering sea Fin 2
Tp	1.0	1.3	2.5	1.0	1.3	1.0	1.3
WP	0.0262	0.0335	0.054	0.0262	0.0335	0.026	0.0344
Surge	0.011	0.0224	0.0836	0.011	0.0125	0.0125	0.0311
Sway	0.0786	0.0068	0.0089	0.0786	0.0762	0.0762	0.0434
Heave	0.0089	0.0139	0.0386	0.0219	0.0144	0.0219	0.0216
Roll	0.9244	1.0734	1.5443	9.083	1.548	9.1384	4.6201
Pitch	1.7994	2.4491	2.9723	2.4285	2.4871	0.7267	1.9841
Yaw	0.3532	1.2532	0.6544	1.349	1.777	1.777	2.2071

Table 6.5: Standard deviation for bare hull and hull with ROV

σ	Head sea Bare hull	Beam sea Bare hull	Quartering sea Bare hull	Head sea Hull w ROV	Quartering sea Hull w ROV
Tp	1.3	1.0	1.3	1.3	1.3
WP	0.0333	0.0251	0.0341	0.034	0.0343
Surge	0.0252	0.0088	0.0292	0.0224	0.0292
Sway	0.0080	0.0684	0.0403	0.0096	0.0436
Heave	0.0386	0.02667	0.405	0.0357	0.0394
Roll	0.9953	9.0207	5.3295	1.2166	5.0722
Pitch	0.9953	0.5418	2.0266	2.4518	1.9548
Yaw	0.5728	0.7472	2.5432	2.41	2.41

Table 6.6: Significant response values for hull with fin 1 and fin 2

$X_{1/3}$	Head sea Fin 1			Beam sea Fin 1	Head sea Fin 2	Beam sea Fin 2	Quartering sea Fin 2
Tp	1.0	1.3	2.5	1.0	1.3	1.0	1.3
WP	0.081	0.1341	0.2159	0.1047	0.1339	0.104	0.1377
Surge	0.0453	0.0898	0.3345	0.0438	0.0499	0.0499	0.1246
Sway	0.0236	0.0271	0.0358	0.3143	0.3047	0.3047	0.1735
Heave	0.0357	0.0554	0.1544	0.0875	0.0574	0.0878	0.0862
Roll	3.70	4.2938	6.1772	36.3319	6.1919	36.5538	18.4806
Pitch	7.1974	9.7963	11.8892	0.6071	9.9483	2.9069	7.9464
Yaw	1.2938	5.0127	2.6176	5.3961	7.1079	7.1079	8.8286

Table 6.7: Significant response values for bare hull and hull with ROV

$X_{1/3}$	Head sea Bare hull	Beam sea Bare hull	Quartering sea Bare hull	Head sea Hull w ROV	Quartering sea Hull w ROV
Tp	1.3	1.0	1.3	1.3	1.3
WP	0.1332	0.1006	0.1363	0.1361	0.137
Surge	0.1010	0.0353	0.1176	0.0897	0.117
Sway	0.032	0.2736	0.1611	0.0897	0.1745
Heave	0.1542	0.1067	0.1621	0.1429	0.1575
Roll	3.9813	36.0829	21.3181	4.8664	20.2889
Pitch	3.9813	2.1671	8.1065	9.807	7.8196
Yaw	3.7	2.9887	10.1727	1.9748	9.6257

6.2 Numerical Results

In this section, the numerical simulations done in WAMIT is presented. To compare the performance of the comparable existing monohull design, WAMIT has been used since only a seakeeping experiment was done for the SWATH due to limited time. The two designs have been compared based on their motion characteristics and the operability of the ROV.

6.2.1 Motion characteristics of designs

For the numerical calculations done in WAMIT, the SWATH's parameters are scaled from the parameters found from the SWATH model in the experiment. The full-scale parameters of the SWATH found from the experiment are presented in Table 6.8. An error related to the SWATH is that it has been modeled without stabilizer fins. To account for the effect of the fins, added damping found from the experiment has been added. From the free decay test performed in

Table 6.8: SWATH parameters from experiment scaled up to full scale

	Value	Unit
Weight	175309.92	kg
COG	-1.057	m
I_{xx}	12958657	kgm^2
I_{yy}	3986988.48	kgm^2

the experiment, the damping coefficient was found. Since WAMIT does not take into account damping, the amplitudes will, in some cases, get unrealistic high. The damping from the free decay test was scaled into the full scale to get a more precise and reasonable comparison. The monohull also has added damping, as explained in subsection 3.2.1. Figure 6.15 shows the monohull and SWATH with and without damping and shows the importance of adding damping for the SWATH to account for the viscous effects.
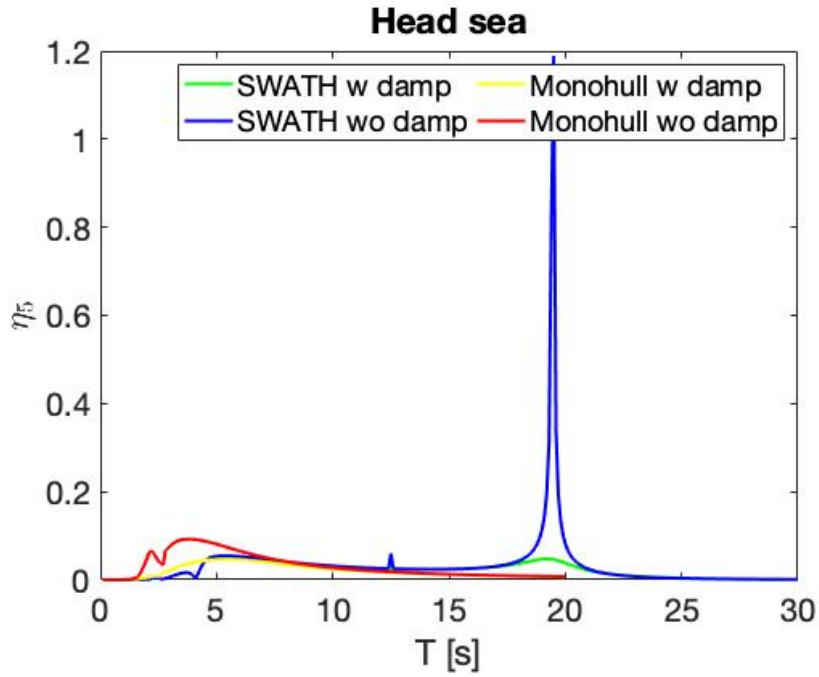
Figure 6.15: SWATH and monohull with and without damping estimated from experiment implemented in study done in WAMIT.

Table 6.9: Natural period for heave and linear and quadratic damping coefficient in full scale

Condition	Natural heave period T_{n3} [s]	Linear damping coefficient B_{33}	Quadratic damping coefficient B_{33}	Total damping term B_{33}^*
Condition 1	17.18	0.13	0.58	$1.35e+05$
Condition 2	18.58	0.27	0.63	$1.77e+05$
Condition 3	12.30	0.0056	4.90	$1.14e+06$

Table 6.10: Natural period for roll and linear and quadratic damping coefficient in full scale

Condition	Natural roll period T_{n4} [s]	Linear damping coefficient B_{44}	Quadratic damping coefficient B_{44}	Total damping term B_{44}^* $[\frac{rad}{s}kgm^2]$
Condition 1	20.40	0.20	0.0028	$1.35e+06$
Condition 2	26.72	0.027	0.72	$3.50e+05$
Condition 3	20.83	0.26	0.019	$1.76e+06$

Table 6.11: Natural period for pitch and linear and quadratic damping coefficient in full scale

Condition	Natural pitch period T_{n5} [s]	Linear damping coefficient B_{55}	Quadratic damping coefficient B_{55}	Total damping term B_{55}^* $[\frac{rad}{s}kgm^2]$
Condition 1	17.73	0.013	0.24	$5.64e+05$
Condition 2	19.94	0.18	0.049	$4.02e+06$
Condition 3	17.00	0.17	0.00	$3.75e+06$

Natural frequency

Table 6.12, Table 6.13 and Table 6.14 presents the natural period for the two designs in head, quartering and beam sea. As explained in subsection 3.2.2, the main idea behind developing a SWATH for the mission of being a suitable support vessel for an ROV, was to make a vessel that has higher natural period than the suggested environmental parameters in Table 4.1. Table 6.12 gives the natural period for the hulls in head sea, where the motion is zero in sway and pitch and Table 6.14 shows zero motion in pitch. The tables present the vessel's motion characteristics, where it is clear that the SWATH has higher natural periods than the monohull, which was the aim of the design of the SWATH.

Table 6.12: Numerical calculation of natural resonance period in head sea

Hull Type	Head Sea				Unit
	Sway	Heave	Roll	Pitch	
Monohull	0.0	5.5	0.0	5.4	s
SWATH	0.0	12.5	0.0	19.5	s

Table 6.13: Numerical calculation of natural resonance period in quartering sea

Hull Type	Quartering Sea				Unit
	Sway	Heave	Roll	Pitch	
Monohull	6.5	4.0	6.5	3.7	s
SWATH	20.3	12.5	20.3	19.5	s

Table 6.14: Numerical calculation of natural resonance period in beam sea

Hull Type	Beam Sea				Unit
	Sway	Heave	Roll	Pitch	
Monohull	6.5	3.6	6.5	0	s
SWATH	20.3	12.5	20.3	0	s

Significant motion amplitude

To evaluate the motion characteristic of the designs, a response spectrum was implemented. It was chosen to use the JONSWAP spectrum with the environmental parameters presented in Table 4.1. The spectral analysis is done for all six DOF in the head, quartering, and beam sea, for $H_S = 2.5$ m, with T_p varying from 4.5-13.5 s. In Figure 6.16, Figure 6.17 and Figure 6.18, the significant motion amplitude in head, quartering, and beam sea is shown for the most critical motions in each heading. The remaining motions that have not been presented can be found in Appendix D.

The significant motion amplitude is used to compare the design in the given sea state. Figure 6.16 shows that the SWATH responds better than the monohull in heave motion. In roll, the monohull has better operability than the SWATH from peak period 10-15 s, while from the lower range, the difference between the two designs is not that significant. The reason why the SWATH increases its significant motion amplitude after $T = 15$ s is that it has its natural period after 15 seconds. Comparing the motions in heave and roll, the significant motions are less in roll than in heave.
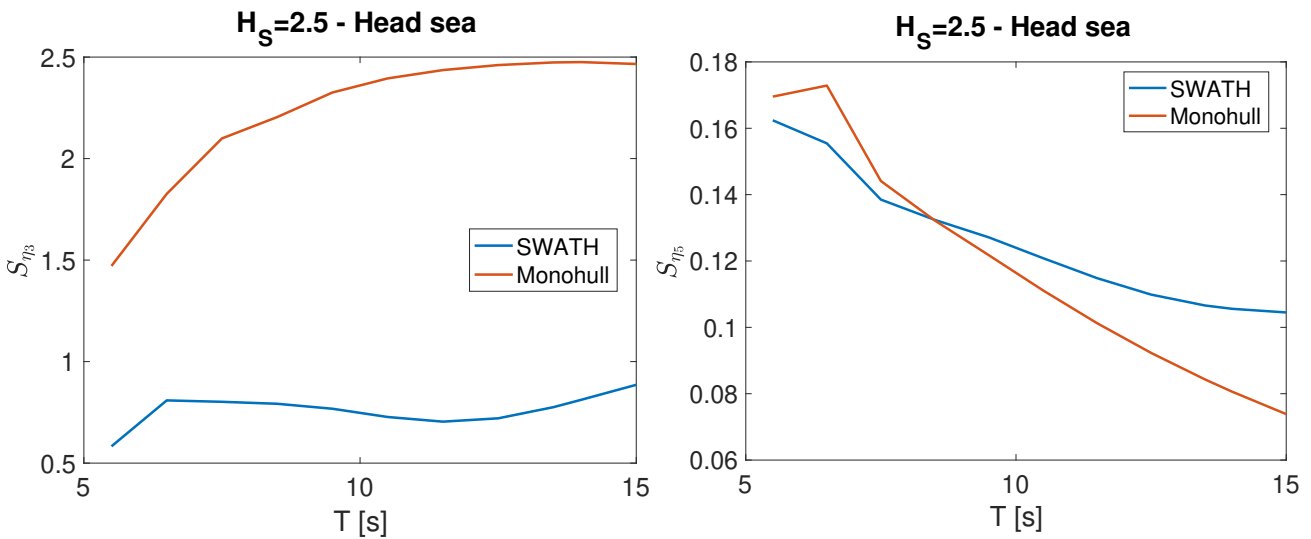

Figure 6.16: Significant motion amplitude of SWATH and monohull for $H_S = 2.5$ in head sea

For significant amplitude motions in quartering sea, as presented in Figure 6.17, the SWATH has as in head sea less motion in heave than the monohull. For roll, the SWATH has less significant motions in the lower peak periods, but increases as the peak period get higher, due to its natural resonance period. In pitch motion, it is noticeable that the monohull has less motions than the SWATH. The SWATH gave larger motions for pitch in quartering sea because, as shown in Figure E.3, the SWATH gets large motion amplitudes for quartering sea in pitch motion whit-in the same region as the monohull.
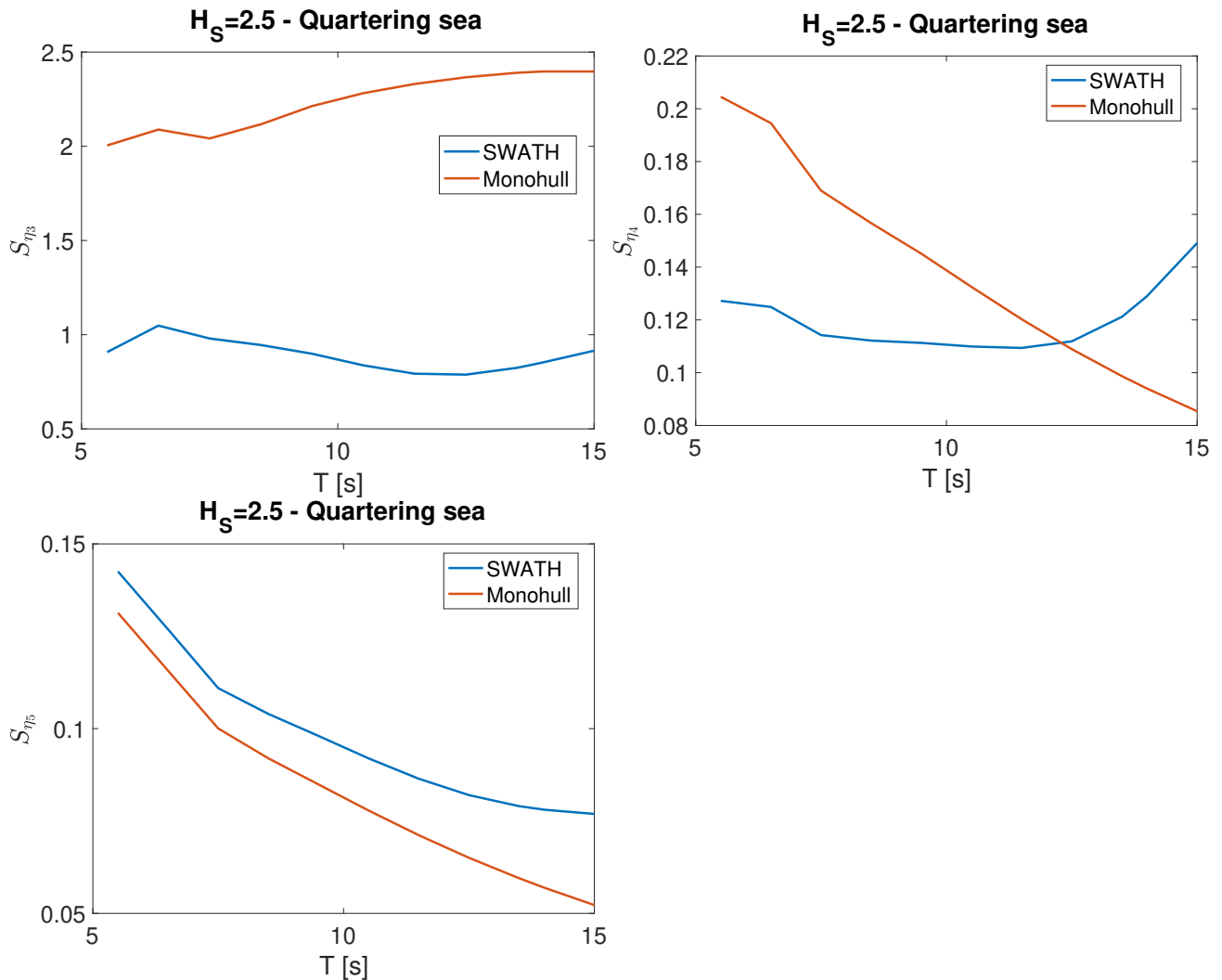
Figure 6.17: Significant motion amplitude of SWATH and monohull for $H_S = 2.5$ in quartering sea

In beam sea, the significant amplitude motions are presented in Figure 6.18 and shows that for heave motion, the motion is less for the SWATH. In roll, the SWATH has better significant motions than the monohull in the lower peak period, but again increases as the wave period increases.

The significant response amplitude presented for the two vessels fulfills the idea behind designing the SWATH. The results show that the SWATH has less significant motions for lower peaks than the monohull, especially in heave motion. One does not have to forget that the SWATH will have higher significant motion amplitudes after $T = 15$ s when the SWATH reaches its natural period domain. The SWATH will be useful in areas with short wave periods since the SWATH has long natural periods. The study shows that the SWATH does have better seakeeping abilities than the monohull in the given sea-condition.
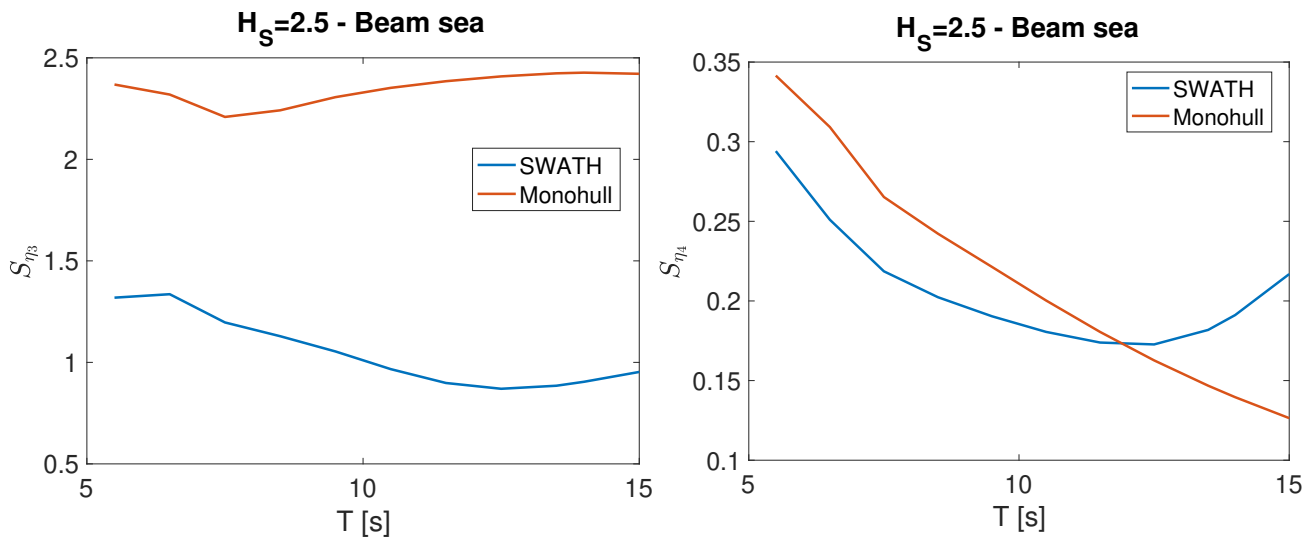
Figure 6.18: Significant motion amplitude of SWATH and monohull for $H_S = 2.5$ in beam sea

6.2.2 Operability of ROV

When studying the operability of the ROV during launch and recovery of the ROV, the relative velocity amplitude between the USV and the ROV was established as a governing requirement. The requirement was established to evaluate if there can arise a collision between the USV and the ROV. The geometry file for the ROV used in WAMIT was made upon the dimensions presented in Table 3.10. When doing the simulations in WAMIT, the ROV was placed 1 m below the USV.

The results presents the relative velocity amplitude between the USV and ROV. The vertical velocity for the ROV was found to be around 1 m/s. The governing equation was then established, saying that the relative velocity amplitude can not be larger than the vertical velocity for the ROV. The black dashed line in Figure 6.19, Figure 6.20 and Figure 6.21 indicates the vertical velocity to the ROV. When the relative velocity amplitude exceeds the dashed line, there is a chance for an impact between the USV and the ROV, which can cause unwanted interaction between the two bodies during the launch and recovery of the ROV. The relative velocity amplitude was established for the SWATH and monohull in the three given wave headings in heave motion. The results show that the relative velocity amplitudes are most significant around five seconds for both the SWATH and the monohull. In all headings, the SWATH does have a higher average relative velocity amplitude than the monohull, except when the monohull has its peak.
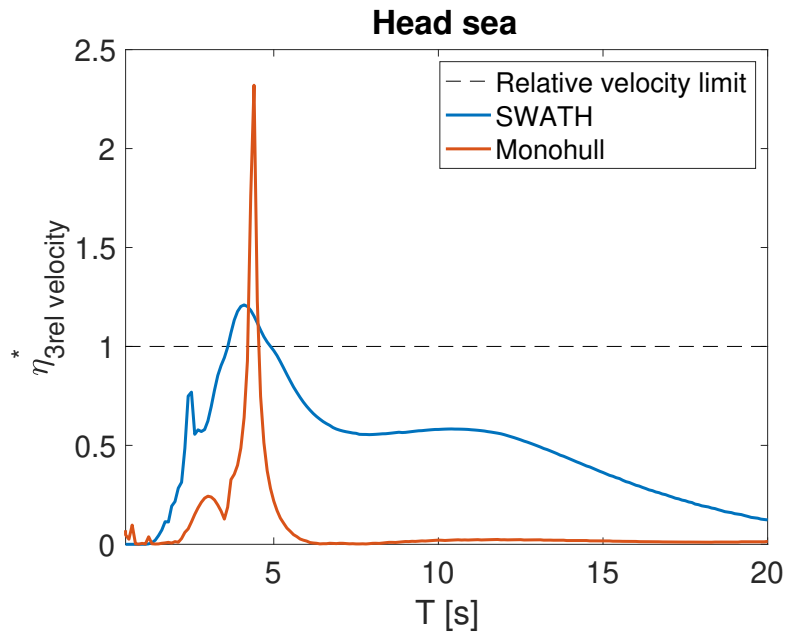
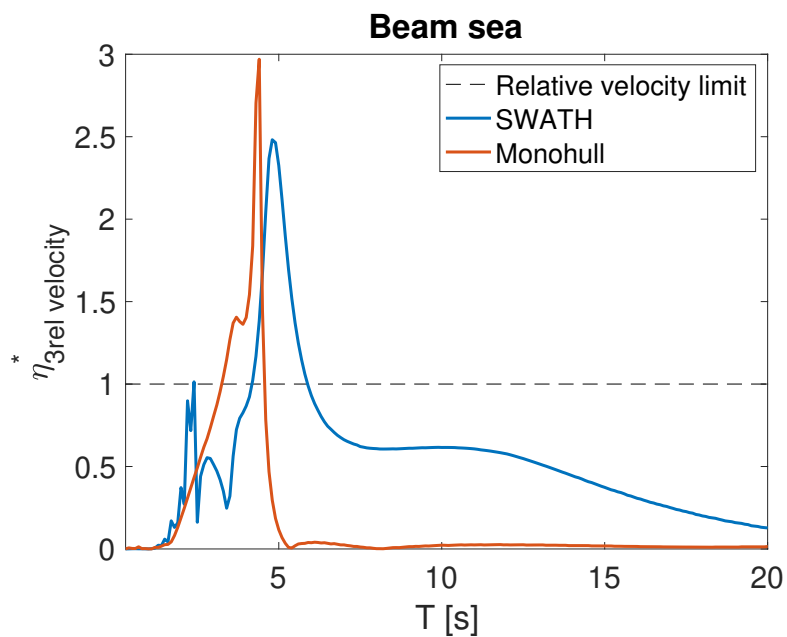Figure 6.19: Relative velocity amplitude between USV and ROV in head sea

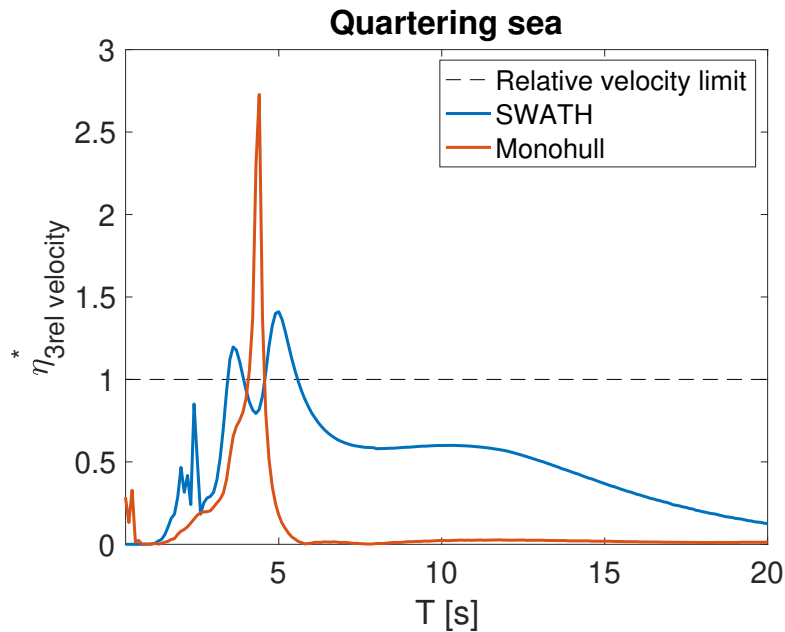Figure 6.20: Relative velocity amplitude between USV and ROV in beam sea

Figure 6.21: Relative velocity amplitude between USV and ROV in quartering sea

One operational requirement can be that the ROV should not be launched and recovered when the wave period is smaller than five seconds. Active heave compensated system does also needs to be implemented to operate in the area where the amplitudes are high. When the wave period is over five seconds, the monohull and ROV relative velocity amplitude is equal to zero, which indicates that it can be a good working window for the launch and recovery of the ROV. One option is also to disregard operation in beam sea, where the amplitudes were high for both the SWATH and the monohull.

6.3 Validation of numerical calculation

To validate if the added damping calculated from the experiment was sufficient, simulation in WAMIT was done for the vessel in the model scale with added damping from the experiment. As explained in subsection 6.1.1, the damping coefficient in heave, roll, and pitch were calculated from the decay test. The damping coefficient was then inserted in WAMIT so that viscous effects were included in the numerical analysis. A more realistic analysis of the monohull and the SWATH could be evaluated. Figure 6.22 and Figure 6.23 shows a good comparison between WAMIT and experiment for heave in head sea and surge and heave motion in beam sea for the model with fin 1. For the rotational motions, the comparison is not as good as for the translator motions. This is because that WAMIT does not take into account for different effects that arise for the rotational motions. An error in the numerical calculations is that the model is modeled without the fore and aft stabilizer fin. However, the viscous effects from the fins are considered from added damping.
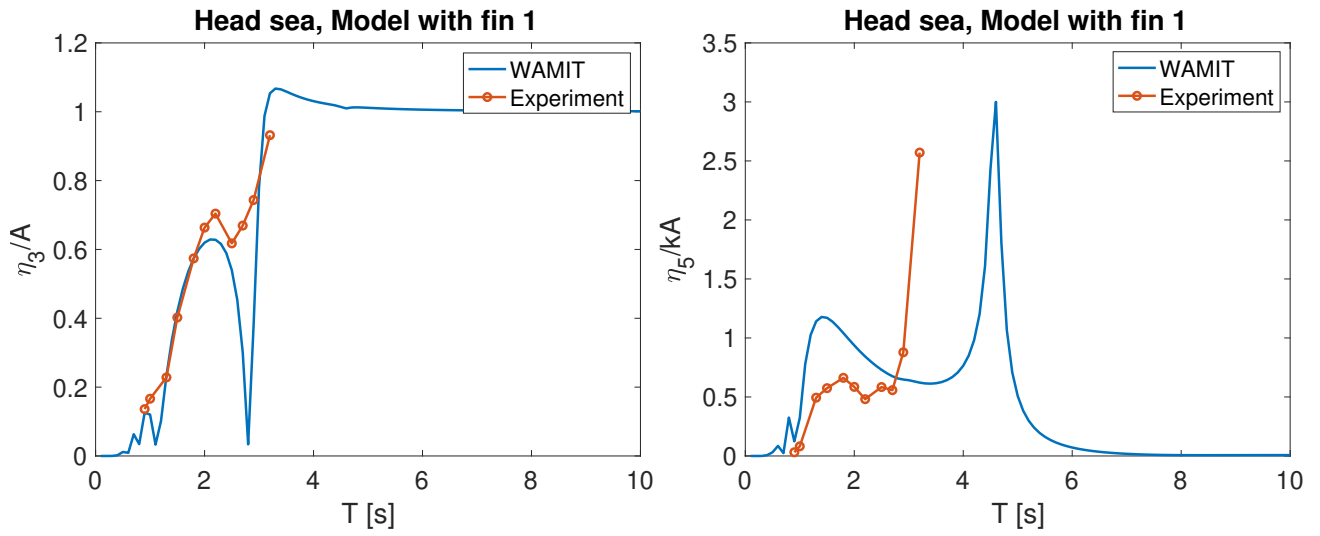
Figure 6.22: Comparison of experimental and numerical results for model with stabiliser fin type 1 in head sea. The numerical results have added damping found from the decay test in the seakeeping experiment.
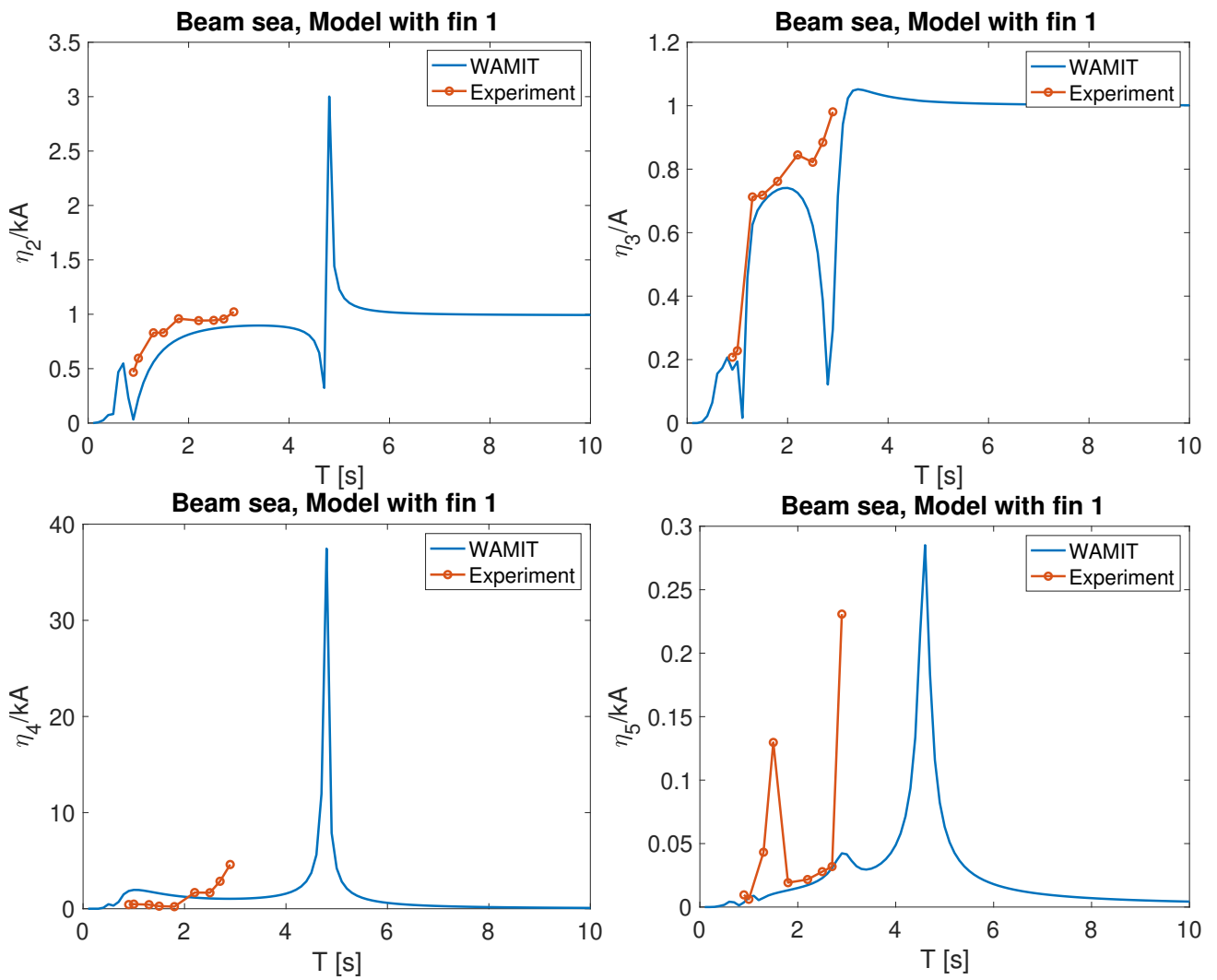
Figure 6.23: RAO validation of model with fin 1 in beam sea

Chapter 7

Discussion

The discussion aims to reflect on the results that are presented in the previous chapter. It begins with a discussion of the experiments that were performed in the towing tank at Sintef, to understand the motions of the SWATH in regular and irregular waves. Further, the two vessel motion characteristics will be discussed and compared. A focus here was to evaluate what design fulfilled the operational requirements the most. Several factors need to be evaluated in the early design stage to find the most suitable design.

In the experiments, the SWATH hull was tested in different conditions: bare hull, hull with two different stabilizer fins, and hull with a connected ROV. Both wave tests in regular and irregular showed a significant effect of implementing stabilizer fins on the SWATH design. It showed that the motion displacement decreases, which is the idea behind implementing the fin in the design of the SWATH. By increasing the dimensions of the stabilizer fins, it was of interest to see how much the fin size would have to say about the seakeeping abilities of the hull. Fin 1 and fin 2 gave in all of the cases close to similar results. Since the fins gave close to similar results, it was decided to only go forward with fin 2 in phase 2.

Testing the operability for ROV operations in the experiments, it was expected that the motions to the vessel should not be changed, due to the large dimension difference between the hull and the ROV. The results were as expected, except for heave motion. The change in heave RAO, as seen both in regular and irregular waves, is found to be due to some faults in the measurement system for the heave motion. For the testing of ROV mounted to the hull, the vertical heave force was measured. The measured non-dimensional heave force showed that the force has its maximum at T=1.0 s, and goes toward zero heave force at T=2.0 s. From the result, it can be seen that the chance for interaction between the vessel and ROV is most likely to exceed for smaller wave period.

Due to limited time, only one repetition for bare hull and hull with fin 1 was performed in

head and beam sea, as presented in Table 5.7. Five repetitions for each run are recommended when finding the mean value and standard deviation from the test. More time should have been planned for repeated runs, to get a more accurate result.

Since experiments were only possible to do on the SWATH, numerical simulations were done in WAMIT to evaluate the seakeeping abilities and the ROV operability in launch and recovery. When adding damping calculated from the decay test, section 6.3 showed a good comparison between the experiment and the simulations done in WAMIT, especially for translation motion. First, the RAO's in head, quartering, and beam sea were established. As anticipated, the SWATH has a higher natural frequency compared to the monohull. Since the SWATH has natural frequencies higher than T=15 s, the vessel is moved out from the given operation sea state, and large motions are avoided due to the natural period. When the RAO's for different heading was established, the significant motion amplitude was established for the given sea state. The SWATH gives less significant motion in the given sea state than the monohull, especially for heave motion.

The measured force on the ROV was found to have a maximum at T=1s in the model scale from the experiment. Scaling the period to full scale where the measured heave force has its maximum, the maximum heave force in full scale is at T=4.24 s. The relative velocity amplitude between the SWATH and the ROV had its maximum peaks around four to five seconds, which states that the assumptions for the relative motion amplitude is reasonable and gives an understanding of where the vessels and the ROV do get high motions. The relative velocity amplitude shows that the monohull has a higher peak for all heading than the SWATH, but only has significant motions in the presented peak range. The SWATH has more relative motions also away from its peak. Launch and recovery of the ROV is an essential operational requirement for the USV. Considering the relative velocity amplitude, the monohull is preferable for wave periods larger than five seconds for launching and recovery of an ROV, since the monohull has equal to zero relative motion amplitude after five seconds. Taylor (1975) compared the seakeeping between three monohull's, two SWATHs, and a catamaran. He also found out that the monohull has better relative motions than the SWATH and the catamaran. He suggested that launching and recovery of the floating object were better suited from a monohull at low stationkeeping speed, than from a SWATH due to the relative motions. The study suggested that the SWATH was a better workboat than the monohull, giving better work conditions for the people on board.

If going for the monohull as the optimum design, some guidelines from the numerical study can be established. Taking the relative motion amplitude into account, the relation between the monohull and SWATH is close to zero from the wave period larger than five seconds and higher. Also, the study showed less motion in head and quartering sea than in beam sea for both designs.

It is not straight forward to say that one design is better than the other. It is, therefore, important to understand the given operation the vessel shall do and what environment it will operate in. In this case, a small USV will be onshore to launch and recover an ROV. It is preferable to have a vessel that can operate in rough sea so that the waiting time will be reduced. The design has to be evaluated based on seakeeping abilities, resistance, cost, and survivability, to name a few important parameters. An autonomous ROV vessel does not need many additional weights. Because it can be customized designed towards the vessels operational profile and requirements. Saying that, an autonomous ROV vessel does not need more deadweight then the fuel for propulsion and hotel power such as lightning, lanterns or for example running of possible internal ship systems. The whole weight of the vessel (ligthshipweight + deadweight) have higher for the SWATH and can be a problem for the requirement of maximum preferable weight. The significant motion amplitude shows that the SWATH does have a better response in the given sea state, which was one of the main reasons for designing the SWATH. Since the USV will be unmanned, it can be onshore for a longer period and therefore need to have good survivability in rough sea. The survival capacity for the two different designs was not examined in this project, and need to be looked into to make a final decision.

Chapter 8

Conclusion

8.1 Conclusion of experiment

Seakeeping experiments were performed on a SWATH model with different features as bare hull, implementation of stabilizer fins with different sizes, and implementation of an ROV. The set-up was designed so that the model was moored in head, beam, and quartering sea in regular and irregular sea. Video recording, six-DOF measurements, and the heave force on the mounted ROV to the model were performed. The effect of stabilizer fins and the attached ROV to the vessel were examined and showed interesting results. Error sources in the experiment are discussed. The outcomes of physical investigations can be summarized as follows:

- A SWATH model is studied to identify its behavior in regular and irregular waves. There were not ran high enough regular waves to determine the natural frequency of the model. Lee & Martin (1976) demonstrated that stabilizer fins should be implemented on a SWATH to secure stability, to obtain damping for heave and pitch, and to maintain reasonable natural periods. Similar effects were identified; the heave motion for the model was improved in head and quartering sea, but in pitch, the effect was not as significant as for heave motion. For beam sea, the stabilizer fins did not have any effect. Stabilizer fins should be included in the model since it provides a significant reduction of the heave motion, which is important for the launch and recovery of the ROV.

- Irregular wave test showed similar results compared to the regular wave test.

- As expected, the ROV does not change the motions to the model. The measured heave force gave the largest non-dimensional force in small wave periods. This implicit says that the relative motion between the model and the ROV is most significant for small periods.

- Linear and quadratic damping were found from the free decay test and implemented in the simulations done in WAMIT to account for viscous effects.

8.2 Optimum design

Both designs has its advantages and disadvantages. It is not easy to categorically recommend these two hull types up against each other. Each design has its advantages and disadvantages that need to be considered carefully against the relevant operational requirements and where to operate. The pros and cons of each design can be summed up in Table 8.1.

Table 8.1: Comparison between SWATH and Monohull based on the study

	SWATH	Monohull
Dimensions	Small L/B	Large L/B
Weight	More weight	Less weight
Weight sensitive	More sensitive	Less sensitive
Deadweight	Less deadweight	More deadweight
Stability	More stable	Less stable
Resistance	Less total resistance	More total resistance
Building cost	More costly	Less costly
Seakeeping	Less motions	More motions
Survivability	Less survivability	Better survivability
Maintenance	More maintenance	Less maintenance

Before taking a final decision for choose of hull design type, the listed features in Table 8.1 should be carefully considered of what is important or not, considering the operational requirements. It is desirable to avoid situations that can lead to; for example, capsize, vessel damage or as in this case, damage of the ROV. As known, when the vessel is at sea, it can be exposed to large waves, driven by powerful winds. From the comparison of the numerical study performed in WAMIT, the SWATH does have better significant motion amplitudes than the monohull. For the requirement of safe launch and recovery of the ROV, a maximum relative velocity amplitude between the USV and the ROV is found to be around 1 m/s. If the operability of the ROV is set as the governing requirement, the relative vertical motion between the USV and the ROV will be the crucial factor for choosing the vessel type. Based on the study and the discussion the following operational requirements can be established for both the SWATH and the monohull:

- Launch and recovery in beam sea should be avoided due to the high relative velocity amplitude between the vessel and ROV.

- Launch and recovery of the ROV should be made in wave periods larger T=5 s.

8.3 Recommendation for further work

- Seakeeping test of the monohull in regular and irregular waves

- Examine survivability of the monohull and the SWATH

- For the numerical analysis that was done, important non-linear effects were not captured. To implement these effects estimation of linear and quadratic damping were found from he experiment. CFD analysis of the vessels and the ROV would be a good solution to get a better understanding of the impact of the motions between the vessel and the ROV during launch and recovery.

Bibliography

Ahvenjärvi, S. (2017), 'The Human Element and Autonomous Ships', *TransNav, the International Journal on Marine Navigation and Safety of Sea Transportation* **10**(3), 517–521.

Bai, Y. & Bai, Q. (2012), 'Installation and Vessels', *Subsea Engineering Handbook* pp. 139–158.

Biran, A. & López-Pulido, R. (2013), *Ship Hydrostatics and Stability: Second Edition*, Elsevier Ltd.

Chakrabarti, S. (2005), *Handbook of Offshore Engineering.*

Christ, R. D. & Wernli, R. L. (2014), *LARS and TMS*, Elsevier Ltd.
URL: *http://dx.doi.org/10.1016/B978-0-08-098288-5.00009-9*

Club, I. (2007), 'Human Error in Shipping', *Springer Series in Reliability Engineering* **20**, 91–103.

DNV (2011), 'Offshore Standard DNV-RP-H103 -Modelling And Analysis Of Marine Operations', *Det Norske Veritas* (April), 150.

DNV GL (2016), 'Standard DNVGL-ST-N001: marine operations and marine warranty (edition: 2016-06)', pp. 1–543.

Faltinsen, O. (1998), *Sea loads on ships and offshore structures*, Cambridge University Press.

Faltinsen, O. M. (2006), *Hydrodynamics of high-speed marine vehicles*, Cambridge University Press.

Faltinsen, O. M. & Timokha, A. N. (2009), *Sloshing*, Cambridge University Press.

G, R. L. (1960), 'The SWATH Concept: Designing Superior Operability Into A Surface Displacement Ship', *Distribution* (May).

Holven, E. B. (2018), 'Control System for ROV Minerva 2', (June).
URL: *https://brage.bibsys.no/xmlui/handle/11250/2564521*

Huse, E. (1994), Experimental Methods in Marine Hydrodynamics, Technical report, Faculty of marine technology - NTNU Trondheim.

INC., W. (n.d.), 'WAMIT USER MANUAL'.
  URL: *WWW.WAMIT.COM*

ITTC (2014*a*), 'ITTC – Recommended Procedures and Guidelines-Seakeeping Experiments', *27th ITTC Seakeeping Committee* pp. 1–22.

ITTC (2014*b*), 'Recommended Procedures and Guidelines: Guide to the Expression of Uncertainty in Experimental Hydrodynamics', *27th International Towing Tank Conference* .

Jamieson, J. & Wilson, L. (2015), 'Effective launch and recovery of autonomous underwater vehicles', *Proceedings of the Annual Offshore Technology Conference* **1**(May), 231–244.

Kongsberg moonpool deployment system (n.d.).
  URL: *https://www.ynfpublishers.com/2012/04/kongsberg-rov-for-forland-new-build*

Lee, C. M. & Martin, M. (1976), 'Determination of Size of Stabilizing Fins for Small Waterplane Area Twin-Hull Ships', *David W Taylor Naval Ship Research and Development Center* (December).
  URL: *https://apps.dtic.mil/dtic/tr/fulltext/u2/a002427.pdf*

Lewi, E. V. (1989), *Principle of Naval Architecture*, 3rd ed. edn.

Medaković, J., Dario, B. & Blagojević, B. (2013), 'A Comparison of Hull Resistances of a Mono-Hull and A SWATH Craft', *International Journal of Enginnering Science and Innovative Technology (IJESIT)* **2**(4), 155–162.

Messalle, R. F. (1987), 'Proceedings of the American Towing Tank Conference (21st) Held in Washington, DC. on 5-7th August 1986'.

Moffat, R. J. (1988), 'Describing the uncertainties in experimental results', *Experimental Thermal and Fluid Science* **1**(1), 3–17.

Myrhaug, D., Lian, W. & Teknikk, N. t.-n. u. I. f. m. (2014), 'Marine dynamics : lecture notes 2009', *TMR4182 Marine dynamics : irregular waves* .

Nagai, T. (1987), 'Critical Review of SWATHs'.

Oritsland, O. & Lehn, E. (1989), 'Hydrodynamic forces and resulting motion of subsea modules during lifting in the splash zone'.

P, S., of Ship, D. & Marine Technology, University of Strathclyde, G. S. (1996), 'Hydrodynamic forces on ROVs near the Air-Sea Interface', **6**(3).

Porathe, T., Hoem, Rødseth, Fjørtoft, K. & Johnsen, S. O. (2018), 'At least as safe as manned shipping? Autonomous shipping, at least as safe as manned shipping? autonomous shipping,safety and "human error"', *Safety and Reliability - Safe Societies in a Changing World - Proceedings of the 28th International European Safety and Reliability Conference, ESREL 2018* pp. 417–426.

Ravinthrakumar, S. (2020), Numerical and Experimental Studies of Resonant Flow in Moonpools in Operational Conditions, PhD thesis, Norwegian University of Science and Technology (NTNU).

SAAB Seaeye leopard (n.d.).
URL: *https://www.saabseaeye.com/solutions/underwater-vehicles/leopard*

Sandford, A. J. (1987), 'Code of practice for the safe and efficient operation of remotely operated vehicles', *Submersible Technology: Adapting to Change: Proceedings of an International Conference (SUBTECH 1987 - Adapting to Change)* (July), 45–50.

Schjølberg, I. & Utne, I. B. (2015), 'Towards autonomy in ROV operations', *IFAC-PapersOnLine* **28**(2), 183–188.

Steen, S. (2015), 'Experimental methods in marine hydrodynamics: statistical analysis', (August).
URL: *http://astorplast.no/wp-content/uploads/AppendixStatisticalAnalysis.pdf*

Taylor, D. W. (1975), 'A seakeeping comaprison between three monohulls, two SWATHs, and a column-stabilized catamaran designed for the same mission', *Resrech and Development Center Bethesda, Maryland* (July).

Wernli, R. L. & Chapman, R. (1986), *ROV '86: Remotely Operated Vehicles.*

Yuan, Z. M., Zhang, X., Ji, C. Y., Jia, L., Wang, H. & Incecik, A. (2018), 'Side wall effects on ship model testing in a towing tank', *Ocean Engineering* .

Appendix A

Production and tilting of the SWATH model

NTNU-prosjekt med modell av Swath for Mohd Atif

Vi har bygget modell av en swath for doktorgrads-student Mohd Atif Siddiqui.
Modellen består av 2 stk 100mm sylindere (aluminiums-rør). Det er limt inn en avrundet PVC-profil i framenden av rørene. I akterenden er det limt inn koniske boss. Disse er delt i lengden med o-ringer i delingen for tetting. Endedelen av bossene kan skrues av for å legge inn ballast. Det er lagt inn senter-rør midt i aluminiums-rørene for ballastering.
Overbygg ble laget av honeycomb-plater og tre-lister. Disse ble skruet og limt sammen. Overbygget ble skruet fast til vinkler som er sveiset fast til aluminiums-rørene.
Ved vipping av modellen viste det seg at vertikal-tyngdepunktet ble for høyt. Dette resulterte i at vi måtte fjerne masse fra overbygget og legge tilsvarende masse i rørene i sylindrene. Ny vipping viste akseptabelt vertikal-tyngdepunkt. Modellforsøk gjøres i forlengelsen i slepetanken i uke 16-2020.

Nye tester skal gjøres i uke 20-2020. Da med en ROV-modell montert mellom skrogene.

Vedlegger vippedata og bilder av modellen

NTNU project with model of Swath for Mohd Atif

We have built a model of a swath for doctoral student Mohd Atif Siddiqui.
The model consists of 2 100mm cylinders (aluminum tubes). A rounded PVC profile is pasted into the front of the pipes. In the stern there is glued conical boss. These are divided into lengths with o-rings in the section for sealing. The end portion of the bosses can be unscrewed to load ballast. Center tubes are inserted in the middle of the aluminum tubes to fill with ballast.
The superstructure was made of honeycomb boards and wood moldings. These were screwed and glued together. The superstructure was screwed to angles welded to the aluminum tubes.
When tilting the model, it turned out that the vertical center of gravity became too high. This meant that we had to remove pulp from the superstructure and put similar mass into the pipes in the cylinders. New tilt showed acceptable vertical center of gravity. Model testing are done in the extension in the towing tank during week 16-2020.

New tests will be done in week 20-2020. Then with an ROV model mounted between the hulls.

attaches tilt data and images of the model

14.04.2020
Trond Innset
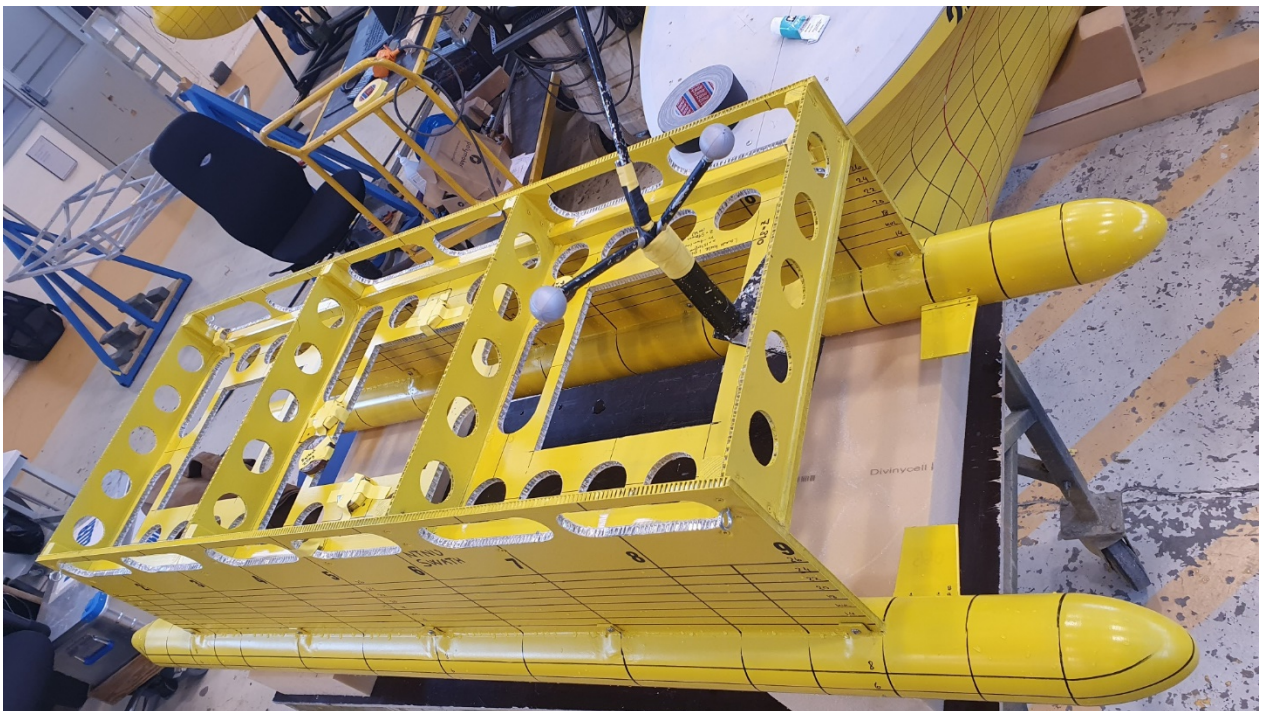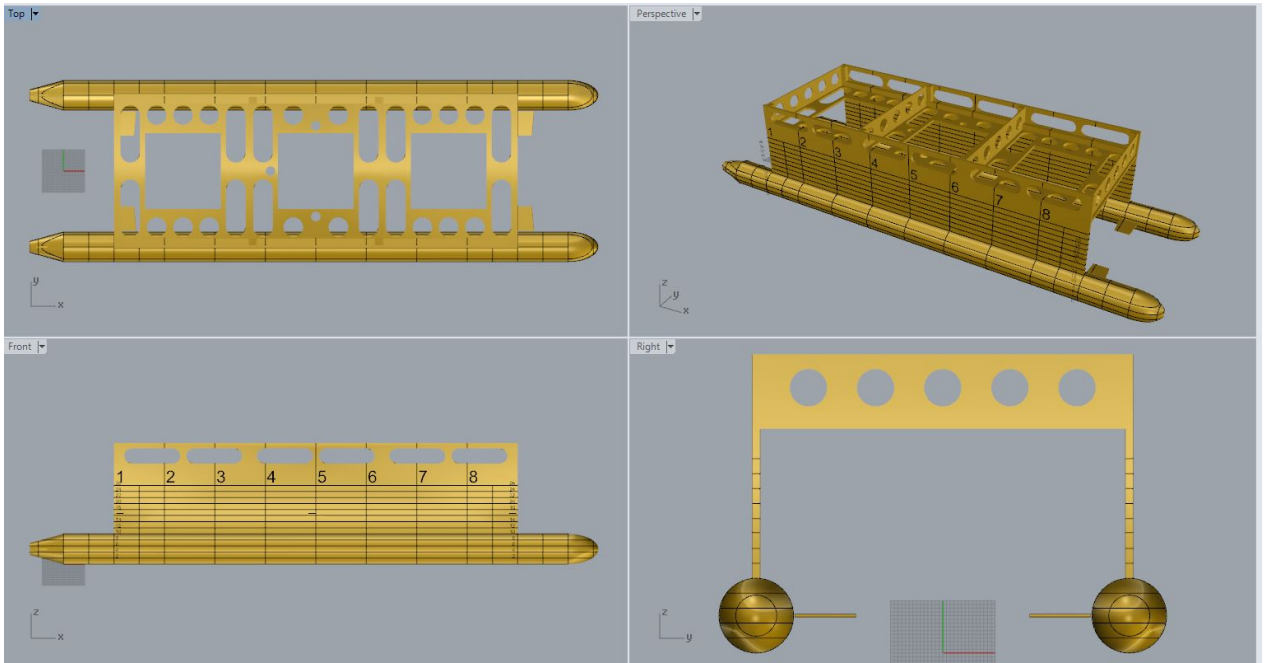
Vektsdata for modeller

MT-K4-S105 Rev.08

Prosjektnr.: Mohd Atif

Prosjekttittel: NTNU-Swath

Modellnr.:

Skala :

Tetthetsforhold: saltvann/ferskvann

Lastekondisjon : 161mm

X-akse :

Y-akse :

Z-akse :

Origo:

SKROG		Fullskala	Modellskala	Målt modell	Avvik (%)
Lengde, Lpp	m	1,668			
Bredde, B	m	0,600			
Dypgang akter, TA	m	0,161			
Dypgang forut, TF	m	0,161			
Deplasement, totalt	tonn, kp	30,06			
Vertikalkomp. stigerør	tonn, kp				
Vertikalkomp. ankerliner	tonn, kp				
KG inkl. vertikalkomp.	m				
XCOG inkl. vertikalkomp.	m				
YCOG inkl. vertikalkomp.	m				

FAIRLEAD-KOORDINATER: FULLSKALA		X	Y	Z
Stigerør	m			
Ankerliner	m			

VIPPING		Fullskala	Modellskala	Målt modell	Avvik (%)
KG ekskl. vertikalkomp.	m	0,000	#DIV/0!	0,101	#DIV/0!
XCOG ekskl. vertikalkomp.	m	0,000	#DIV/0!	0,838	#DIV/0!
YCOG ekskl. vertikalkomp.	m	0,000	#DIV/0!	0,000	#DIV/0!
Vekt ekskl. vertikalkomp.	tonn, kp	30	#DIV/0!	30,060	#DIV/0!
Ixx ekskl. vertikalkomp.	t m2/kg m2	0	#DIV/0!	2,110	#DIV/0!
Iyy ekskl. vertikalkomp.	t m2/kg m2	0	#DIV/0!	6,858	#DIV/0!
Izz ekskl. vertikalkomp.	t m2/kg m2	0	#DIV/0!		
Rxx ekskl. vertikalkomp.	m			0,265	#VERDI!
Ryy ekskl. vertikalkomp.	m			0,478	#VERDI!
Rzz ekskl. vertikalkomp.	m				

KRENGEPRØVE		Fullskala	Modellskala	Målt modell	Avvik (%)
Vekt inkl. vertikalkomp.	tonn, kp				
GMxx inkl. vertikalkomp.	m				
GMyy inkl. vertikalkomp.	m				
Txx med vekter	s				
Tyy med vekter	s				

C:\TROND-NTNU-tegnearkiv\NTNU-Mohd-Atif-Siddiqui\Mohd Atif swath 2020\NTNU-Swath-Endelig_resultat_
Rev8_Vektsdata_for_modeller.xls

14.04.2020

SHIFTING KNIVES

Project No.			
Title	VIPPING AV SWATH (NTNU-MOHD ATIF)	07.04.2020	**Date:**
Client	VIPPING PITCH	kl.09.00	
		T.I.	**Sign.:**

EMPTY CRADLE	Mass	8,760	kg
	Moment of inertia about COG	0,607	kg m2
	Distance from lower knife to COG (+ downwards)	0,214	m
	Distance between knives	0,100	
	Distance from lower knife to base line (+ downwards)	0,200	m
MODEL	Mass	30,060	kg
OSCILLATION PERIODS	Oscillation period, lower knife	2,597	s
	Oscillation period, upper knife	2,093	s
RESULTS	Moment of inertia, lower knife	7,157	kg m2
	Distance from lower knife to COG (+ downwards)	0,100	m
	Moment of inertia about COG	6,858	kg m2
	KG	0,100	m
	Radii of gyration	0,478	m

SHIFTING KNIVES

Project No.	VIPPING AV SWATH (NTNU-MOHD ATIF)	07.04.2020	**Date:**
Title	VIPPING RULL	kl.09.30	
Client		T.I.	**Sign.:**

EMPTY CRADLE	Mass	8,760	kg
	Moment of inertia about COG	0,607	kg m2
	Distance from lower knife to COG (+ downwards)	0,214	m
	Distance between knives	0,100	
	Distance from lower knife to base line (+ downwards)	0,200	m
MODEL	Mass	30,060	kg
OSCILLATION PERIODS	Oscillation period, lower knife	1,688	s
	Oscillation period, upper knife	1,484	s
RESULTS	Moment of inertia, lower knife	2,397	kg m2
	Distance from lower knife to COG (+ downwards)	0,098	m
	Moment of inertia about COG	2,110	kg m2
	KG	0,102	m
	Radii of gyration	0,265	m

MERKING AV MODELL:

M- NTNU-Swath-Mohd-Atif

MT-K4-S118 Rev.02

Merkeversjon: 1

Dato: 14.04.20

ALLE DATA I mm:

LPP =	**1667,7**	
SKALA =	**1,000**	
SLAGRADIUS =		
AVST. SPEIL =	**-111**	

SLINGREKJØL:

HØYDE OVER BL

V/ MAKSSPANT= **0,0**   ST= **5**

I MODELLSKALA

FULLSKALA

WL NR.	DYPGANG	TRIM
DWL	161,1	0
WL 1	0	0
WL 2	0	0
WL 3	0	0
WL 4	0	0
WL 5	0	0

MODELLDATA I mm:

Avstand fra FP til forkant bulb: **100,0**

SPANT		AVSTAND 0
SPEIL	=	-111,0
0	=	0,0
1/2	=	83,4
1	=	166,8
1 1/2	=	250,2
2	=	333,5
3	=	500,3
4	=	667,1
5	=	833,8
6	=	1000,6
7	=	1167,4
8	=	1334,1
8 1/2	=	1417,5
9	=	1500,9
9 1/2	=	1584,3
10	=	1667,7

VANNLINJE: DWL

0	ST 1	ST 5	ST 9	ST 10
161,1	161,1	161,1	161,1	161,1

VANNLINJE: WL 1

0	ST 1	ST 5	ST 9	ST 10
0,0	0,0	0,0	0,0	0,0

VANNLINJE: WL 2

0	ST 1	ST 5	ST 9	ST 10
0,0	0,0	0,0	0,0	0,0

VANNLINJE: WL 3

0	ST 1	ST 5	ST 9	ST 10
0,0	0,0	0,0	0,0	0,0

RUTENETT/VANNLINJER I MM

20	=	20,0	
40	=	40,0	Aktenfor
60	=	60,0	st. 3
80	=	80,0	
100	=	100,0	Forenfor
120	=	120,0	st. 7
140	=	140,0	
KVL 161,1	=	161,1	
180	=	180,0	
200	=	200,0	
220	=	220,0	
240	=	240,0	
260	=	260,0	
0	=	0,0	
0	=	0,0	
0	=	0,0	

VANNLINJE: WL 4

0	ST 1	ST 5	ST 9	ST 10
0,0	0,0	0,0	0,0	0,0

VANNLINJE: WL 5

0	ST 1	ST 5	ST 9	ST 10
0,0	0,0	0,0	0,0	0,0

Kommenterer:

Kontrollert:

merkeskjema-NTNU-Swath-endelig.xls

Appendix B

Free decay test
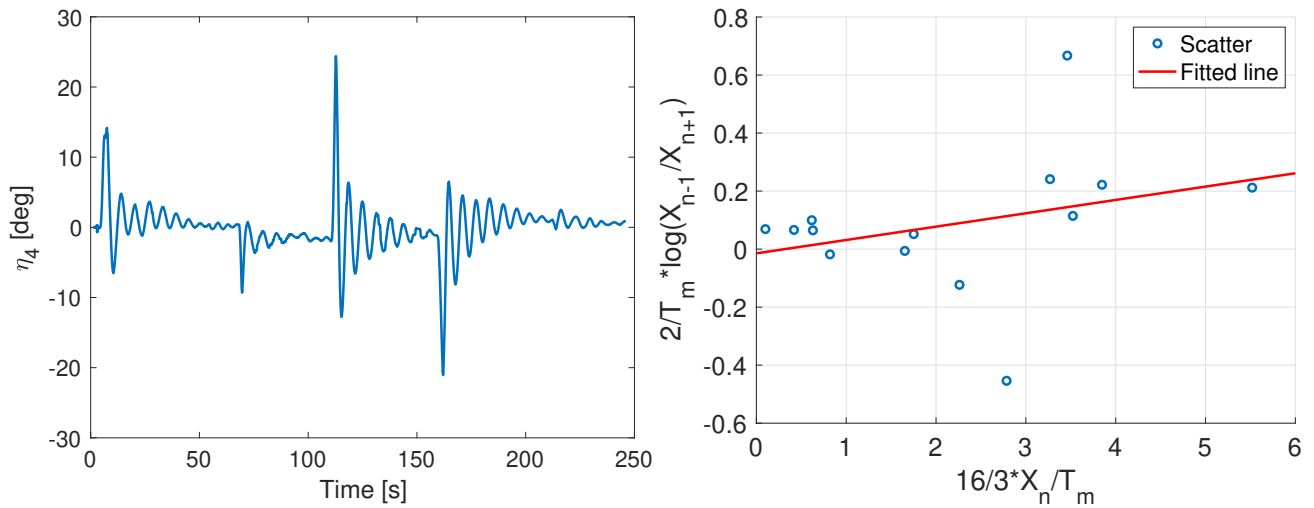
Figure B.1: Estimation of damping coefficient for hull with fin 1 in roll motion
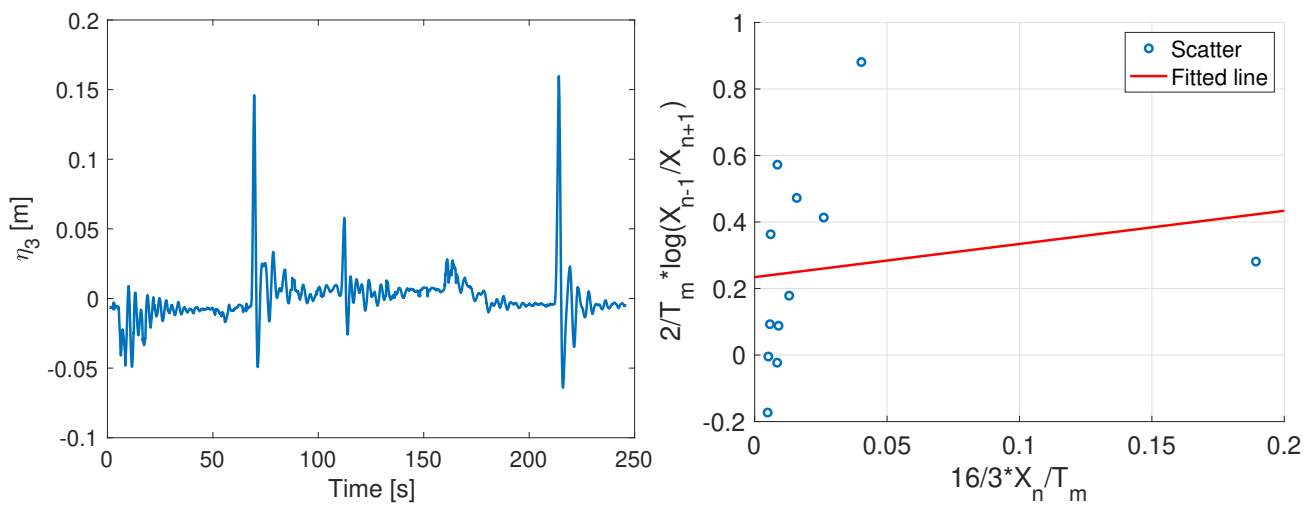
Figure B.2: Estimation of damping coefficient for hull with fin 1 in heave motion
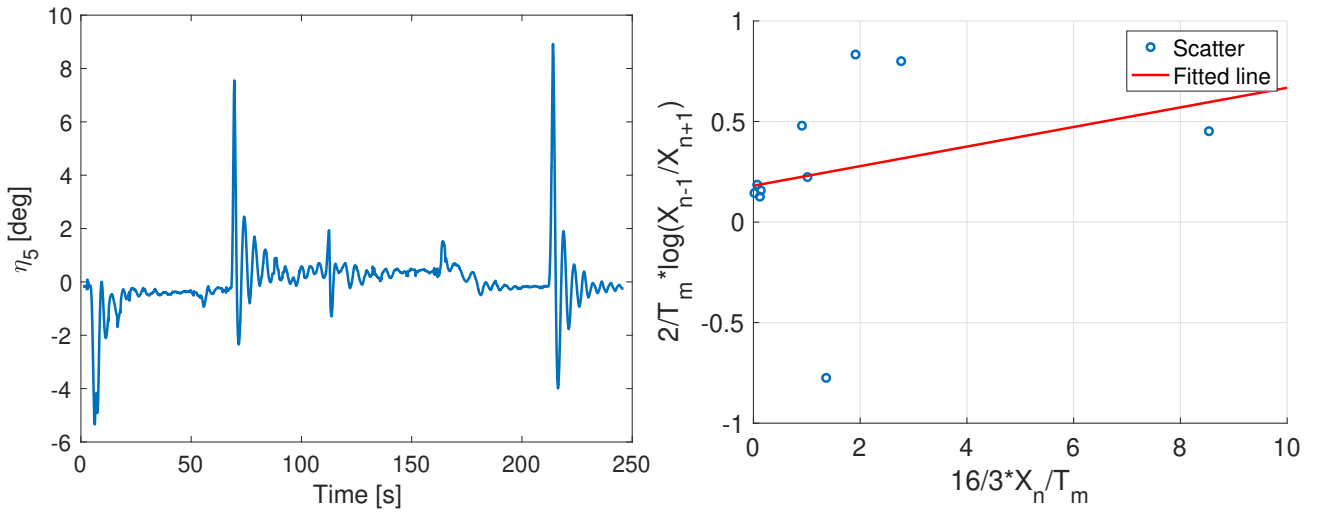
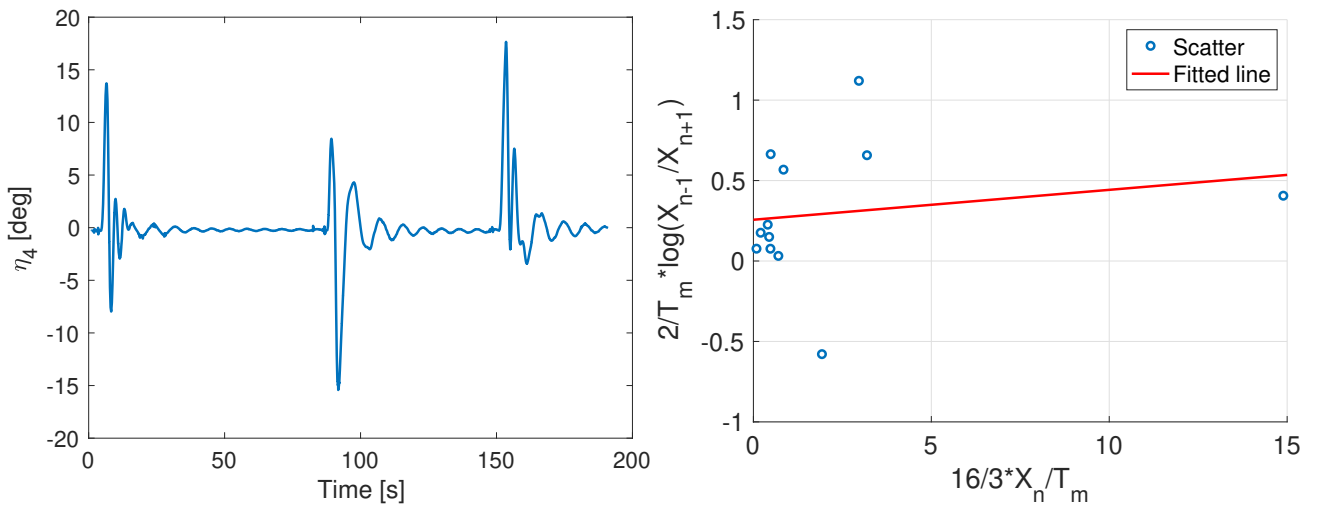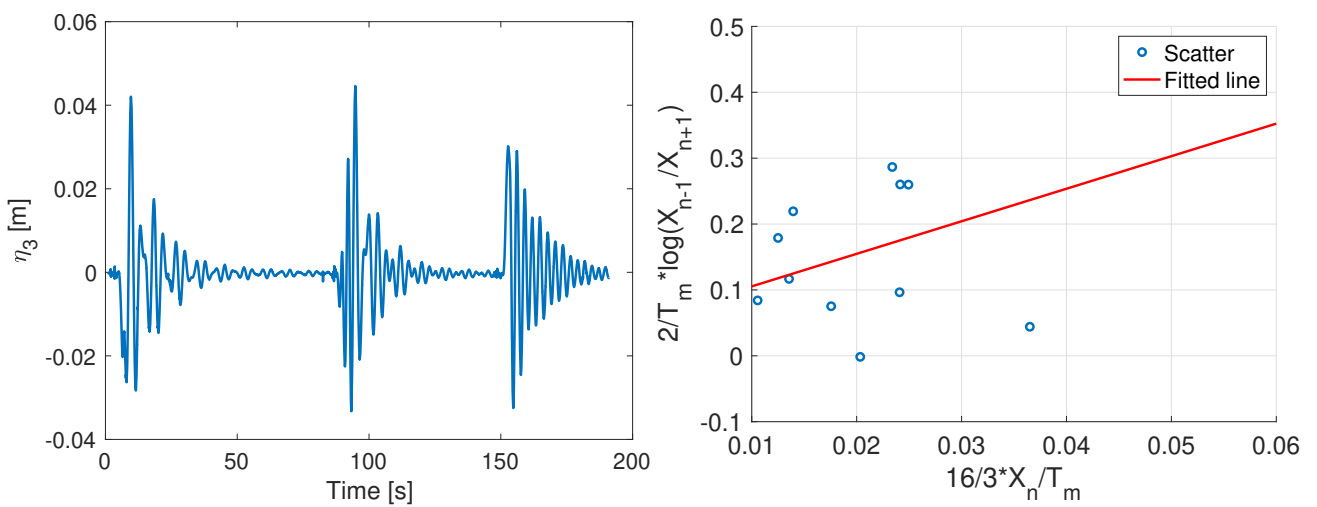Figure B.3: Estimation of damping coefficient for hull with fin 1 in pitch motion
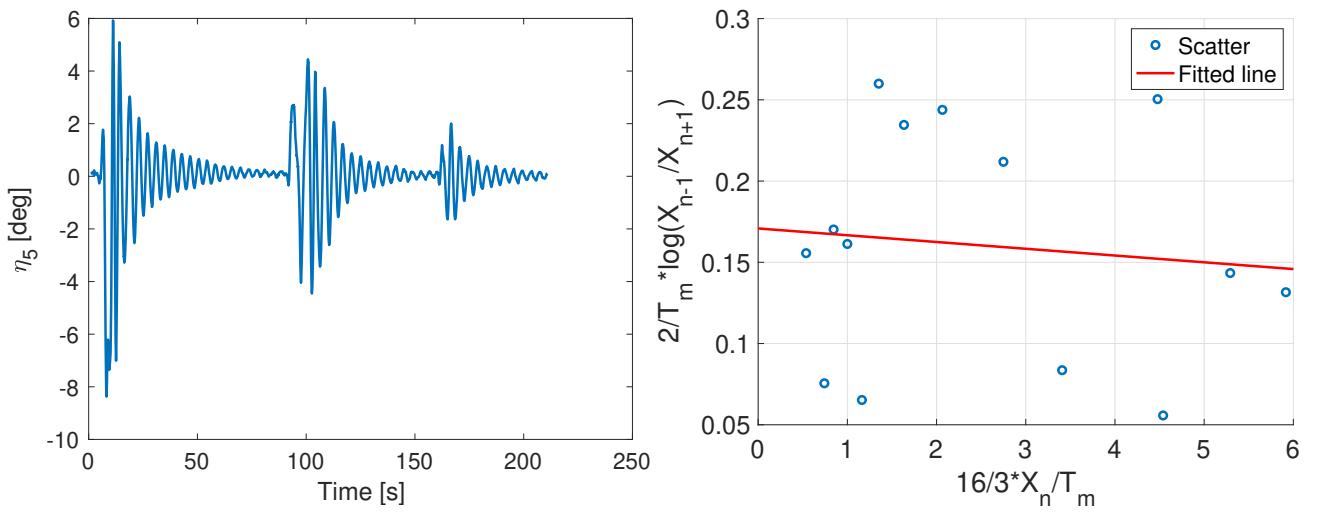
Figure B.4: Estimation of damping coefficient for condition 1 in pitch motion
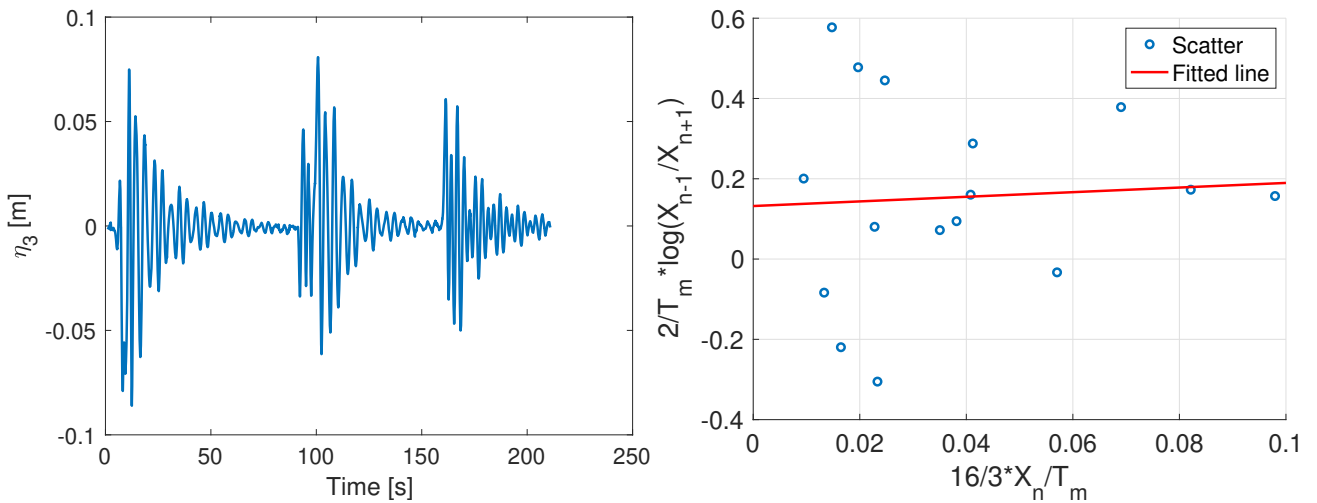
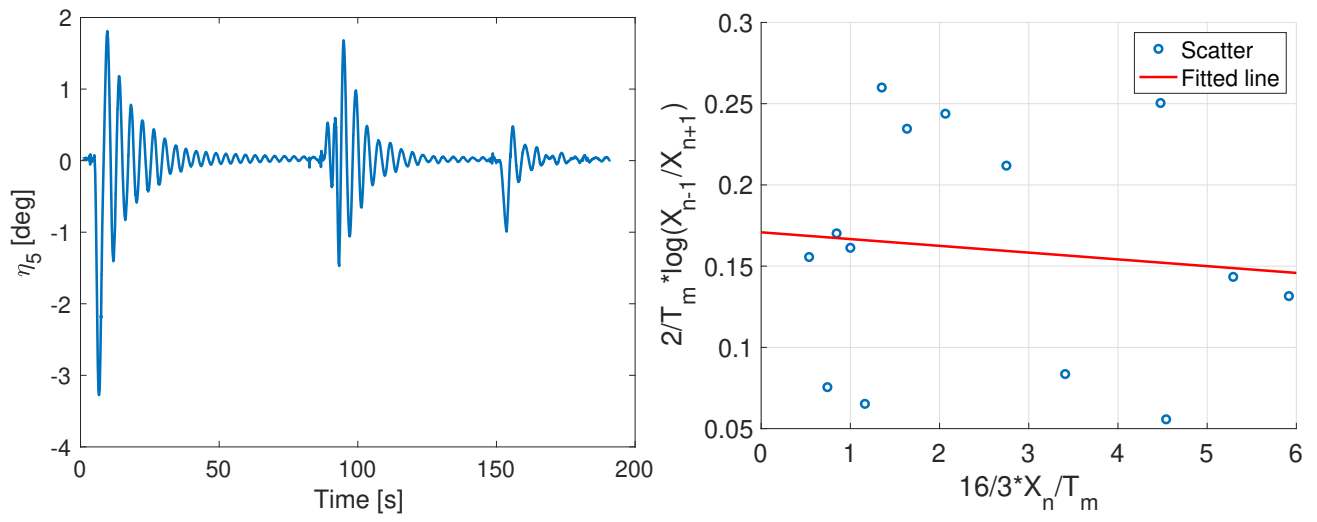Figure B.5: Estimation of damping coefficient for condition 1 in heave motion
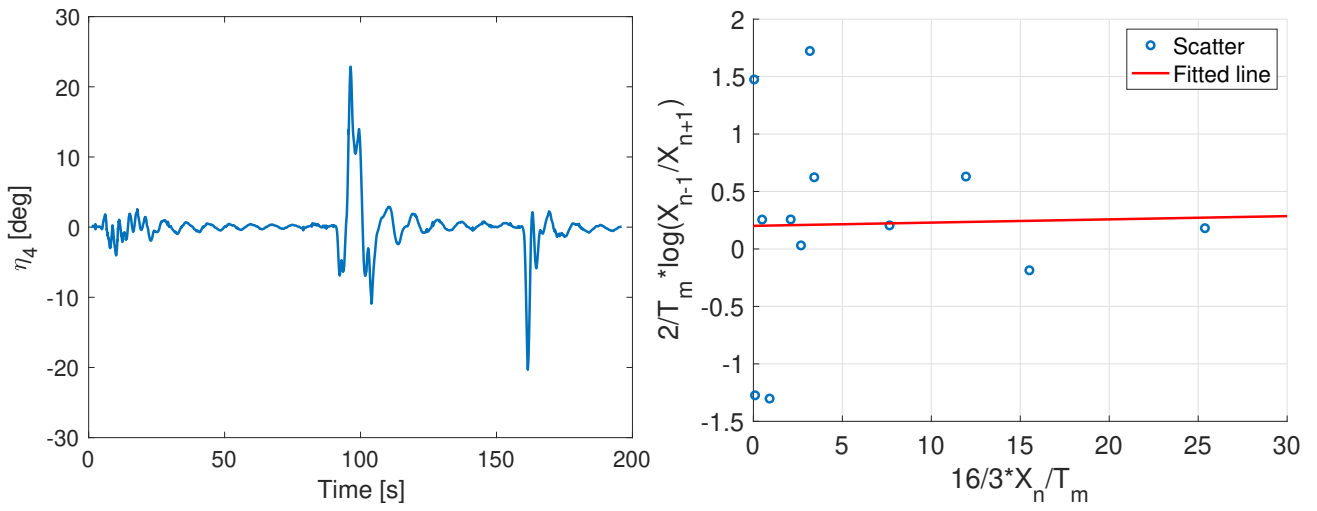
Figure B.6: Estimation of damping coefficient for condition 1 in roll motion

Figure B.7: Estimation of damping coefficient for condition 3 in roll motion

Figure B.8: Estimation of damping coefficient for condition 3 in heave motion

Figure B.9: Estimation of damping coefficient for condition 3 in pitch motion

Appendix C

RAO from experiment

In this chapter the remaining RAO that was not presented in subsection 6.1.2, is present here.

(a) Head sea, surge RAO

(b) Head sea, sway RAO

(c) Head sea, roll RAO

(d) head sea, yaw motion
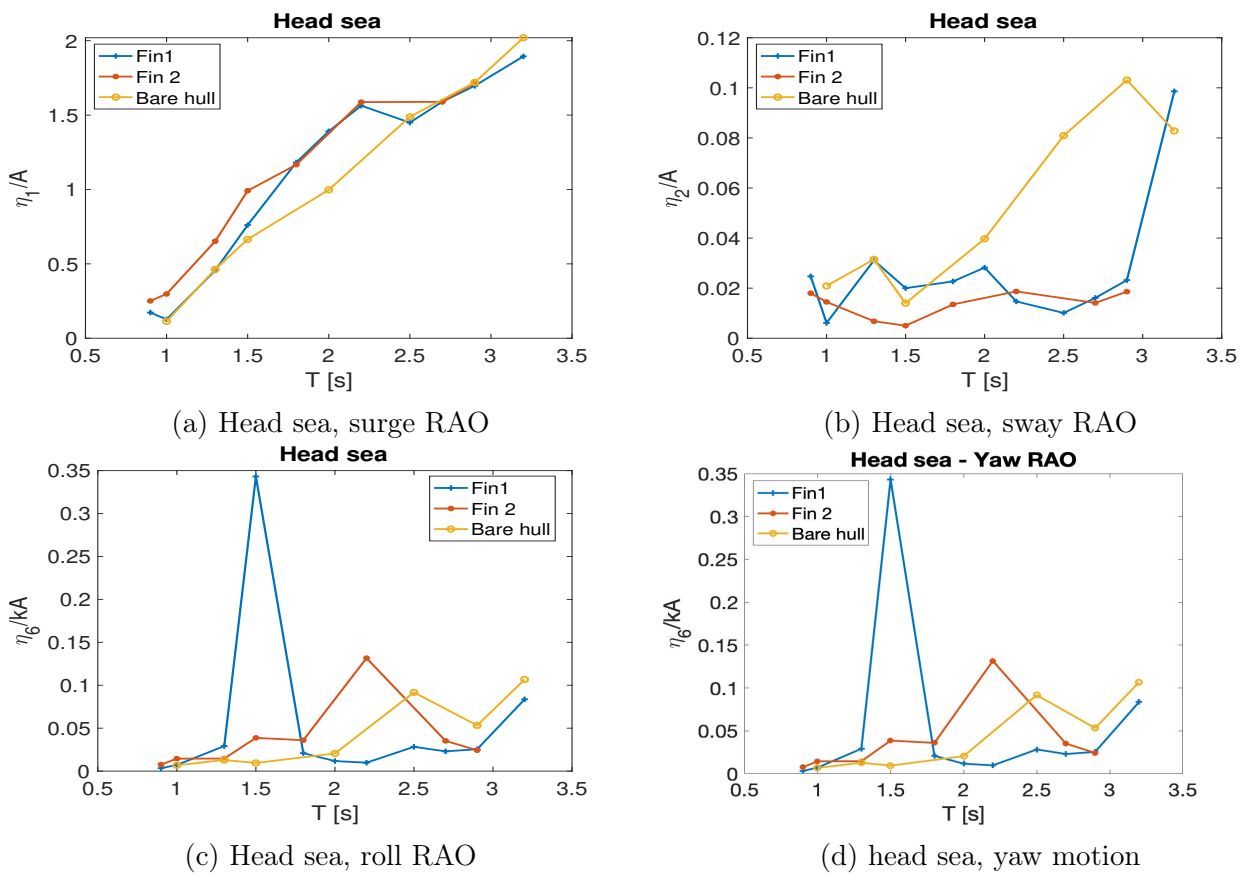
Figure C.1: Remaining presentation of RAO for head sea in regular waves
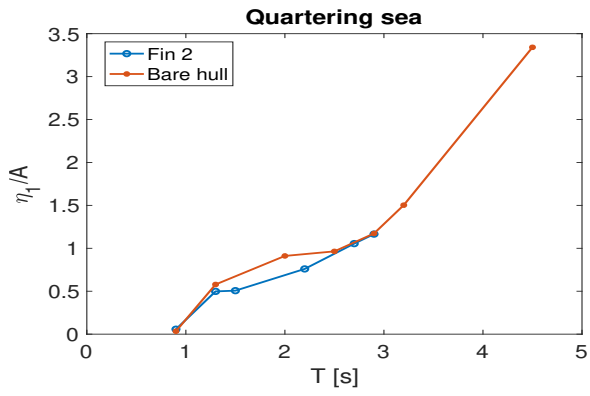
(a) Quartering sea, surge RAO
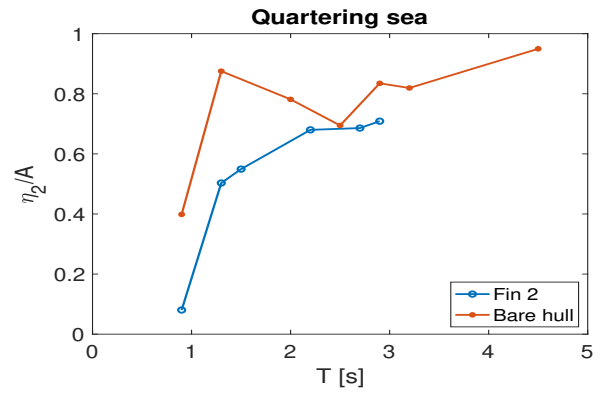
(b) Quartering sea, sway RAO
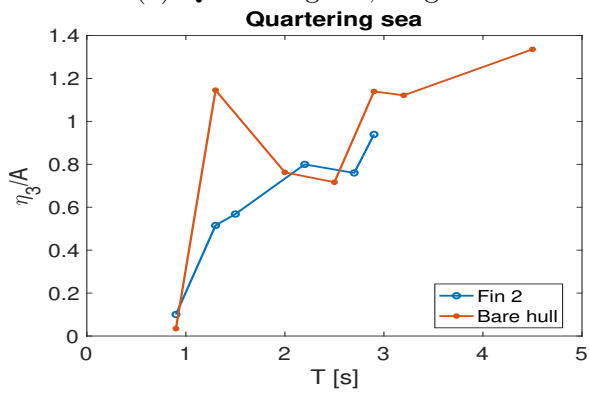
(c) Quartering sea, pitch RAO
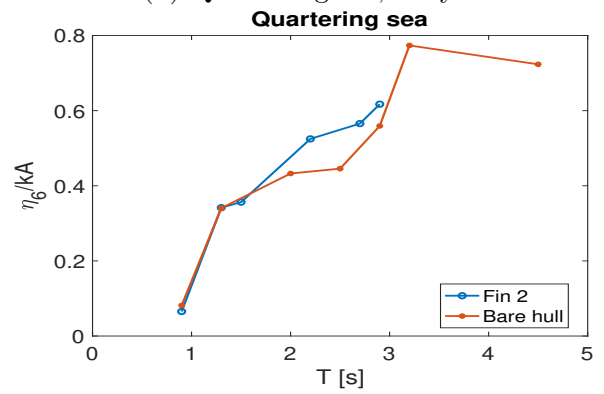
(d) Quartering sea, yaw motion

Figure C.2: Remaining presentation of RAO for quartering sea in regular waves
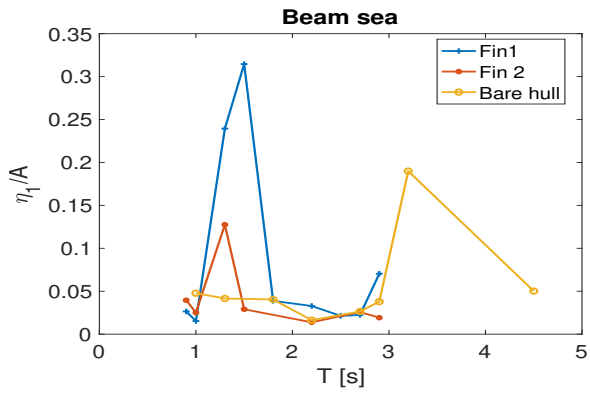
(a) Beam sea, surge RAO
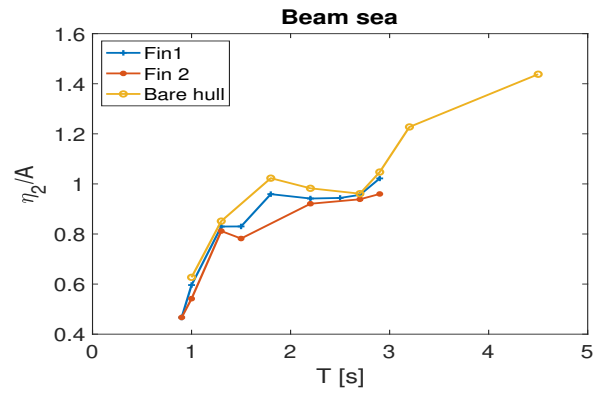
(b) Beam sea, sway RAO
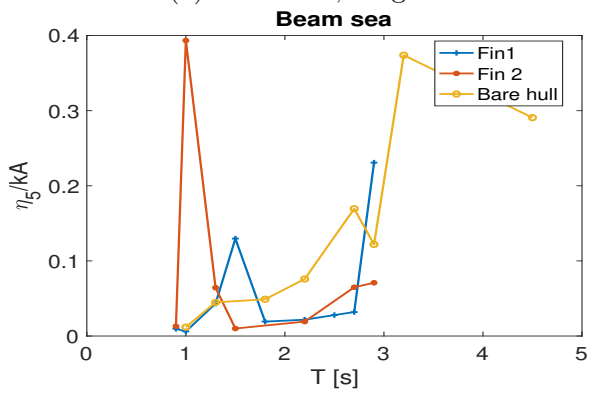
(c) Beam sea, pitch RAO
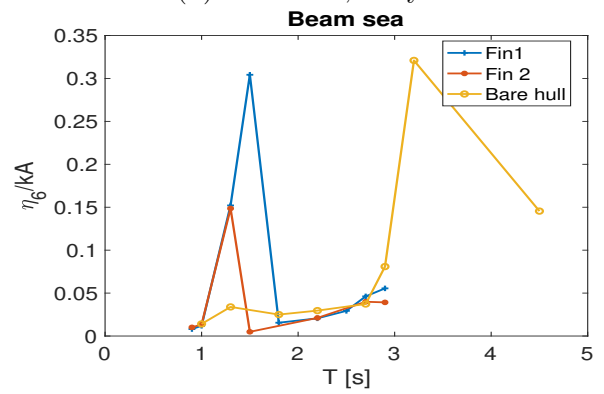
(d) Beam sea, yaw motion

Figure C.3: Remaining presentation of RAO for beam sea in regular waves

Appendix D

Significant motion amplitude

The remaining motions that were not presented in section 6.2.1, is presented below.
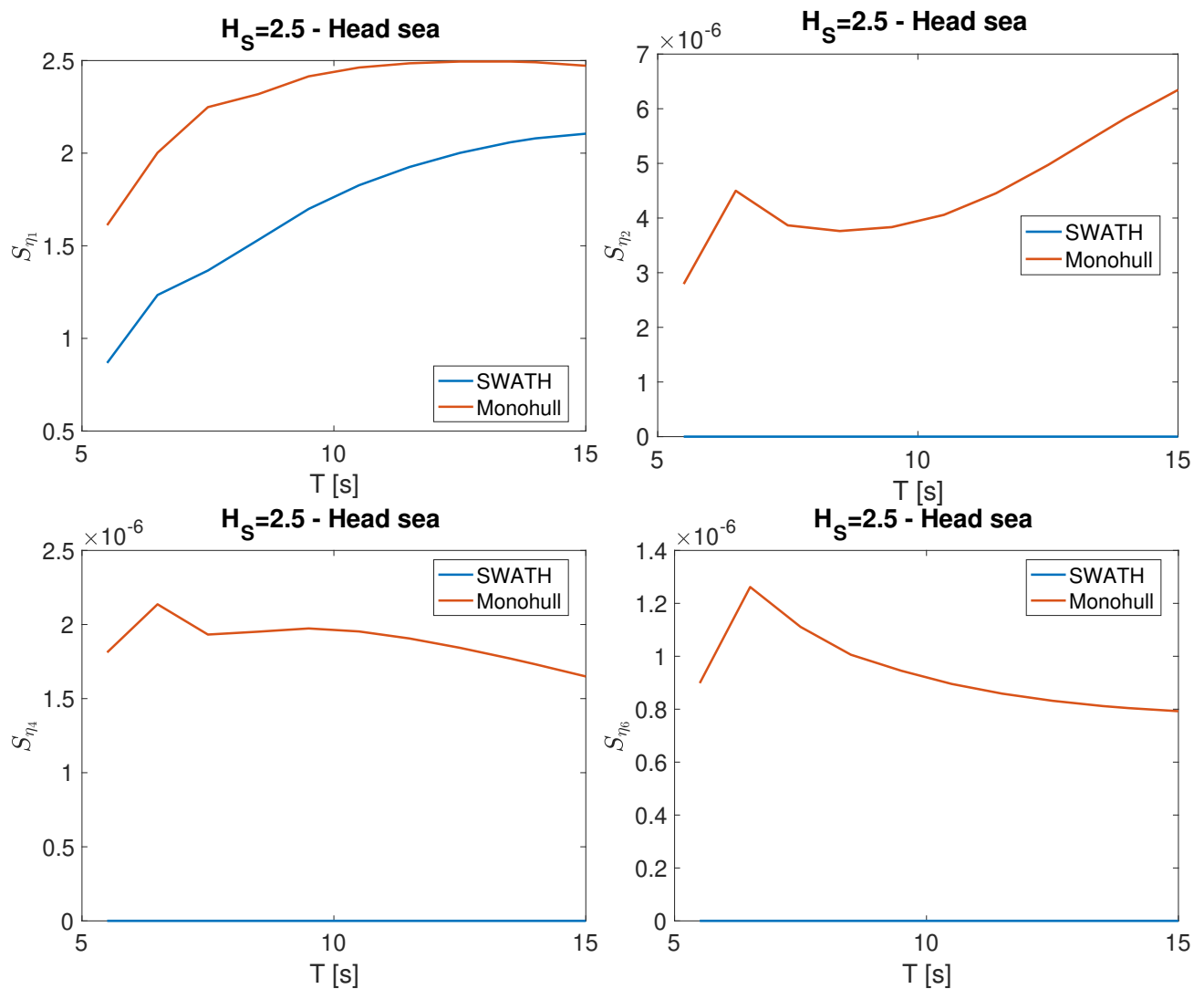
Figure D.1: Significant motion amplitude of SWATH and monohull for $H_S = 2.5$ in head sea
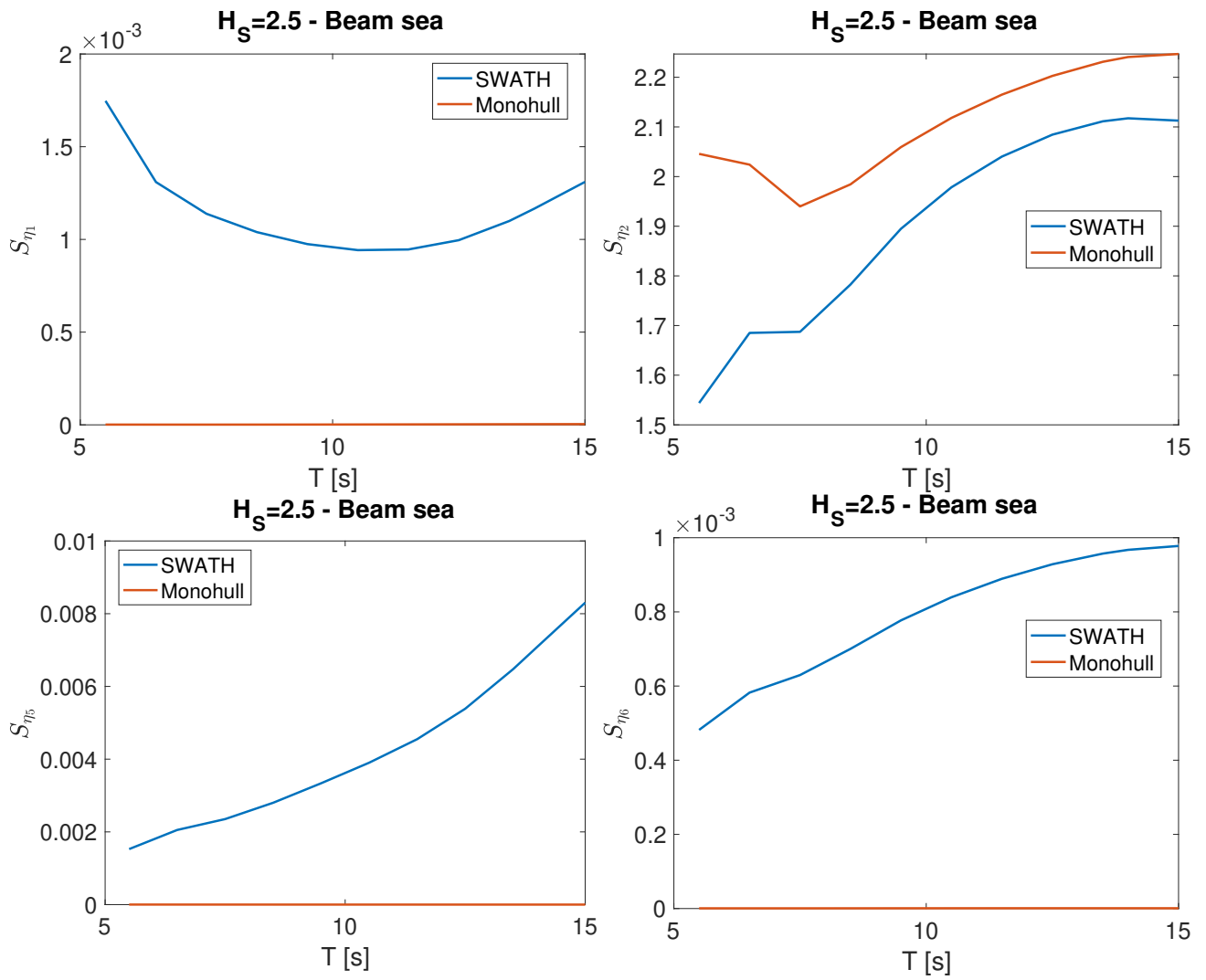
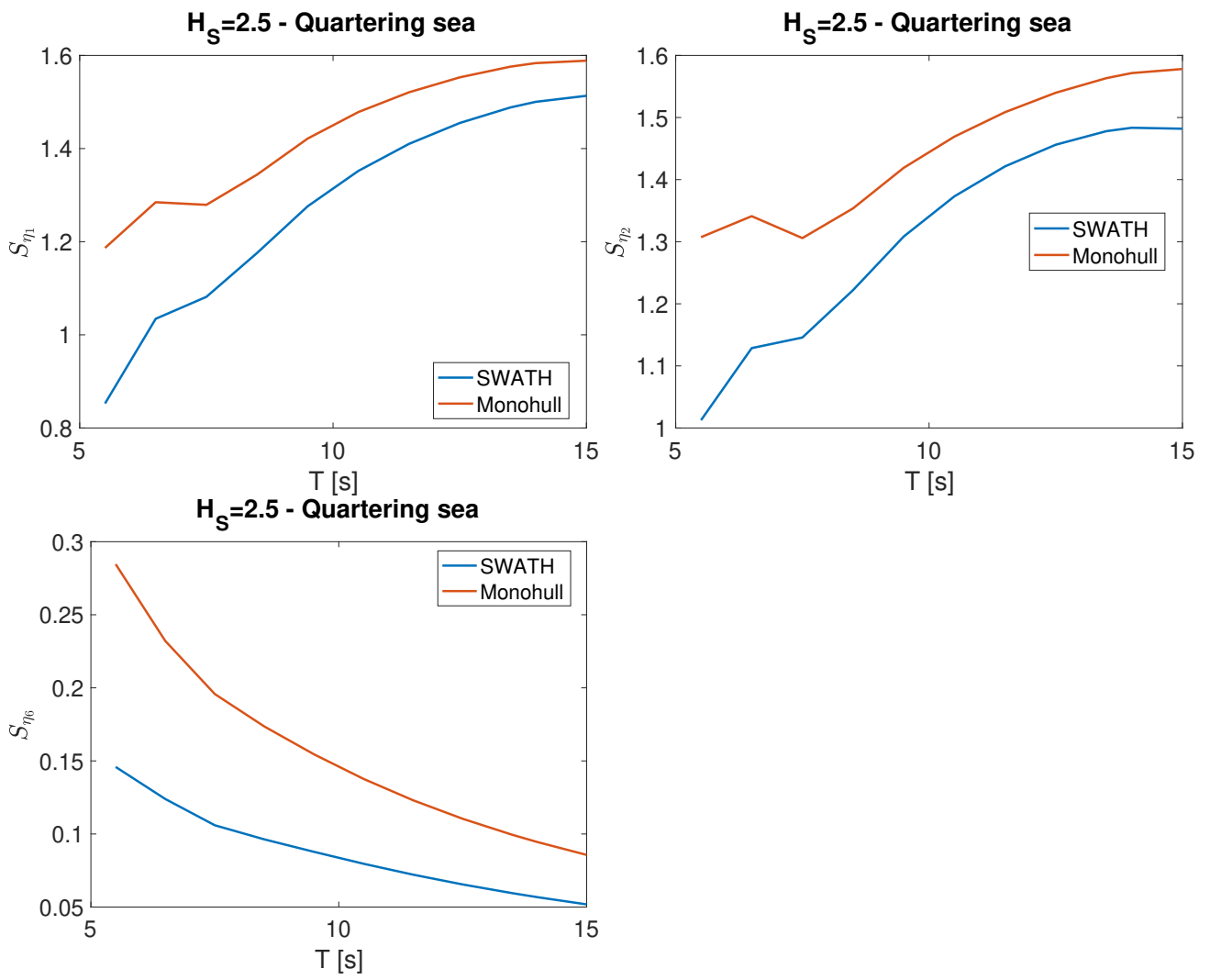Figure D.2: Significant motion amplitude of SWATH and monohull for $H_S = 2.5$ in beam sea

Figure D.3: Significant motion amplitude of SWATH and monohull for $H_S = 2.5$ in quartering sea
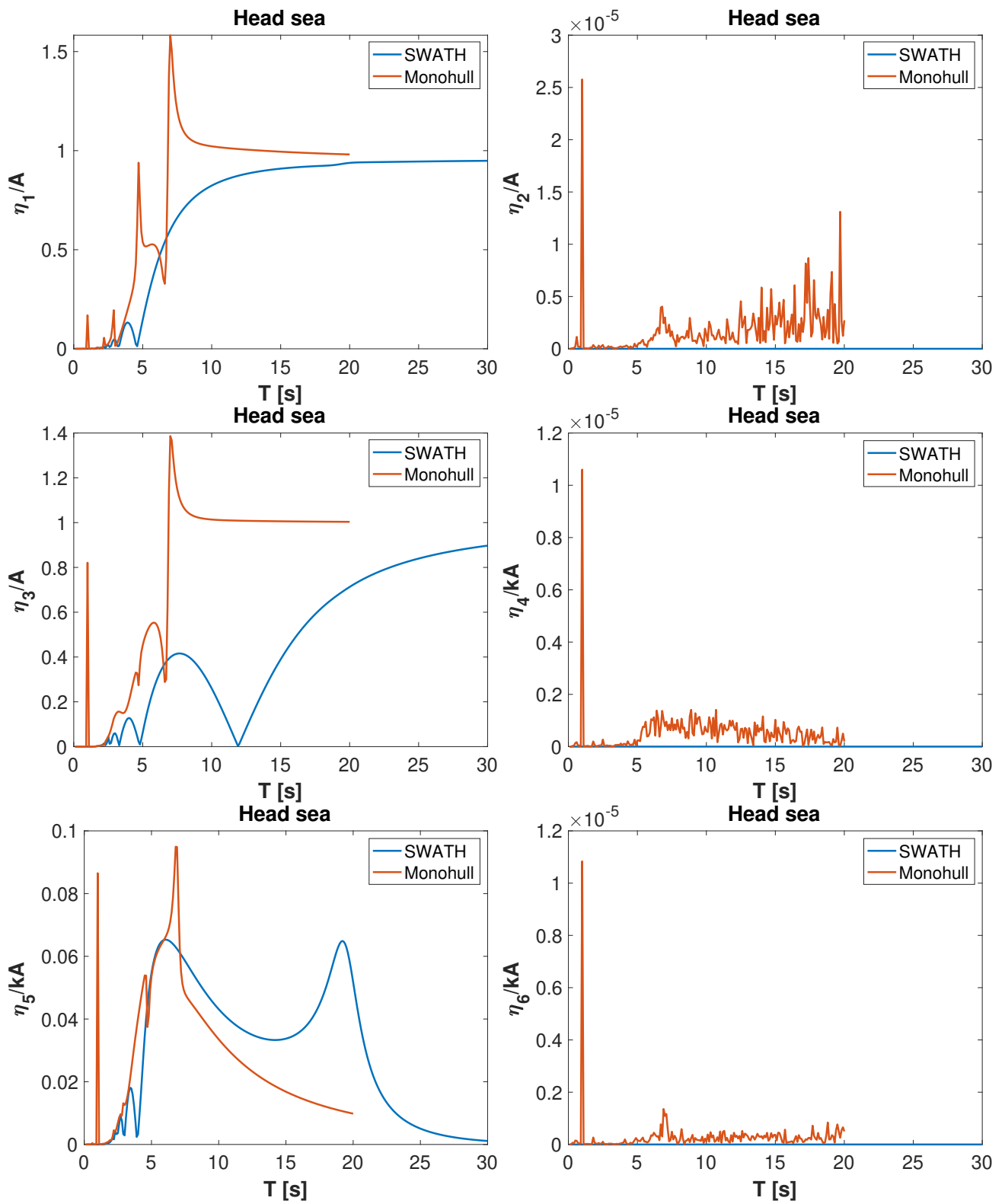
Appendix E
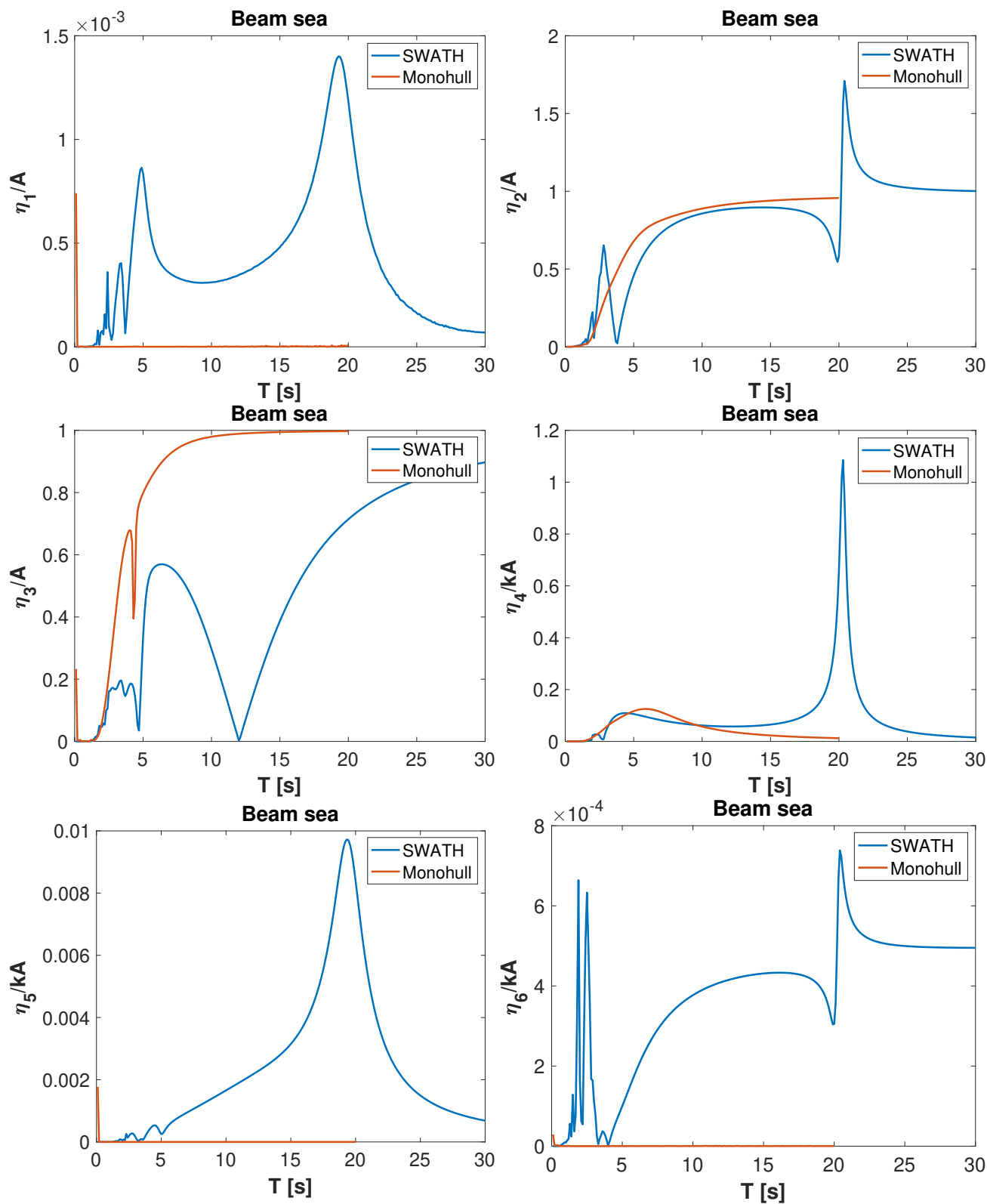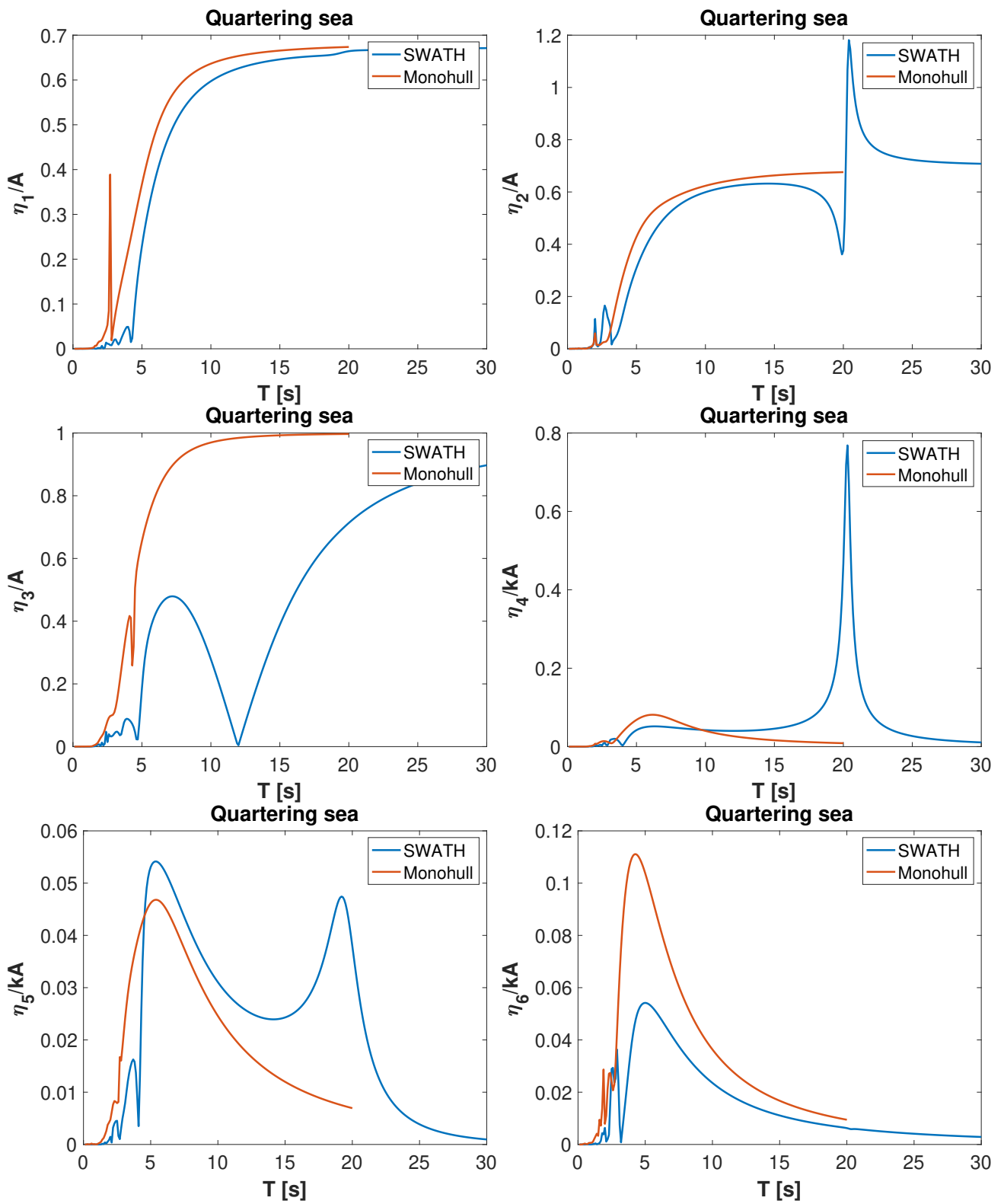
RAO from WAMIT with damping

Figure E.1: RAO in beam sea

Figure E.2: RAO in beam sea

Figure E.3: RAO in quartering sea

Sofie Kopperstad Gjerde

Hydrodynamic design of an autonomous ROV vessel

NTNU
Norwegian University of
Science and Technology